Evaluating the effects of variable *NR2E1* levels on gene expression, behaviour, and neural and ocular development

by

Bibiana Ka Yan Wong

B.Sc., University of British Columbia, 2001

A THESIS SUBMITTED IN PARTIAL FULFILLMENT OF
THE REQUIREMENTS FOR THE DEGREE OF

DOCTOR OF PHILOSOPHY

in

The Faculty of Graduate Studies

(Medical Genetics)

THE UNIVERSITY OF BRITISH COLUMBIA

(Vancouver)

December 2009

Abstract

Nuclear receptor 2E1 (*Nr2e1*) is expressed in the developing and adult brain and eye, and controls proliferation and differentiation of neural and retinal stem/progenitor cells by regulating genes important in these cellular processes. The Simpson laboratory discovered and characterized a spontaneous deletion of mouse *Nr2e1* (the *fierce* allele, *frc*) and demonstrated the functional equivalence of human and mouse NR2E1 when the behavioural and neuroanatomical phenotypes of $Nr2e1^{frc/frc}$ mutants were rescued by introducing human *NR2E1*. *NR2E1* has recently been implicated in human psychiatric disorders and variants in *NR2E1* were identified in patients with brain and behavioural abnormalities, including bipolar I disorder (BPI). Although *NR2E1* had been implicated in BPI, the validity of $Nr2e1^{frc/frc}$ mice to model BPI has not yet been tested. In anticipation of subtle behavioural phenotypes, the hypothesis that dark-phase testing affects the outcome of high-throughput behavioural tests was tested. We demonstrated that dark-phase testing improved discrimination between genetically distinct inbred mouse strains. This result was integrated into the experimental design for evaluating $Nr2e1^{frc/frc}$ mice as a model for BPI by behavioural measures and lithium treatment. $Nr2e1^{frc/frc}$ mice exhibited behavioural traits used to model BPI in rodents, including hyperactivity and learning deficits; however, adult $Nr2e1^{frc/frc}$ mice were resistant to the effects of lithium treatment, and therefore our results did not provide support for $Nr2e1^{frc/frc}$ mice as an appropriate pharmacological model for BPI. Since the nature of patient variants in *NR2E1* is likely regulatory, resulting in transcriptional alterations, and the effects of variable levels of *Nr2e1* are currently unknown, I tested the hypothesis that variable *Nr2e1* levels will affect gene expression and neurological and ocular development. Mice overexpressing *Nr2e1* showed alterations in transcription

levels of key target genes in both the brain and the eye, significant increase in neural

stem/progenitor cell proliferation in the subventricular zone of the adult brain, and severe eye

abnormalities. Gene expression changes in *Gfap*, *Gsk3β*, *Pax6*, and *Nr2e3* suggest a role for

Nr2e1 in genetic pathways important in psychiatric and eye disorders, including BP,

Alzheimer Disease, cancer, Aniridia, and enhanced S-cone syndrome. Collectively, these

results justify the further investigation of *NR2E1* in these human disorders.

Table of contents

List of tables

List of figures

List of abbreviations

129S1/SvImJ	129
Auditory brainstem response	ABR
Bacterial artificial chromosome	BAC
Bipolar disorder	BP
Bipolar I disorder	BPI
Bipolar II disorder	BPII
Bromodeoxyuridine	BrdU
C57BL/6J	B6
Clumped pigmentary retinal degeneration	CPRD
Cycle threshold	Ct
Dentate gyrus	DG
DNA-binding domain	DBD
Embryonic day	E
Enhanced S-cone syndrome	ESCS
Fierce allele – spontaneous deletion of mouse *Nr2e1*	*frc*
Fluorescence *in situ* hybridization	FISH
Ganglion cell layer	GCL
Goldmann-Favre syndrome	GFS
Inner nuclear layer	INL
Inner plexiform layer	IPL
Ligand-binding domain	LBD
Light-dark	L/D
Lithium chloride	LiCl
Logarithm of odds	LOD
Long-term potentiation	LTP
Neural stem/progenitor cell	NSC
Nuclear receptor subfamily 2 group E member 1 – Human gene	*NR2E1*
Nuclear receptor subfamily 2 group E member 1 – Mouse gene	*Nr2e1*
Nuclear receptor subfamily 2 group E member 1 – Human protein	NR2E1
Nuclear receptor subfamily 2 group E member 1 – Mouse protein	Nr2e1
Outer nuclear layer	ONL
Outer plexiform layer	OPL
Phage artificial chromosome	PAC
Photoreceptor outer segment	OS
Polymerase chain reaction	PCR
Postnatal day	P
Quantitative reverse-transcriptase PCR	qRT-PCR
Retinal progenitor cell	RPC
Retinitis pigmentosa	RP
Retinoic acid	RA
Revolutions per minute	RPM
Room temperature	RT
Single nucleotide polymorphism	SNP

Subventricular zone	SVZ
Transgenic	Tg
Untranslated region	UTR
Ventricular zone	VZ
Wildtype	Wt

Acknowledgments

I would like to thank my supervisory committee, Drs. Elizabeth Simpson (supervisor), Leigh Field, Blair Leavitt, Anthony Phillips, and Fabio Rossi, for all their support and expert guidance over the years. To the many administrative support staff, Dora Pak, Tracey Weir, Veronica Yakoleff, Rhonda Ellwyn, Heather Baker, Anna Moorhouse, and Tammy Philippo, I am grateful for all your assistance throughout my studies, from scheduling seemingly impossible meetings, to helping with grant applications, manuscript preparation, and thesis proofreading. To the wonderful students I had the honour of mentoring, John Chen, Emilija Todorovic, Jasmen Sze, Jason Cheng, Catherine Tam, Winnie Yang, and Glen Ottmann; thank you for all your help and giving me the opportunity to experience my own little "lab" within a lab. I would also like to thank the numerous Simpson lab members that I have had the pleasure of working with throughout the *many* years I have been here. There are too many of you to name, but I appreciate all the meaningful discussions, technical and emotional support, and friendships that have been formed. To my fellow Simpson lab Ph.D. students, old and new, Drs. Brett Abrahams and Ravi Kumar, Charles de Leeuw, Jean-François (Jeff) Schmouth, and Ximena Corso-Dìaz, thank you for all your scientific insights and ideas and support especially through rejected manuscripts, failed experiments, and unexpected results. I would especially like to thank Kathy Banks, my lab manager and my bay mate of over 5 years, and a voice of strength and reason through many of my trials and tribulations at and away from the lab. My graduate experience would also not have been the same without many other CMMT staff and students; you have all touched my life in your own unique ways and I am forever grateful for all the wonderful memories.

I would like to thank all my family and friends for their love and steadfast support, without them I would not have made it this far. To all my friends, you know who you are, without you this would not have been possible. To my two amazing grandmothers, all my aunts, uncles, and cousins thank you for your words of wisdom, your delectable food, and your constant encouragement. To the only grandfather I have known, sorry I took so long to graduate that you could not be here to share this with me. To make up for it, I dedicate this work to your memory. To my parents, thank you for supporting me in everything I do and allowing me the freedom to pursue my dreams. I hope that I can live up to all your expectations and be someone you are proud of.

I thank God everyday for all the amazing people He has surrounded me with to help me through this stage of my life.

To the loving memory of my grandfather (1925 – 2009)

Thank you for always believing in me.

Co-authorship statement

Chapter 2

The project described in this chapter was conceived and initiated by Dr. E.M. Simpson. The project became focused under the direction of Dr. S.M. Hossain. Dr. S.M. Hossain performed all behaviour testing. I analyzed the data, created all tables and figures, edited, and saw the manuscript through to publication.

Chapter 3

The project described in this chapter was conceived and initiated by Dr. E.M. Simpson. The initial characterization of $Nr2e1^{frc/frc}$ mice was performed under the direction of Dr. S.M. Hossain, and students he trained (ET and SB). After Dr. Hossain's departure from the laboratory, I took over, focused, and directed the project by independently reproducing the original behavioural observations and further characterizing $Nr2e1^{frc/frc}$ mice with and without lithium treatment. I was also in charge of the collaboration with Dr. Q.Y. Zhen. I generated all the data presented in this chapter. A student (GAO), whom I trained, assisted in capturing images for quantification of cell proliferation. I performed all data analysis, wrote the paper, created all the figures, edited and saw the manuscript to submission.

Chapter 4

The project described in this chapter was conceived and initiated by Dr. E.M. Simpson. The project became focused under my direction. Dr. E.R. Linnell generated the four transgenic strains studied in this chapter. Initial screening of the transgenic strains was

performed by Ms. M.L. Berry. Dr. B.S. Abrahams analyzed, using fluorescent in situ

hybridization, the genomic integration site, with the help of Dr. M.B. Valentine and Ms.

A.C.O. Chong, of the four transgenic strains (resulting in Fig. 4.1). Students (JS, JCYC, CT,

WHWY, and GAO), whom I trained, assisted in sample preparation and image collection and

tracing. Ms. A.E. Borrie assisted in the harvesting of the eye samples. I generated the results

presented, performed all data analysis, wrote the paper, and created all the figures for this

manuscript in preparation.

Chapter 1: General introduction

1.1 Nuclear receptor superfamily

The nuclear receptor superfamily is made up of numerous transcription factors important in the regulation of gene expression involved in processes including, but not limited to, metabolism, inflammation, cancer, neural and organ development, and cell proliferation and differentiation, metamorphosis, and organ physiology (Lee *et al.*, 2008, Mangelsdorf *et al.*, 1995, Yang *et al.*, 2006). Nuclear receptors bind specific DNA elements via their DNA-binding domain (DBD) and their function is largely controlled by conformational changes through binding of ligands to the receptor's ligand binding domain (LBD). These receptors include: thyroid hormone receptors (TR), peroxisome proliferator-activated receptors (PPAR), retinoic acid receptors (RAR), and the steroid receptor group containing glucocorticoid receptor (GR), mineralocorticoid receptors (MR), progesterone receptor (PR), and androgen receptors (AR) (Maglich *et al.*, 2001). However, there is a class of nuclear receptors, known as orphan nuclear receptors that have no known ligand; some of these have been shown to function in the absence of a ligand. For example, the function of Nr4e2, also known as Nurr1, is regulated by stable conformational folding of its LBD that resembles a ligand-bound nuclear receptor (Wang *et al.*, 2003). Many members of the orphan nuclear receptor family are involved in the development of the central nervous system (Armentano *et al.*, 2006, Chen *et al.*, 2001, Lutz *et al.*, 1994, Zetterstrom *et al.*, 1997). One of these orphan nuclear receptors, nuclear receptor 2e1 (Nr2e1) and its role in neural and ocular development, cell proliferation, and behaviour, is the focus of this thesis.

1.2 The importance of Nr2e1 in neurodevelopment and cell cycle regulation

1.2.1 Structure and interspecies homology of *Nr2e1*

Nr2e1, previously known as *MTll*, *Tlx*, was first identified in *Drosophila melanogaster* with similarity in its DBD and LBD to steroid hormone receptors. When mutated, *Drosophila Nr2e1* affects the embryonic development of the anterior and posterior poles (Pignoni *et al.*, 1990). Vertebrate *Nr2e1* was first cloned and investigated in chicken (Yu *et al.*, 1994), then in mouse (Monaghan *et al.*, 1995), and finally in human (Jackson *et al.*, 1998). The DBD of vertebrate *Nr2e1* contains two distinct differences when compared to other nuclear receptors. First, the proximal box (P box) sequence contains a serine residue in place of the canonical lysine residue that is found in all other nuclear receptors (Figure 1.1). Secondly, the distal box (D box) sequence encodes for seven amino acids instead of the typical five in other nuclear receptors (Figure 1.1). DNA-binding assays showed that the Nr2e1 DBD binds to a target sequence AAGTCA, either as a monomer to a single half-site or as dimers to a pair of half-sites (Kobayashi *et al.*, 1999, Yu *et al.*, 1994). The human and mouse Nr2e1 proteins are 385 amino acids large in size and show 100% and 99.5% conservation in the DBD and LBD, respectively (Kobayashi *et al.*, 2000). Genomic analysis of *Nr2e1* also showed elements of extreme conservation from human to mouse down to *F. rubripes* (Fugu), indicative of regulatory and functional importance (Abrahams *et al.*, 2002).

```
P box consensus sequence                    EGCKG

Nr2e1 (chick)    CKVCGDRSSGKHYGVYAC DGCSG FFKRSIRRNRTYVC KSGNQGG CPVDKTHRNQCRACRLKKCLEVNMNKDAVQHERGPRTSTIRK
                                     | | | |              | |   | |
Tll (Drosophila) CKVCRDRHSGKHYGIYAC DGCAG FFKRSIRRSRQYVC KSQKQGL CVVDKTHRNQCRACRLRKCFEVGMNKDAVQHERGPRNSTLRR
                                    P box               D box
Conserved C    1   2              3   4              5        6       7   8   9
```
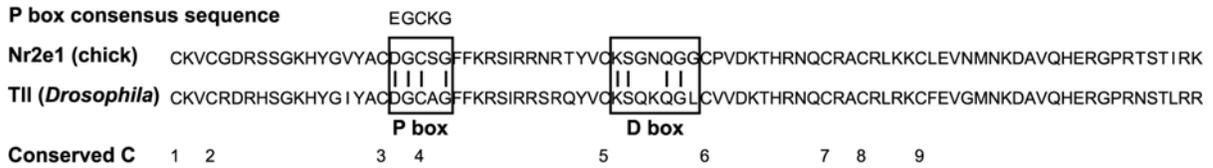
Figure 1.1 DNA-binding domain of Nr2e1 contains two distinct differences

Amino-acid sequences of the DNA-binding domain of chick Nr2e1 and *Drosophila* Tll show two distinct differences compared to other nuclear receptors. The proximal box (P box) and distal box (D box) are boxed and labelled. The P box sequences differ from the consensus sequence such that both encode aspartic acid (D) instead of glutamic acid (E); in addition, a lysine (K) that is absolutely conserved in all other members is substituted with either serine (S) or alanine (A). The D box encodes 7 amino acids between the 5th and 6th coserved cysteines (C) instead of the usual 5 amino acids. Vertical lines identify sequence homology between chick and *Drosophila* Nr2e1 within the P and D boxes. (Modified from (Yu *et al.*, 1994))

1.2.2 Expression pattern of *Nr2e1* in the developing and adult brain

In mouse, *Nr2e1* transcription is first detected at the 5-somite stage (embryonic day (E)8) in a few cells adjacent to the neural epithelium caudal to the anterior limit of developing proscencephalon (Monaghan *et al.*, 1995). By E8.5, expression has spread caudally into the presumptive diencephalon and can be detected in newly formed optic and olfactory evaginations. At E12.5, *Nr2e1* transcripts are restricted to a subset of forebrain periventricular zones and presumptive amygdala, except for transcripts remaining in the neural retina and olfactory epithelium. *Nr2e1* expression decreases to undetectable levels perinatally, but by adulthood expression is again observable in a subset of cells in the subgranular layer of the dentate gyrus (DG) of the hippocampus and the subventricular zone (SVZ) lining the lateral ventricles of the adult brain (Monaghan *et al.*, 1995, Shi *et al.*, 2004). Furthermore, antibody staining revealed that Nr2e1 protein is localized in the cell nucleus (Li *et al.*, 2008).

In humans, detailed information about expression patterns is lacking; however, *NR2E1* transcripts are detected in adult tissues including the amygdala, caudate nucleus, cerebral cortex (including frontal lobe, occipital lobe, putamen, temporal lobe), corpus callosum, hippocampus, substantia nigra, subthalamic nucleus, and thalamus (Jackson *et al.*, 1998, Kumar *et al.*, 2008).

1.2.3 Targeted and spontaneous deletions of *Nr2e1* in mice

The use of *Nr2e1*-null mouse mutants has provided significant insight into the function of *Nr2e1*. Several laboratories have used homologous recombination to generate mice carrying deletions of exons two and three (Monaghan *et al.*, 1997) and exons three, four, and five (Yu *et al.*, 2000) of *Nr2e1*. Alternatively, the Simpson laboratory has reported on mice homozygous for the *Nr2e1^{frc}* allele, which is a spontaneous deletion of all nine exons of *Nr2e1* as well as its proximal promoter, without disruption of neighbouring genes (Figure 1.2) (Kumar *et al.*, 2004). These various *Nr2e1*-null mice present similar phenotypes and will be discussed as a whole below. The work in Chapter 3 was done using *Nr2e1^{frc/frc}* homozygous mice from the Simpson laboratory.
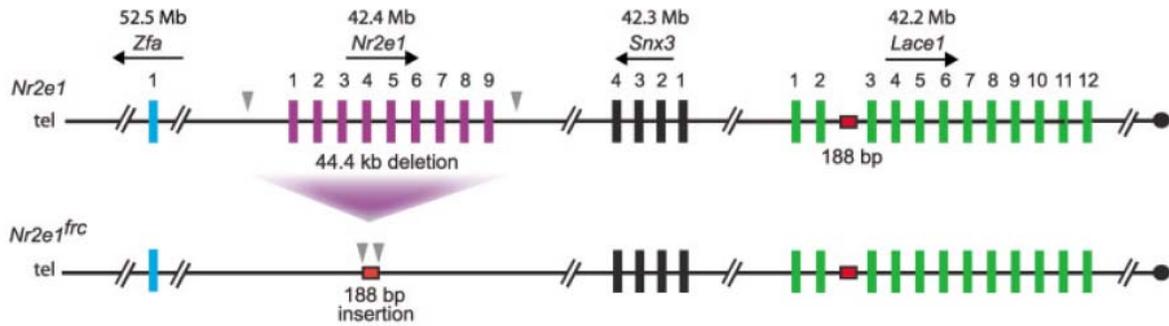
Figure 1.2 *Nr2e1^frc* deletion results in the loss of all *Nr2e1* exons
A schematic representation of Wt *Nr2e1* and *Nr2e1^frc* loci illustrating the 44.4 kb deletion of *Nr2e1* and the transposition of 188-bp sequence (red box) from *Lace1*. Grey arrowheads indicate deletion boundaries. Diagonal hatched lines represent discontinuous DNA sequence. Number above each gene indicates distance from the centromere. Horizontal arrows below each gene indicate transcriptional direction. Horizontal bars represent exons of each gene. (Modified from (Kumar *et al.*, 2004))

1.2.4 Role of *Nr2e1* in neurodevelopment and neurogenesis

The critical role of *Nr2e1* in normal neurodevelopment is obvious when one examines the extreme neuroanatomical phenotypes in *Nr2e1*-null mice. The earliest neurological phenotypes observed from E9.5 to E14.5 are increased staining of two panneural markers, Tuj1 and Map2, and a marker for Cajal-Retzius cells, Cr, in *Nr2e1*-null compared to wild-type (Wt) telencephalon; this increase in neuronal differentiation is attributable to shorter cell cycle as demonstrated using bromodeoxyuridine (BrdU) birthdating analysis (Roy *et al.*, 2004). By E12.5, *Nr2e1*-null mice show reduced populations of dorsal telencephalon progenitor-derived excitatory neurons and, ventrally, medial ganglionic eminence (MGE)-generated inhibitory interneurons (Roy *et al.*, 2004). This reduction in cell proliferation is also revealed by the flattening of the lateral ganglionic eminence (LGE) and MGE in the *Nr2e1*-null telencephalon by E12.5 (Roy *et al.*, 2004). After E14.5, depletion and slower cell division rate of *Nr2e1*-null neural progenitor cells result in reduction of the superficial layers

of the cortex, namely layers 2 and 3 (Li *et al.*, 2008, Roy *et al.*, 2004, Shi *et al.*, 2004, Sun *et al.*, 2007). Since TUNEL assay showed no difference in apoptosis between *Nr2e1*-null and Wt mice (Li *et al.*, 2008), the 20% reduction of neocortical thickness is a result of the inability of the *Nr2e1*-null progenitor cell population to be sustained throughout late prenatal development (Land & Monaghan, 2003). *Nr2e1* has been shown to be essential for patterning in the lateral telencephalon, in establishing the pallio-subpallial boundary through its interaction with *Pax6* (Stenman *et al.*, 2003a, Stenman *et al.*, 2003b). Recently, *in utero* electroporation studies also showed that *Nr2e1* has a role in regulating cell migration from the VZ into the intermediate zone and cortical plate during embryogenesis (Li *et al.*, 2008).

This deficit in the proliferative potential of *Nr2e1*-null progenitor cells is also evident in the adult mouse forebrain, where *Nr2e1*-null cells showed reduced proliferation and increased gliogenesis *in vitro* and *in vivo* (Shi *et al.*, 2004). Furthermore, these cellular phenotypes can be corrected by viral reintroduction of *Nr2e1 in vitro* (Shi *et al.*, 2004).

1.2.5 Genetic and protein interactions of *Nr2e1* in the brain

The mechanism by which *Nr2e1* exerts its control on cell proliferation and differentiation is by directly binding to the AAGTCA consensus sequence in the promoters of *Pten*, *Gfap*, *S100β*, and *Aqp4*, thereby repressing the expression of these genes (Shi *et al.*, 2004, Yu *et al.*, 2000, Zhang *et al.*, 2008). Nr2e1 has also shown direct binding to histone demethylase, LSD1 and histone deacetylases, HDAC3, 5, and 7, to recruit these protein complexes for transcription repression (Sun *et al.*, 2007, Yokoyama *et al.*, 2008). The level of *Nr2e1* is itself regulated by a negative feedback loop by microRNA-9 (miR-9) that binds to the 3′ UTR of the *Nr2e1* mRNA. The overexpression of miR-9 results in a decrease of *Nr2e1* transcripts leading to reduced proliferation, premature differentiation, and outward

migration of neural stem cells (Zhao *et al.*, 2009). Further analysis of the miR-9 locus also

identified multiple Nr2e1 binding sites downstream of the mature miR-9 sequence (Zhao *et al.*, 2009), supporting the role of Nr2e1 in repression of miR-9.

1.3 The lack of Nr2e1 results in adult neuroanatomical and behavioural abnormalities

1.3.1 Neuroanatomical anomalies

In the adult, gross neuroanatomical abnormalities can be seen in *Nr2e1*-null brains

including: hypoplasia of the cerebral cortex, olfactory bulb, hippocampus, corpus callosum

and amygdala; increased volume of the lateral ventricles; reduced thickness in superficial

cortical layers II and III; reduced population of excitatory neurons and inhibitory

interneurons; reduced neurogenesis in the dentate gyrus (DG) and subventricular zone

(SVZ); reduced dendritic branching of DG granule neurons, and long-term potentiation

(LTP) deficit in granule neurons of the DG (Christie *et al.*, 2006, Land & Monaghan, 2003,

Monaghan *et al.*, 1997, Roy *et al.*, 2004, Roy *et al.*, 2002, Shi *et al.*, 2004, Stenman *et al.*,

2003a, Stenman *et al.*, 2003b, Young *et al.*, 2002). *Nr2e1*-null mice also show slower weight

gain during development and small stature compared to Wt mice (Young *et al.*, 2002). The

characterization of DG granule neuron branching and LTP deficit was work I did in

collaboration with Dr. Brian Christie and the subsequent publication is presented in the

appendix of this thesis (Appendix A).

1.3.2 Behavioural abnormalities

Nr2e1-null mice exhibit various behavioural abnormalities. Most striking of these behaviours is their pathological aggression, with *Nr2e1*-null males often killing their siblings or intended mates (Young *et al.*, 2002). Depending upon strain background, *Nr2e1*-null females also showed aggression and poor maternal behaviour (Young *et al.*, 2002). When handled by humans, *Nr2e1*-null mice exhibit a 'hard to handle' phenotype, characterized by vocalization, struggling, jumping, and biting (Young *et al.*, 2002). Furthermore, impaired olfaction and vision were revealed during sensorimotor examination of *Nr2e1*-null mice (Young *et al.*, 2002). They also show reduced anxiety and memory for fear and hyperresponsiveness (Roy *et al.*, 2002).

More recently, conditional knockouts of *Nr2e1* have been analyzed to decipher the developmental versus adult role of *Nr2e1* in behaviour. Of particular interest are (1) mice deleted for the floxed *Nr2e1* allele using a tamoxifen-induced *cre* in the adult brain show significant reduction in stem cell proliferation that corresponds to impairments only in spatial learning, but not to contextual fear conditioning, locomotion, or diurnal rhythmic activities (Zhang *et al.*, 2008), and (2) mice deleted for the floxed *Nr2e1* allele using CaMKIIα-Cre during brain development but sparing the eye (eye phenotypes are discussed below) show reduced anxiety and aggression, but no impairment in fear conditioning and Morris water-maze compared to Wt mice (Belz *et al.*, 2007). These results suggest that disruptions in contextual fear conditioning, locomotion, or diurnal rhythmic activities are likely the result of developmental abnormalities and that learning and memory paradigms are dependent on reduced vision in *Nr2e1*-null mice (Belz *et al.*, 2007, Zhang *et al.*, 2008).

Interestingly, human *NR2E1*, with its endogenous promoter and regulatory regions, when reintroduced into *Nr2e1*-null mice has been shown to rescue the mutant neuroanatomical and behavioural phenotypes (Abrahams *et al.*, 2005). This result suggests that the regulation and function of human *NR2E1* is equivalent to that of mouse *Nr2e1*, which is supported by the high conservation observed at both the genomic and amino acid sequence level.

1.4 The importance of Nr2e1 in eye development

As mentioned previously, *Nr2e1* transcripts are detected at E8.5 in the optic evagination and are expressed in the mouse neural retina throughout development and into adulthood (Monaghan *et al.*, 1995). *Nr2e1* expression during early eye development has also been demonstrated in chicken (Yu *et al.*, 1994), *Xenopus* (Hollemann *et al.*, 1998), and Medaka (*Oryzias latipes*) (Nguyen *et al.*, 1999). Ectopic expression of the Nr2e1-DBD fused with the engrailed repressor domain in *Xenopus* showed reduced *Pax6* expression and inhibition of eye vesicle evagination (Hollemann *et al.*, 1998). In addition to the interaction of *Nr2e1* and *Pax6* in establishing boundaries in the brain (Stenman *et al.*, 2003a, Stenman *et al.*, 2003b), this is the second piece of evidence for an interaction between *Nr2e1* and *Pax6*, a gene that encodes for a transcription factor essential for normal vertebrate eye development (Grindley *et al.*, 1995, Ramaesh *et al.*, 2005).

Excess and/or deficiency of retinoic acid (RA) can also cause eye malformations (Cvekl & Wang, 2009, Fujieda *et al.*, 2009); and a *cis* element, named the silencing element relieved by TLX (SET), found in the RA receptor β2 (*RARβ2*) promoter supports a regulatory role for *Nr2e1* in the expression of *RARβ2* in the eye (Kobayashi *et al.*, 2000).

Furthermore, *Pax2*, a gene involved in both human and mouse retinal development, contains the *Nr2e1* consensus binding site in its promoter and is a direct target of *Nr2e1* (Yu *et al.*, 2000).

1.4.1 Adult eye anomalies in *Nr2e1*-null mice

Given that *Nr2e1* is expressed in the developing eye and the above evidence supporting its role in eye development, it is not surprising that *Nr2e1*-null adult mice have numerous ocular abnormalities. The adult neural retina consists of 5 layers: the outer nuclear layer (ONL), the outer plexiform layer (OPL), the inner nuclear layer (INL), the inner plexiform layer (IPL), and the ganglion cell layer (GCL) (Figure 1.3). Ocular phenotypes seen in *Nr2e1*-null mice include: optic nerve hypoplasia; retinal degeneration and dystrophy, especially the INL and the ONL, which are later forming; enhanced S-cone generation; shortened axons and dendrites of rods, cones, and bipolar, horizontal, and ganglion cells as evident by reduced thickness of the IPL, OPL, and photoreceptor outer segment (OS); impaired astrocyte network formation on the inner retinal surface; diminished retinal vascularization; impaired regression of hyaloid vessels; and reduced to flat electroretinogram (Miyawaki *et al.*, 2004, Young *et al.*, 2002, Yu *et al.*, 2000, Zhang *et al.*, 2006).
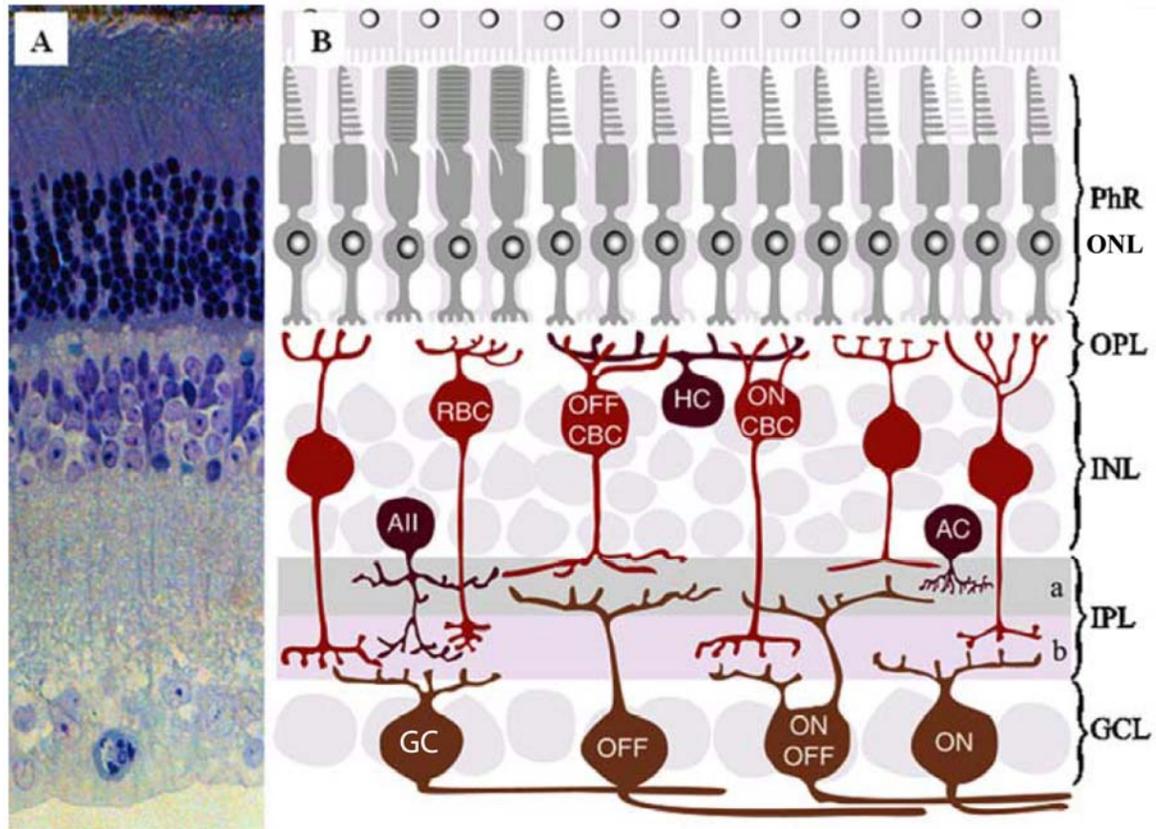
Figure 1.3 Cellular structure of mature mouse retina

(A) A cross section of an adult mouse retina. (B) A schematic representation of the layers and its cellular components. Cell bodies of photoreceptors (PhR; rods and cones) make up the outer nuclear layer (ONL). In the outer plexiform layer (OPL), PhR synapse with bipolar (RBC) and horizontal cells (HC). Cell bodies of RBC, HC, and amacrine cells (AC) are located in the inner nuclear layer (INL). In the inner plexiform layer (IPL), ganglion cells (GC) synapses with RBC, HC, and AC. The cell bodies of GC are located in the ganglion cell layer (GCL). (Modified from (Tian, 2004)).

1.4.2 Genetic and protein interactions of *Nr2e1* in the eye

Mechanistically, Nr2e1 acts in similar cellular processes in the eye and the brain. *Nr2e1* is expressed in retinal progenitor cells (RPCs) and regulates cell cycle progression by directly regulating *Pten* expression, which then dictates the levels of cyclinD1 and p27[Kip1] (Miyawaki *et al.*, 2004, Zhang *et al.*, 2006). In the mature retina, *Nr2e1* expression is restricted in Müller cells, glial cells of the eye, and is shown to be necessary for their proper development (Miyawaki *et al.*, 2004). Nr2e1 also recruits co-repressor Atrophin1 (Atn1) for coordinating retina-specific proliferation and differentiation (Wang *et al.*, 2006a, Zhang *et al.*, 2006). The expression of *Nr2e1* in retinal astrocytes can be regulated by oxygen concentration and is proposed to participate in the formation of proangiogenic scaffolds under hypoxic conditions (Uemura *et al.*, 2006).

1.4.3 The function of *Nr2e3*, a relative of *Nr2e1*, in the eye

The role of *Nr2e1* in eye development and disorders is further supported by the function of *Nr2e3* in eye. *Nr2e3*, also known as photoreceptor-specific nuclear receptor (PNR) is the closest relative to *Nr2e1*. *Nr2e3* is expressed in the photoreceptor layer of the neural retina during chick embryogenesis (Kobayashi *et al.*, 2008) and when mutated causes enhanced S-cone syndrome, a disorder of retinal cell fate determination (Akhmedov *et al.*, 2000, Corbo & Cepko, 2005, Escher *et al.*, 2009, Haider *et al.*, 2000, Schorderet & Escher, 2009).

1.5 The emerging role of Nr2e1 in cancer

Nr2e1 directly controls the expression of *Pten*, plays a critical role in regulating cell cycle, and has now been implicated in cancers, such as retinoblastomas and neurocytomas (Sim *et al.*, 2006, Yokoyama *et al.*, 2008). *Nr2e1* is expressed in Y79 retinoblastoma cells and acts as an inhibitor of *Pten* (Sun *et al.*, 2007, Yokoyama *et al.*, 2008). Overexpression of *Nr2e1* has also been found in neurocytoma (Sim *et al.*, 2006)

1.6 NR2E1: A candidate gene for bipolar disorder

1.6.1 Genetics of bipolar disoder

Bipolar disorder (BP) is mainly characterized by mood disturbances ranging from extreme elation (mania) to extreme depression with a lifetime prevalence of 0.4 to 1.6% (American Psychiatric Association., 2000). A manic episode is defined by at least 1 week (or less if hospitalization is required) of elevated, expansive, or irritable mood. This mood disturbance must be accompanied by at least three to four additional symptoms from a list that includes: inflated self-esteem or grandiosity, decreased need for sleep, pressure of speech, flight of ideas, distractibility, increased involvement in goal-directed activities (e.g. sexual and social behaviours) or psychomotor agitation, and excessive involvement in pleasurable activities with a high potential for painful consequences (American Psychiatric Association., 2000). A major depressive episode lasts a period of at least two weeks during which there is either depressed mood or the loss of interest or pleasure in nearly all activities, and may include persistent feelings of sadness, anxiety, guilty, anger, isolation, or hopelessness; disturbances in sleep and appetite; fatigue; problems concentrating; apathy or indifference; loss of interest in sexual activity; social anxiety; irritability; and morbid suicidal

ideation (American Psychiatric Association., 2000). There are two main subtypes of BP, bipolar I disorder (BPI) and bipolar II disorder (BPII). The clinical course for BPI is the occurrence of one or more manic episodes, and often also one or more major depressive episodes. Patients have to have one or more major depressive episodes accompanied by at least one hypomanic episode, a mild to moderate level of mania, for a diagnostic of BPII. The average age of onset for BP is 20 for both men and women, with BPII more common in women.

There are lines of evidence supporting a strong genetic influence for BP. Twin studies have shown high heritability for BP (60-85%) (Burmeister *et al.*, 2008) with concordance rates for monozygotic twins ranging from 40-97% and 5-38% for dizygotic twins (Angst *et al.*, 1980, Kieseppa *et al.*, 2004, Mcguffin *et al.*, 2003). Family studies show increased risk in first-degree relatives of individuals with BP to exhibit earlier age of onset and to develop BP and other related psychiatric disorders, including hypomania and schizoaffective disorder (Baron *et al.*, 1982, Gershon *et al.*, 1988, Kendler *et al.*, 1993, Maier *et al.*, 1993, Winokur *et al.*, 1982). Linkage studies of BP and other psychiatric disorders have also identified several reproducible loci of interest, including the 6q region containing *NR2E1* (Dick *et al.*, 2003, Hayden & Nurnberger, 2006, Kohn & Lerer, 2005, Mcqueen *et al.*, 2005, Middleton *et al.*, 2004, Pato *et al.*, 2005, Pato *et al.*, 2004, Schulze *et al.*, 2004). Because of the complex inheritance and other external factors underlying BP, causative genes are only beginning to be identified (Craddock & Sklar, 2009, Le-Niculescu *et al.*, 2009, Martinowich *et al.*, 2009, Ogden *et al.*, 2004).

1.6.2 Genetic support for *NR2E1* in brain disorders

Human *NR2E1* is mapped to chromosome location 6q21. In the largest meta-analysis of BP to date, this 108.5 Mb region (6q21-22) showed the highest LOD score (4.19) specifically for bipolar I disorder (BPI), the subtype dominated by mania (Figure 1.4) (Mcqueen *et al.*, 2005). A follow up study by this group identified a significant association between BPI and a single nucleotide polymorphism (SNP) near the solute carrier family 22, member 16 gene (SLC22A16) (Fan *et al.*). Under this same linkage peak, the Simpson laboratory found a significant association between a SNP in *NR2E1* (marker rs217520, for the A allele) and BPI (Table 1.1) (Kumar *et al.*, 2008). Novel regulatory mutations in *NR2E1* that were absent in controls were also identified in patients with impulsive-aggressive disorder, schizophrenia, BP, and microcephaly (Kumar *et al.*, 2007, Kumar *et al.*, 2008).
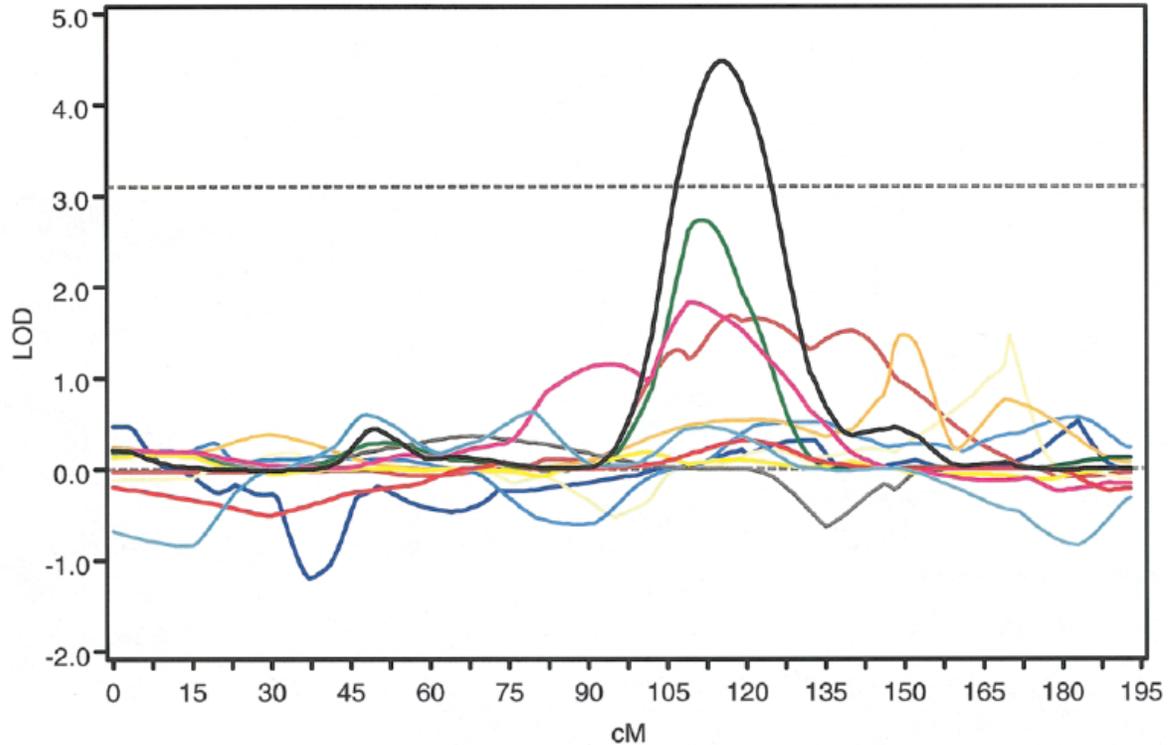
Figure 1.4 *NR2E1* located near a putative bipolar I disorder susceptibility locus

The highest LOD score to date (4.19) from pooled analysis of original genotype data from 11 BP genomewide linkage scans was identified at physical location 108.5 Mb (115 cM), a region close to where *NR2E1* maps (108.6 Mb). The LOD scores from the pooled analysis (solid black line) are overlaid with the LOD scores from the data set-specific analysis (solid non-black lines). Genomewide significance threshold (3.03) is indicated by the horizontal dotted line. (Modified from (Mcqueen *et al.*, 2005))

Table 1.1 Significant association between *NR2E1* SNP and bipolar I disorder

| Marker | Case-control | n[a] | Allele[b] | | χ^2 | OR (95% CI) | P | |
			A	C				
rs217520	Bipolar disorder (I and II)	374	417 (0.56)	331 (0.44)	6.11	0.77 (0.62–0.95)	0.013*	0.036*
	Bipolar I disorder	341	380 (0.56)	302 (0.44)	5.89	0.77 (0.62–0.96)	0.015*	0.041*
	Bipolar II disorder	34	37 (0.54)	31 (0.46)	1.54	0.73 (0.43–1.24)	0.215	
	Schizophrenia	376	438 (0.58)	314 (0.42)	2.26	0.85 (0.69–1.06)	0.133	
	Control	369	458 (0.62)	280 (0.38)	—	—	—	

[a]Number of subjects examined.
[b]Number of alleles; values in parenthesis refer to frequencies.
[c]g, numbering based on Antonarakis and the Nomenclature Working Group [1998], where A of the initiator Met codon in exon 1 is denoted nucleotide +1. Human genomic *NR2E1* sequence: NCBI AL078596.
*Significant P values.

(Modified from (Kumar *et al.*, 2008))

Furthermore, alterations in genes that interact with *NR2E1* have also been identifed in brain-behavioural disorders, including: *NURR1* (Buervenich *et al.*, 2000, Carmine *et al.*, 2003)*, PAX6* (Ellison-Wright *et al.*, 2004, Heyman *et al.*, 1999)*, RARβ2* (Van Neerven *et al.*, 2008)*, GFAP* (Barley *et al.*, 2009, Steffek *et al.*, 2008), and *S100β* (Schroeter *et al.*, 2009, Steiner *et al.*, 2006).

1.6.3 Role of neural stem/progenitor cells in brain disorders

The role of neural stem/progenitor cells has also been implicated in various neurological and psychiatric disorders, including BP. For example: neuroprotective effects can be triggered by deep brain stimulation treatment that increases proliferation in the dentate gyrus (Toda *et al.*, 2008); lithium treatment for mania in BPI acts through the Gsk3β pathway to induce neurogenesis (Wada *et al.*, 2005); and Parkinson's and Alzheimer's animal models have shown motor and cognitive improvement through stem cell implantation (Bjorklund & Lindvall, 2000, Wang *et al.*, 2006b). Since *Nr2e1* plays an important role in the regulation of neural stem/progenitor cells and brain development that results in abnormal behavioural phenotypes, *NR2E1* is both a strong positional and functional candidate for psychiatric disorders, especially BPI.

1.6.4 Different mouse "models" of bipolar disorder

The heterogeneity and complexity of behavioural traits represented in patients with BP is difficult, if not impossible, to accurately model in animals. Therefore, it is commonly accepted to study facets of this disease in rodent models (Einat, 2006a, Einat, 2006b). Since BP is a disorder diagnosed by abnormal behavioural traits, many current mouse models are supported by the presence of behavioural phenotypes exhibited in patients (Table 1.2). The

mania component of BP is often modeled in increased spontaneous and psychostimulant-induced hyperactivity, increased aggressive behaviours, and decreased anxiety-like behaviours (Einat & Manji, 2006). Depressive behaviours are measured in rodents as attempts to escape during tests such as the forced swim, tail suspension, and learned helplessness test. Cognitive impairments are also noted in some patients with BP, and therefore, are examined in rodent models using learning and memory tasks such as the Morris water maze, conditioned and passive avoidance, and fear conditioning.

Table 1.2 Mouse behavioural tests used to evaluate phenotypes similar to bipolar disorder symptoms

Bipolar disorder symptoms	Mouse behaviour tests
Facets of mania	
Increased energy and activity	Locomotor activity
Irritability	Vocal and physical reactions to minute stimuli; struggle
Reduced sleep	Measures of sleep
Aggression	Social interaction; resident-intruder
Increased sexual drive	Sexual behaviour
Response to drugs	Operant paradigms; conditioned place preference; sensitization
Hedonistic behaviour	Preference for reinforcement
Distractibility and reduced concentration	Learning tasks: Y-maze; Barnes maze; Morris water maze
Poor judgement (risk-taking)	Anxiety-like behaviour: elevated plus maze; open-field arena
Facets of depression	
Depression; despair	Learned helplessness: tail suspension; Porsolt forced swim
Sleep disturbances	Measures of sleep
Irritability	Vocal and physical reactions to minute stimuli; struggle
Distractibility and reduced concentration	Learning tasks: Y-maze; Barnes maze; Morris water maze
Social anxiety	Social interaction
Decreased sexual drive	Sexual behaviour

(Modified from (Einat, 2006b))

1.6.4.1 Genetic mouse models

Candidate genes of BP, identified in human linkage and genome-wide association studies, are being tested in genetic mouse models. There are several single-gene knockout and transgenic mice that have been useful in deciphering the involvement of these genes in

BP. Neuronal nitric oxide synthase (nNOS) metabolism has been suggested to contribute to pathogenesis and pathophysiology of BP (Bernstein *et al.*, 1998, Lauer *et al.*, 2005, Reif *et al.*, 2006). *nNOS* knockout mice have now been shown to exhibit hyperlocomotor activity, increased social behaviours, reduced depressive-like behaviours, and impaired spatial memory retention (Tanda *et al.*, 2009). Given the sleep disturbances and dysregulation in patients with BP, circadian rhythm genes have also been indicated in susceptibility of BP (Shi *et al.*, 2008). *Clock* mutant mice exhibit behaviours similar to those seen in patients with mania including hyperactivity, decreased sleep, reduced depression-like behaviour, lower anxiety, and enhanced behavioural responses to reward (e.g. cocaine, sucrose, and medial forebrain bundle stimulation; these behaviours were also attenuated by chronic administration of lithium (Roybal *et al.*, 2007). Transgenic mice overexpressing *glycogen synthase kinase 3β* (*Gsk3β*), a gene downregulated by lithium treatment, showed increased locomotor activity and acoustic startle response, and decreased habituation to the open field and to acoustic startle (Prickaerts *et al.*, 2006). Recently, reduced expression of *Disrupted in schizophrenia 1* (*Disc1*) has been shown to result in premature proliferation and differentiation of neuronal progenitors that can be compensated by treating with *Gsk3β* inhibitors (Mao *et al.*, 2009). Interestingly, mice expressing truncated Disc1 showed neurological abnormalities such as those seen in *Nr2e1*-null mutants, including: enlarged ventricles, reduced cerebral cortex, especially thinning of layers II/III, hypoplasia of corpus callosum and hippocampus, and reduced dendritic branching and length (Shen *et al.*, 2008). Behaviours of mice carrying *Disc1* mutations range from hyperactivity, increased immobility during depression-related tests, impaired conditioned response, and abnormal sensorimotor gating (Hikida *et al.*, 2007, Shen *et al.*, 2008).

1.6.4.2 Drug-induced model of hyperactivity

Another common approach to modeling mania in BP is the use of drugs, in particular a mixture of D-amphetamine and chlordiazepoxide, to induce hyperactivity in rodents (Aylmer et al., 1987, Gould et al., 2007). D-amphetamine/chlordiazepoxide-induced hyperactivity in rodents became a widely used model of manic behaviour because of its response to lithium treatment. Lithium, the drug of choice for treating BP, can attenuate this drug-induced hyperactivity without affecting spontaneous activity levels (Gould et al., 2001).

1.7 Thesis objectives

1.7.1 General hypothesis and sub-hypotheses

Work presented in this thesis tested the general hypothesis that variable levels of *Nr2e1* in mice, ranging from no expression to overexpression, will result in neurological, ocular, and gene expression phenotypes that reflect traits observed in human psychiatric and eye disorders. The first two chapters of this thesis focused on evaluating *Nr2e1$^{frc/frc}$* mice as a model for bipolar I disorder (BPI) and tested two sub-hypotheses. These sub-hypotheses were: (1) that dark-phase testing is more etiologically-correct and, therefore, will improve discrimination between genetically distinct mouse strains (Chapter 2); and (2) that *Nr2e1$^{frc/frc}$* mice will exhibit behavioural anomalies similar to those seen in some patients with BPI (Chapter 3). Based on *Nr2e1*-null brain and eye phenotypes, Chapter 4 evaluated the sub-hypothesis that *Nr2e1* overexpression will also result in dysmorphia of neuroanatomical and ocular development, and that target gene transcription levels will inversely correlate with *Nr2e1* levels.

1.7.2 Evaluation of $Nr2e1^{frc/frc}$ as a model for bipolar I disorder

Since *NR2E1* has been implicated in BPI and the *Nr2e1*-null mice have not yet been studied as a potential mouse model, this is the focus of the first two manuscript-based chapters. We anticipated that there might be subtle behavioural phenotypes in modeling aspects of BPI in mice, and therefore Chapter 2 evaluated the effect of light-phase versus dark-phase testing on detection of behavioural differences in genetically different inbred mouse strains to establish best practice standards to be used in Chapter 3. The focus of Chapter 3 was to use a battery of behavioural tests to examine $Nr2e1^{frc/frc}$ mice for behavioural traits used in other mouse models of BP, including activity levels, cognition, information processing, and cell proliferation in neurogenic regions. I also tested the effect of lithium treatment on these parameters to assess the pharmacological validity of this model.

1.7.3 Evaluation of overexpression of *Nr2e1* in mice

Mice lacking *Nr2e1* have been studied in detail by the Simpson laboratory and many others; however, the genetic, neurological, and ocular consequence of *Nr2e1* overexpression has not been examined. Our laboratory has previously established four random insertion transgenic strains, two carrying a bacterial artificial chromosome (BAC) containing mouse *Nr2e1* and two carrying a phage artificial chromosome (PAC) spanning human *NR2E1*. The strains carrying the PACs, when bred onto the fierce background, rescue the $Nr2e1^{frc/frc}$ phenotype to demonstrate functional conservation of mouse and human *NR2E1* (Abrahams *et al.*, 2005). In Chapter 4, I first quantified the expression of *Nr2e1* in these four transgenic strains and then further examined changes in transcript levels of genes previously known to be altered by the absence of *Nr2e1*. Gross neurological measurements and presence of eye phenotypes were also studied. The B6-bacEMS4A strain was chosen, based on *Nr2e1*

expression and showing the most affected gross neurological and eye phenotypes, for quantification of cell proliferation in neurogenic regions. Given the lack of *Nr2e1* overexpression in the B6-bacEMS4B strain and low penetrance of eye phenotypes in the PAC strains, detailed gene expression and histology of the eye were only performed on the B6-bacEMS4A strain.

1.8 References

Abrahams, B.S., Kwok, M.C., Trinh, E., Budaghzadeh, S., Hossain, S.M. & Simpson, E.M. (2005) Pathological aggression in "fierce" mice corrected by human nuclear receptor 2E1. *J Neurosci,* **25,** 6263-6270.

Abrahams, B.S., Mak, G.M., Berry, M.L., Palmquist, D.L., Saionz, J.R., Tay, A., Tan, Y.H., Brenner, S., Simpson, E.M. & Venkatesh, B. (2002) Novel vertebrate genes and putative regulatory elements identified at kidney disease and NR2E1/fierce loci. *Genomics,* **80,** 45-53.

Akhmedov, N.B., Piriev, N.I., Chang, B., Rapoport, A.L., Hawes, N.L., Nishina, P.M., Nusinowitz, S., Heckenlively, J.R., Roderick, T.H., Kozak, C.A., Danciger, M., Davisson, M.T. & Farber, D.B. (2000) A deletion in a photoreceptor-specific nuclear receptor mRNA causes retinal degeneration in the rd7 mouse. *Proc Natl Acad Sci U S A,* **97,** 5551-5556.

American Psychiatric Association. (2000) *Diagnostic and Statistical Manual of Mental Disorders IV Text Revision,* American Psychiatric Association.

Angst, J., Frey, R., Lohmeyer, B. & Zerbin-Rudin, E. (1980) Bipolar manic-depressive psychoses: results of a genetic investigation. *Hum Genet,* **55,** 237-254.

Armentano, M., Filosa, A., Andolfi, G. & Studer, M. (2006) COUP-TFI is required for the formation of commissural projections in the forebrain by regulating axonal growth. *Development,* **133,** 4151-4162.

Aylmer, C.G., Steinberg, H. & Webster, R.A. (1987) Hyperactivity induced by dexamphetamine/chlordiazepoxide mixtures in rats and its attenuation by lithium pretreatment: a role for dopamine? *Psychopharmacology (Berl),* **91,** 198-206.

23

Barley, K., Dracheva, S. & Byne, W. (2009) Subcortical oligodendrocyte- and astrocyte-associated gene expression in subjects with schizophrenia, major depression and bipolar disorder. *Schizophr Res,* **112,** 54-64.

Baron, M., Gruen, R., Asnis, L. & Kane, J. (1982) Schizoaffective illness, schizophrenia and affective disorders: morbidity risk and genetic transmission. *Acta Psychiatr Scand,* **65,** 253-262.

Belz, T., Liu, H.K., Bock, D., Takacs, A., Vogt, M., Wintermantel, T., Brandwein, C., Gass, P., Greiner, E. & Schutz, G. (2007) Inactivation of the gene for the nuclear receptor tailless in the brain preserving its function in the eye. *Eur J Neurosci,* **26,** 2222-2227.

Bernstein, H.G., Stanarius, A., Baumann, B., Henning, H., Krell, D., Danos, P., Falkai, P. & Bogerts, B. (1998) Nitric oxide synthase-containing neurons in the human hypothalamus: reduced number of immunoreactive cells in the paraventricular nucleus of depressive patients and schizophrenics. *Neuroscience,* **83,** 867-875.

Bjorklund, A. & Lindvall, O. (2000) Cell replacement therapies for central nervous system disorders. *Nat Neurosci,* **3,** 537-544.

Buervenich, S., Carmine, A., Arvidsson, M., Xiang, F., Zhang, Z., Sydow, O., Jonsson, E.G., Sedvall, G.C., Leonard, S., Ross, R.G., Freedman, R., Chowdari, K.V., Nimgaonkar, V.L., Perlmann, T., Anvret, M. & Olson, L. (2000) NURR1 mutations in cases of schizophrenia and manic-depressive disorder. *Am J Med Genet,* **96,** 808-813.

Burmeister, M., McInnis, M.G. & Zollner, S. (2008) Psychiatric genetics: progress amid controversy. *Nat Rev Genet,* **9,** 527-540.

Carmine, A., Buervenich, S., Galter, D., Jonsson, E.G., Sedvall, G.C., Farde, L., Gustavsson, J.P., Bergman, H., Chowdari, K.V., Nimgaonkar, V.L., Anvret, M., Sydow, O. &

Olson, L. (2003) NURR1 promoter polymorphisms: Parkinson's disease, schizophrenia, and personality traits. *Am J Med Genet B Neuropsychiatr Genet,* **120B,** 51-57.

Chen, Y.H., Tsai, M.T., Shaw, C.K. & Chen, C.H. (2001) Mutation analysis of the human NR4A2 gene, an essential gene for midbrain dopaminergic neurogenesis, in schizophrenic patients. *Am J Med Genet,* **105,** 753-757.

Christie, B.R., Li, A.M., Redila, V.A., Booth, H., Wong, B.K., Eadie, B.D., Ernst, C. & Simpson, E.M. (2006) Deletion of the nuclear receptor Nr2e1 impairs synaptic plasticity and dendritic structure in the mouse dentate gyrus. *Neuroscience,* **137,** 1031-1037.

Corbo, J.C. & Cepko, C.L. (2005) A hybrid photoreceptor expressing both rod and cone genes in a mouse model of enhanced S-cone syndrome. *PLoS Genet,* **1,** e11.

Craddock, N. & Sklar, P. (2009) Genetics of bipolar disorder: successful start to a long journey. *Trends Genet,* **25,** 99-105.

Cvekl, A. & Wang, W.L. (2009) Retinoic acid signaling in mammalian eye development. *Exp Eye Res,* **89,** 280-291.

Dick, D.M., Foroud, T., Flury, L., Bowman, E.S., Miller, M.J., Rau, N.L., Moe, P.R., Samavedy, N., El-Mallakh, R., Manji, H., Glitz, D.A., Meyer, E.T., Smiley, C., Hahn, R., Widmark, C., McKinney, R., Sutton, L., Ballas, C., Grice, D., Berrettini, W., Byerley, W., Coryell, W., DePaulo, R., MacKinnon, D.F., Gershon, E.S., Kelsoe, J.R., McMahon, F.J., McInnis, M., Murphy, D.L., Reich, T., Scheftner, W. & Nurnberger, J.I., Jr. (2003) Genomewide linkage analyses of bipolar disorder: a new

sample of 250 pedigrees from the National Institute of Mental Health Genetics

Initiative. *Am J Hum Genet,* **73,** 107-114.

Einat, H. (2006a) Establishment of a Battery of Simple Models for Facets of Bipolar

Disorder: A Practical Approach to Achieve Increased Validity, Better Screening and

Possible Insights into Endophenotypes of Disease. *Behav Genet.*

Einat, H. (2006b) Modelling facets of mania - new directions related to the notion of

endophenotypes. *J Psychopharmacol.*

Einat, H. & Manji, H.K. (2006) Cellular plasticity cascades: genes-to-behavior pathways in

animal models of bipolar disorder. *Biol Psychiatry,* **59,** 1160-1171.

Ellison-Wright, Z., Heyman, I., Frampton, I., Rubia, K., Chitnis, X., Ellison-Wright, I.,

Williams, S.C., Suckling, J., Simmons, A. & Bullmore, E. (2004) Heterozygous

PAX6 mutation, adult brain structure and fronto-striato-thalamic function in a human

family. *Eur J Neurosci,* **19,** 1505-1512.

Escher, P., Gouras, P., Roduit, R., Tiab, L., Bolay, S., Delarive, T., Chen, S., Tsai, C.C.,

Hayashi, M., Zernant, J., Merriam, J.E., Mermod, N., Allikmets, R., Munier, F.L. &

Schorderet, D.F. (2009) Mutations in NR2E3 can cause dominant or recessive retinal

degenerations in the same family. *Hum Mutat,* **30,** 342-351.

Fan, J., Ionita-Laza, I., McQueen, M.B., Devlin, B., Purcell, S., Faraone, S.V., Allen, M.H.,

Bowden, C.L., Calabrese, J.R., Fossey, M.D., Friedman, E.S., Gyulai, L., Hauser, P.,

Ketter, T.B., Marangell, L.B., Miklowitz, D.J., Nierenberg, A.A., Patel, J.K., Sachs,

G.S., Thase, M.E., Molay, F.B., Escamilla, M.A., Nimgaonkar, V.L., Sklar, P., Laird,

N.M. & Smoller, J.W. Linkage disequilibrium mapping of the chromosome 6q21-

22.31 bipolar I disorder susceptibility locus. *Am J Med Genet B Neuropsychiatr Genet,* **153B,** 29-37.

Fujieda, H., Bremner, R., Mears, A.J. & Sasaki, H. (2009) Retinoic acid receptor-related orphan receptor alpha regulates a subset of cone genes during mouse retinal development. *J Neurochem,* **108,** 91-101.

Gershon, E.S., DeLisi, L.E., Hamovit, J., Nurnberger, J.I., Jr., Maxwell, M.E., Schreiber, J., Dauphinais, D., Dingman, C.W., 2nd & Guroff, J.J. (1988) A controlled family study of chronic psychoses. Schizophrenia and schizoaffective disorder. *Arch Gen Psychiatry,* **45,** 328-336.

Gould, T.D., O'Donnell, K.C., Picchini, A.M. & Manji, H.K. (2007) Strain differences in lithium attenuation of d-amphetamine-induced hyperlocomotion: a mouse model for the genetics of clinical response to lithium. *Neuropsychopharmacology,* **32,** 1321-1333.

Gould, T.J., Keith, R.A. & Bhat, R.V. (2001) Differential sensitivity to lithium's reversal of amphetamine-induced open-field activity in two inbred strains of mice. *Behav Brain Res,* **118,** 95-105.

Grindley, J.C., Davidson, D.R. & Hill, R.E. (1995) The role of Pax-6 in eye and nasal development. *Development,* **121,** 1433-1442.

Haider, N.B., Jacobson, S.G., Cideciyan, A.V., Swiderski, R., Streb, L.M., Searby, C., Beck, G., Hockey, R., Hanna, D.B., Gorman, S., Duhl, D., Carmi, R., Bennett, J., Weleber, R.G., Fishman, G.A., Wright, A.F., Stone, E.M. & Sheffield, V.C. (2000) Mutation of a nuclear receptor gene, NR2E3, causes enhanced S cone syndrome, a disorder of retinal cell fate. *Nat Genet,* **24,** 127-131.

Hayden, E.P. & Nurnberger, J.I., Jr. (2006) Molecular genetics of bipolar disorder. *Genes Brain Behav,* **5,** 85-95.

Heyman, I., Frampton, I., van Heyningen, V., Hanson, I., Teague, P., Taylor, A. & Simonoff, E. (1999) Psychiatric disorder and cognitive function in a family with an inherited novel mutation of the developmental control gene PAX6. *Psychiatr Genet,* **9,** 85-90.

Hikida, T., Jaaro-Peled, H., Seshadri, S., Oishi, K., Hookway, C., Kong, S., Wu, D., Xue, R., Andrade, M., Tankou, S., Mori, S., Gallagher, M., Ishizuka, K., Pletnikov, M., Kida, S. & Sawa, A. (2007) Dominant-negative DISC1 transgenic mice display schizophrenia-associated phenotypes detected by measures translatable to humans. *Proc Natl Acad Sci U S A,* **104,** 14501-14506.

Hollemann, T., Bellefroid, E. & Pieler, T. (1998) The Xenopus homologue of the Drosophila gene tailless has a function in early eye development. *Development,* **125,** 2425-2432.

Jackson, A., Panayiotidis, P. & Foroni, L. (1998) The human homologue of the Drosophila tailless gene (TLX): characterization and mapping to a region of common deletion in human lymphoid leukemia on chromosome 6q21. *Genomics,* **50,** 34-43.

Kendler, K.S., McGuire, M., Gruenberg, A.M., O'Hare, A., Spellman, M. & Walsh, D. (1993) The Roscommon Family Study. I. Methods, diagnosis of probands, and risk of schizophrenia in relatives. *Arch Gen Psychiatry,* **50,** 527-540.

Kieseppa, T., Partonen, T., Haukka, J., Kaprio, J. & Lonnqvist, J. (2004) High concordance of bipolar I disorder in a nationwide sample of twins. *Am J Psychiatry,* **161,** 1814-1821.

Kobayashi, M., Hara, K., Yu, R.T. & Yasuda, K. (2008) Expression and functional analysis of Nr2e3, a photoreceptor-specific nuclear receptor, suggest common mechanisms in retinal development between avians and mammals. *Dev Genes Evol,* **218,** 439-444.

Kobayashi, M., Takezawa, S., Hara, K., Yu, R.T., Umesono, Y., Agata, K., Taniwaki, M., Yasuda, K. & Umesono, K. (1999) Identification of a photoreceptor cell-specific nuclear receptor. *Proc Natl Acad Sci U S A,* **96,** 4814-4819.

Kobayashi, M., Yu, R.T., Yasuda, K. & Umesono, K. (2000) Cell-type-specific regulation of the retinoic acid receptor mediated by the orphan nuclear receptor TLX. *Mol Cell Biol,* **20,** 8731-8739.

Kohn, Y. & Lerer, B. (2005) Excitement and confusion on chromosome 6q: the challenges of neuropsychiatric genetics in microcosm. *Mol Psychiatry,* **10,** 1062-1073.

Kumar, R.A., Chan, K.L., Wong, A.H., Little, K.Q., Rajcan-Separovic, E., Abrahams, B.S. & Simpson, E.M. (2004) Unexpected embryonic stem (ES) cell mutations represent a concern in gene targeting: lessons from "fierce" mice. *Genesis,* **38,** 51-57.

Kumar, R.A., Leach, S., Bonaguro, R., Chen, J., Yokom, D.W., Abrahams, B.S., Seaver, L., Schwartz, C.E., Dobyns, W., Brooks-Wilson, A. & Simpson, E.M. (2007) Mutation and evolutionary analyses identify NR2E1-candidate-regulatory mutations in humans with severe cortical malformations. *Genes Brain Behav,* **6,** 503-516.

Kumar, R.A., McGhee, K.A., Leach, S., Bonaguro, R., Maclean, A., Aguirre-Hernandez, R., Abrahams, B.S., Coccaro, E.F., Hodgins, S., Turecki, G., Condon, A., Muir, W.J., Brooks-Wilson, A.R., Blackwood, D.H. & Simpson, E.M. (2008) Initial association of NR2E1 with bipolar disorder and identification of candidate mutations in bipolar

disorder, schizophrenia, and aggression through resequencing. *Am J Med Genet B Neuropsychiatr Genet,* **147B,** 880-889.

Land, P.W. & Monaghan, A.P. (2003) Expression of the transcription factor, tailless, is required for formation of superficial cortical layers. *Cereb Cortex, 13,* 921-931.

Lauer, M., Johannes, S., Fritzen, S., Senitz, D., Riederer, P. & Reif, A. (2005) Morphological abnormalities in nitric-oxide-synthase-positive striatal interneurons of schizophrenic patients. *Neuropsychobiology,* **52,** 111-117.

Le-Niculescu, H., Patel, S.D., Bhat, M., Kuczenski, R., Faraone, S.V., Tsuang, M.T., McMahon, F.J., Schork, N.J., Nurnberger, J.I., Jr. & Niculescu, A.B., 3rd (2009) Convergent functional genomics of genome-wide association data for bipolar disorder: comprehensive identification of candidate genes, pathways and mechanisms. *Am J Med Genet B Neuropsychiatr Genet,* **150B,** 155-181.

Lee, J.S., Kim, K.I. & Baek, S.H. (2008) Nuclear receptors and coregulators in inflammation and cancer. *Cancer Lett*.

Li, W., Sun, G., Yang, S., Qu, Q., Nakashima, K. & Shi, Y. (2008) Nuclear receptor TLX regulates cell cycle progression in neural stem cells of the developing brain. *Mol Endocrinol,* **22,** 56-64.

Lutz, B., Kuratani, S., Cooney, A.J., Wawersik, S., Tsai, S.Y., Eichele, G. & Tsai, M.J. (1994) Developmental regulation of the orphan receptor COUP-TF II gene in spinal motor neurons. *Development,* **120,** 25-36.

Maglich, J.M., Sluder, A., Guan, X., Shi, Y., McKee, D.D., Carrick, K., Kamdar, K., Willson, T.M. & Moore, J.T. (2001) Comparison of complete nuclear receptor sets

from the human, Caenorhabditis elegans and Drosophila genomes. *Genome Biol,* **2,** RESEARCH0029.

Maier, W., Lichtermann, D., Minges, J., Hallmayer, J., Heun, R., Benkert, O. & Levinson, D.F. (1993) Continuity and discontinuity of affective disorders and schizophrenia. Results of a controlled family study. *Arch Gen Psychiatry,* **50,** 871-883.

Mangelsdorf, D.J., Thummel, C., Beato, M., Herrlich, P., Schutz, G., Umesono, K., Blumberg, B., Kastner, P., Mark, M., Chambon, P. & Evans, R.M. (1995) The nuclear receptor superfamily: the second decade. *Cell,* **83,** 835-839.

Mao, Y., Ge, X., Frank, C.L., Madison, J.M., Koehler, A.N., Doud, M.K., Tassa, C., Berry, E.M., Soda, T., Singh, K.K., Biechele, T., Petryshen, T.L., Moon, R.T., Haggarty, S.J. & Tsai, L.H. (2009) Disrupted in schizophrenia 1 regulates neuronal progenitor proliferation via modulation of GSK3beta/beta-catenin signaling. *Cell,* **136,** 1017-1031.

Martinowich, K., Schloesser, R.J. & Manji, H.K. (2009) Bipolar disorder: from genes to behavior pathways. *J Clin Invest,* **119,** 726-736.

McGuffin, P., Rijsdijk, F., Andrew, M., Sham, P., Katz, R. & Cardno, A. (2003) The heritability of bipolar affective disorder and the genetic relationship to unipolar depression. *Arch Gen Psychiatry,* **60,** 497-502.

McQueen, M.B., Devlin, B., Faraone, S.V., Nimgaonkar, V.L., Sklar, P., Smoller, J.W., Abou Jamra, R., Albus, M., Bacanu, S.A., Baron, M., Barrett, T.B., Berrettini, W., Blacker, D., Byerley, W., Cichon, S., Coryell, W., Craddock, N., Daly, M.J., Depaulo, J.R., Edenberg, H.J., Foroud, T., Gill, M., Gilliam, T.C., Hamshere, M., Jones, I., Jones, L., Juo, S.H., Kelsoe, J.R., Lambert, D., Lange, C., Lerer, B., Liu, J.,

Maier, W., Mackinnon, J.D., McInnis, M.G., McMahon, F.J., Murphy, D.L., Nothen, M.M., Nurnberger, J.I., Pato, C.N., Pato, M.T., Potash, J.B., Propping, P., Pulver, A.E., Rice, J.P., Rietschel, M., Scheftner, W., Schumacher, J., Segurado, R., Van Steen, K., Xie, W., Zandi, P.P. & Laird, N.M. (2005) Combined analysis from eleven linkage studies of bipolar disorder provides strong evidence of susceptibility loci on chromosomes 6q and 8q. *Am J Hum Genet,* **77,** 582-595.

Middleton, F.A., Pato, M.T., Gentile, K.L., Morley, C.P., Zhao, X., Eisener, A.F., Brown, A., Petryshen, T.L., Kirby, A.N., Medeiros, H., Carvalho, C., Macedo, A., Dourado, A., Coelho, I., Valente, J., Soares, M.J., Ferreira, C.P., Lei, M., Azevedo, M.H., Kennedy, J.L., Daly, M.J., Sklar, P. & Pato, C.N. (2004) Genomewide linkage analysis of bipolar disorder by use of a high-density single-nucleotide-polymorphism (SNP) genotyping assay: a comparison with microsatellite marker assays and finding of significant linkage to chromosome 6q22. *Am J Hum Genet,* **74,** 886-897.

Miyawaki, T., Uemura, A., Dezawa, M., Yu, R.T., Ide, C., Nishikawa, S., Honda, Y., Tanabe, Y. & Tanabe, T. (2004) Tlx, an orphan nuclear receptor, regulates cell numbers and astrocyte development in the developing retina. *J Neurosci,* **24,** 8124-8134.

Monaghan, A.P., Bock, D., Gass, P., Schwager, A., Wolfer, D.P., Lipp, H.P. & Schutz, G. (1997) Defective limbic system in mice lacking the tailless gene. *Nature,* **390,** 515-517.

Monaghan, A.P., Grau, E., Bock, D. & Schutz, G. (1995) The mouse homolog of the orphan nuclear receptor tailless is expressed in the developing forebrain. *Development,* **121,** 839-853.

Nguyen, V., Deschet, K., Henrich, T., Godet, E., Joly, J.S., Wittbrodt, J., Chourrout, D. & Bourrat, F. (1999) Morphogenesis of the optic tectum in the medaka (Oryzias latipes): a morphological and molecular study, with special emphasis on cell proliferation. *J Comp Neurol,* **413,** 385-404.

Ogden, C.A., Rich, M.E., Schork, N.J., Paulus, M.P., Geyer, M.A., Lohr, J.B., Kuczenski, R. & Niculescu, A.B. (2004) Candidate genes, pathways and mechanisms for bipolar (manic-depressive) and related disorders: an expanded convergent functional genomics approach. *Mol Psychiatry,* **9,** 1007-1029.

Pato, C.N., Middleton, F.A., Gentile, K.L., Morley, C.P., Medeiros, H., Macedo, A., Azevedo, M.H. & Pato, M.T. (2005) Genetic linkage of bipolar disorder to chromosome 6q22 is a consistent finding in Portuguese subpopulations and may generalize to broader populations. *Am J Med Genet B Neuropsychiatr Genet,* **134,** 119-121.

Pato, C.N., Pato, M.T., Kirby, A., Petryshen, T.L., Medeiros, H., Carvalho, C., Macedo, A., Dourado, A., Coelho, I., Valente, J., Soares, M.J., Ferreira, C.P., Lei, M., Verner, A., Hudson, T.J., Morley, C.P., Kennedy, J.L., Azevedo, M.H., Daly, M.J. & Sklar, P. (2004) Genome-wide scan in Portuguese Island families implicates multiple loci in bipolar disorder: fine mapping adds support on chromosomes 6 and 11. *Am J Med Genet B Neuropsychiatr Genet,* **127,** 30-34.

Pignoni, F., Baldarelli, R.M., Steingrimsson, E., Diaz, R.J., Patapoutian, A., Merriam, J.R. & Lengyel, J.A. (1990) The Drosophila gene tailless is expressed at the embryonic termini and is a member of the steroid receptor superfamily. *Cell,* **62,** 151-163.

Prickaerts, J., Moechars, D., Cryns, K., Lenaerts, I., van Craenendonck, H., Goris, I., Daneels, G., Bouwknecht, J.A. & Steckler, T. (2006) Transgenic mice overexpressing glycogen synthase kinase 3beta: a putative model of hyperactivity and mania. *J Neurosci,* **26,** 9022-9029.

Ramaesh, T., Ramaesh, K., Martin Collinson, J., Chanas, S.A., Dhillon, B. & West, J.D. (2005) Developmental and cellular factors underlying corneal epithelial dysgenesis in the Pax6+/- mouse model of aniridia. *Exp Eye Res,* **81,** 224-235.

Reif, A., Strobel, A., Jacob, C.P., Herterich, S., Freitag, C.M., Topner, T., Mossner, R., Fritzen, S., Schmitt, A. & Lesch, K.P. (2006) A NOS-III haplotype that includes functional polymorphisms is associated with bipolar disorder. *Int J Neuropsychopharmacol,* **9,** 13-20.

Roy, K., Kuznicki, K., Wu, Q., Sun, Z., Bock, D., Schutz, G., Vranich, N. & Monaghan, A.P. (2004) The Tlx gene regulates the timing of neurogenesis in the cortex. *J Neurosci,* **24,** 8333-8345.

Roy, K., Thiels, E. & Monaghan, A.P. (2002) Loss of the tailless gene affects forebrain development and emotional behavior. *Physiol Behav,* **77,** 595-600.

Roybal, K., Theobold, D., Graham, A., DiNieri, J.A., Russo, S.J., Krishnan, V., Chakravarty, S., Peevey, J., Oehrlein, N., Birnbaum, S., Vitaterna, M.H., Orsulak, P., Takahashi, J.S., Nestler, E.J., Carlezon, W.A., Jr. & McClung, C.A. (2007) Mania-like behavior induced by disruption of CLOCK. *Proc Natl Acad Sci U S A,* **104,** 6406-6411.

Schorderet, D.F. & Escher, P. (2009) NR2E3 mutations in enhanced S-cone sensitivity syndrome (ESCS), Goldmann-Favre syndrome (GFS), clumped pigmentary retinal degeneration (CPRD), and retinitis pigmentosa (RP). *Hum Mutat*.

Schroeter, M.L., Abdul-Khaliq, H., Krebs, M., Diefenbacher, A. & Blasig, I.E. (2009) Neuron-specific enolase is unaltered whereas S100B is elevated in serum of patients with schizophrenia--original research and meta-analysis. *Psychiatry Res,* **167,** 66-72.

Schulze, T.G., Buervenich, S., Badner, J.A., Steele, C.J., Detera-Wadleigh, S.D., Dick, D., Foroud, T., Cox, N.J., MacKinnon, D.F., Potash, J.B., Berrettini, W.H., Byerley, W., Coryell, W., DePaulo, J.R., Jr., Gershon, E.S., Kelsoe, J.R., McInnis, M.G., Murphy, D.L., Reich, T., Scheftner, W., Nurnberger, J.I., Jr. & McMahon, F.J. (2004) Loci on chromosomes 6q and 6p interact to increase susceptibility to bipolar affective disorder in the national institute of mental health genetics initiative pedigrees. *Biol Psychiatry,* **56,** 18-23.

Shen, S., Lang, B., Nakamoto, C., Zhang, F., Pu, J., Kuan, S.L., Chatzi, C., He, S., Mackie, I., Brandon, N.J., Marquis, K.L., Day, M., Hurko, O., McCaig, C.D., Riedel, G. & St Clair, D. (2008) Schizophrenia-related neural and behavioral phenotypes in transgenic mice expressing truncated Disc1. *J Neurosci,* **28,** 10893-10904.

Shi, J., Wittke-Thompson, J.K., Badner, J.A., Hattori, E., Potash, J.B., Willour, V.L., McMahon, F.J., Gershon, E.S. & Liu, C. (2008) Clock genes may influence bipolar disorder susceptibility and dysfunctional circadian rhythm. *Am J Med Genet B Neuropsychiatr Genet,* **147B,** 1047-1055.

Shi, Y., Chichung Lie, D., Taupin, P., Nakashima, K., Ray, J., Yu, R.T., Gage, F.H. & Evans, R.M. (2004) Expression and function of orphan nuclear receptor TLX in adult neural stem cells. *Nature,* **427,** 78-83.

Sim, F.J., Keyoung, H.M., Goldman, J.E., Kim, D.K., Jung, H.W., Roy, N.S. & Goldman, S.A. (2006) Neurocytoma is a tumor of adult neuronal progenitor cells. *J Neurosci, 26,* 12544-12555.

Steffek, A.E., McCullumsmith, R.E., Haroutunian, V. & Meador-Woodruff, J.H. (2008) Cortical expression of glial fibrillary acidic protein and glutamine synthetase is decreased in schizophrenia. *Schizophr Res, 103,* 71-82.

Steiner, J., Bielau, H., Bernstein, H.G., Bogerts, B. & Wunderlich, M.T. (2006) Increased cerebrospinal fluid and serum levels of S100B in first-onset schizophrenia are not related to a degenerative release of glial fibrillar acidic protein, myelin basic protein and neurone-specific enolase from glia or neurones. *J Neurol Neurosurg Psychiatry, 77,* 1284-1287.

Stenman, J., Yu, R.T., Evans, R.M. & Campbell, K. (2003a) Tlx and Pax6 co-operate genetically to establish the pallio-subpallial boundary in the embryonic mouse telencephalon. *Development, 130,* 1113-1122.

Stenman, J.M., Wang, B. & Campbell, K. (2003b) Tlx controls proliferation and patterning of lateral telencephalic progenitor domains. *J Neurosci, 23,* 10568-10576.

Sun, G., Yu, R.T., Evans, R.M. & Shi, Y. (2007) Orphan nuclear receptor TLX recruits histone deacetylases to repress transcription and regulate neural stem cell proliferation. *Proc Natl Acad Sci U S A, 104,* 15282-15287.

Tanda, K., Nishi, A., Matsuo, N., Nakanishi, K., Yamasaki, N., Sugimoto, T., Toyama, K., Takao, K. & Miyakawa, T. (2009) Abnormal social behavior, hyperactivity, impaired remote spatial memory, and increased D1-mediated dopaminergic signaling in neuronal nitric oxide synthase knockout mice. *Mol Brain, 2,* 19.

Tian, N. (2004) Visual experience and maturation of retinal synaptic pathways. *Vision Res,* **44,** 3307-3316.

Toda, H., Hamani, C., Fawcett, A.P., Hutchison, W.D. & Lozano, A.M. (2008) The regulation of adult rodent hippocampal neurogenesis by deep brain stimulation. *J Neurosurg,* **108,** 132-138.

Uemura, A., Kusuhara, S., Wiegand, S.J., Yu, R.T. & Nishikawa, S. (2006) Tlx acts as a proangiogenic switch by regulating extracellular assembly of fibronectin matrices in retinal astrocytes. *J Clin Invest,* **116,** 369-377.

van Neerven, S., Kampmann, E. & Mey, J. (2008) RAR/RXR and PPAR/RXR signaling in neurological and psychiatric diseases. *Prog Neurobiol,* **85,** 433-451.

Wada, A., Yokoo, H., Yanagita, T. & Kobayashi, H. (2005) Lithium: potential therapeutics against acute brain injuries and chronic neurodegenerative diseases. *J Pharmacol Sci,* **99,** 307-321.

Wang, L., Rajan, H., Pitman, J.L., McKeown, M. & Tsai, C.C. (2006a) Histone deacetylase-associating Atrophin proteins are nuclear receptor corepressors. *Genes Dev,* **20,** 525-530.

Wang, Q., Matsumoto, Y., Shindo, T., Miyake, K., Shindo, A., Kawanishi, M., Kawai, N., Tamiya, T. & Nagao, S. (2006b) Neural stem cells transplantation in cortex in a mouse model of Alzheimer's disease. *J Med Invest,* **53,** 61-69.

Wang, Z., Benoit, G., Liu, J., Prasad, S., Aarnisalo, P., Liu, X., Xu, H., Walker, N.P. & Perlmann, T. (2003) Structure and function of Nurr1 identifies a class of ligand-independent nuclear receptors. *Nature,* **423,** 555-560.

Winokur, G., Tsuang, M.T. & Crowe, R.R. (1982) The Iowa 500: affective disorder in relatives of manic and depressed patients. *Am J Psychiatry,* **139,** 209-212.

Yang, X., Downes, M., Yu, R.T., Bookout, A.L., He, W., Straume, M., Mangelsdorf, D.J. & Evans, R.M. (2006) Nuclear receptor expression links the circadian clock to metabolism. *Cell,* **126,** 801-810.

Yokoyama, A., Takezawa, S., Schule, R., Kitagawa, H. & Kato, S. (2008) Transrepressive function of TLX requires the histone demethylase, LSD1. *Mol Cell Biol*.

Young, K.A., Berry, M.L., Mahaffey, C.L., Saionz, J.R., Hawes, N.L., Chang, B., Zheng, Q.Y., Smith, R.S., Bronson, R.T., Nelson, R.J. & Simpson, E.M. (2002) Fierce: a new mouse deletion of Nr2e1; violent behaviour and ocular abnormalities are background-dependent. *Behav Brain Res,* **132,** 145-158.

Yu, R.T., Chiang, M.Y., Tanabe, T., Kobayashi, M., Yasuda, K., Evans, R.M. & Umesono, K. (2000) The orphan nuclear receptor Tlx regulates Pax2 and is essential for vision. *Proceedings of the National Academy of Sciences USA,* **97,** 2621-2625.

Yu, R.T., McKeown, M., Evans, R.M. & Umesono, K. (1994) Relationship between Drosophila gap gene tailless and a vertebrate nuclear receptor Tlx. *Nature,* **370,** 375-379.

Zetterstrom, R.H., Solomin, L., Jansson, L., Hoffer, B.J., Olson, L. & Perlmann, T. (1997) Dopamine neuron agenesis in Nurr1-deficient mice. *Science,* **276,** 248-250.

Zhang, C.L., Zou, Y., He, W., Gage, F.H. & Evans, R.M. (2008) A role for adult TLX-positive neural stem cells in learning and behaviour. *Nature,* **451,** 1004-1007.

Zhang, C.L., Zou, Y., Yu, R.T., Gage, F.H. & Evans, R.M. (2006) Nuclear receptor TLX prevents retinal dystrophy and recruits the corepressor atrophin1. *Genes Dev,* **20,** 1308-1320.

Zhao, C., Sun, G., Li, S. & Shi, Y. (2009) A feedback regulatory loop involving microRNA-9 and nuclear receptor TLX in neural stem cell fate determination. *Nat Struct Mol Biol,* **16,** 365-371.

Chapter 2: The dark phase improves genetic discrimination for some high throughput mouse behavioural phenotyping[1]

2.1 Introduction

Behaviour testing in mice is undergoing a rapid evolution as genetically modified and chemically mutated mice are being applied to the field. Now is the time to set the standards for test conditions (Brown *et al.*, 2000, Crabbe *et al.*, 1999, Crawley & Paylor, 1997, Van Der Staay & Steckler, 2002, Würbel, 2002). An important and often overlooked parameter is the effect of light-dark (L/D) cycle (Wahlsten, 2001). Mice are nocturnal animals and thus more active in the dark phase (Whishaw *et al.*, 1999). Ironically, most researchers conduct behaviour testing during the day, when mice are normally sleeping and less active (Marques & Waterhouse, 1994) and in the light, a condition mice normally avoid. Although convenient, this practice is ethologically incorrect. The alternative is to test mice in the dark phase. Some of the inconvenience of dark-phase testing can be minimized through the use of reverse light cycle (lights on 23:00 hr to 11:00), dim red light, and low-light level camera - but is the effort warranted?

The importance of dark-phase test conditions may depend on the type of testing being done. We consider mouse behavioural phenotyping to consist of a continuum of situations with three principle nodes.

The first is the 'classical' testing situation, paralleling many rat studies, in which a strain is fully characterized and at least three tests purported to measure a specific attribute

---

[1] A version of this chapter has been published. Hossain, S.M., Wong, B.K.Y., Simpson, E.M. (2004) The Dark Phase Improves Genetic Discrimination for Some High Throughput Mouse Behavioral Phenotyping. Genes, Brain, and Behavior 3(3): 167-77. [PMID 15140012]

are applied before a conclusion regarding the strain's ability or psychosocial state is drawn. Such studies are often combined with brain analyses that reveal features supportive of the conclusion. Often such classical testing is driven by a specific hypothesis regarding the interaction of brain and behaviour. Examples of classical testing would include the Morris water task to assess learning and memory, or the elevated plus maze to assess anxiety, both performed with pretest conditioning or training and no particular concern for throughput. Although not always done, from an ethological standpoint, it makes sense to conduct these tests in the dark since the purpose is to learn about the abilities and state of the strain. Previous experimental findings demonstrate that dark-phase testing may affect the outcome. For example, behavioural responses such as emotional reactivity, acoustic startle response, memory performance, and locomotor activity were influenced by lighting conditions (Kopp, 2001, Valentinuzzi *et al.*, 2000). During a water tank social interaction test, mice were more willing to wade in search of food in the dark phase than in the light phase (Nejdi *et al.*, 1996).

The second is the 'mutant versus wild type' testing situation. In such a situation the test battery is often not sufficiently comprehensive to permit strong conclusions about overall abilities or psychosocial states. In contrast, the panel of tests, some of which may have been adapted for high throughput, is designed to identify a phenotypic difference between two cohorts of mice that differ by only one modified gene. Often there is no a priori hypothesis and the search is focused on finding a test that can discriminate mutant and wild type. A positive result from such a study would be appropriately followed up with a 'classical' test situation before a strong conclusion about ability or psychosocial state could be made. Although the effect of dark-phase testing in the mutant versus wild type test situation has not been thoroughly studied, its value has been demonstrated. Discrimination between wild type

and mutant mice by wheel running activity was observed only in dark-phase testing (Kriegsfeld *et al.*, 1999).

The third is the 'screening' test situation. Such a situation has developed out of the application of mouse behaviour to the world of genomics; as exemplified by quantitative trait loci analyses and ENU mutagenesis. These applications require screening thousands of genetically variant mice to identify unknown phenotypes using high throughput phenotyping, with the goal of rapid discrimination of rare outliers. For this work, tests such as the SHIRPA primary screen (Rogers *et al.*, 1997), coupled with non-invasive high throughput assays for major behavioural domains (e.g. open field), are employed to allow rapid assessments and identification of a subset of mice worth further study. Such studies are resource-driven and conclusions about the ability or psychosocial state of the animal cannot be appropriately made. However, with heritability testing and the generation of a cohort of mice, testing situations mutant versus wild type and classical can subsequently be applied. The value of dark-phase testing in the screening situation has not been investigated.

Since the importance of ethological correctness and the effect of L/D cycle on high throughput behavioural tests, such as those required of 'mutant versus wild type' and 'screening' situations, are poorly characterized or unknown, we set out to test two hypotheses: 1) Dark-phase testing affects the outcome of high throughput behavioural tests, and 2) dark-phase testing improves discrimination between genetically distinct mice using high throughput behavioural tests. Our study includes an initial assessment of home cage activity and the following behavioural tests conducted in a high throughput manner: open-field, SHIRPA primary screen, social interaction, social recognition, rotarod, tail-flick, and hot-plate test performed on three strains: C57BL/6J (B6) inbred, 129S1/SvImJ (129) inbred,

and B6129F1 (F1) hybrid. The tests were chosen for their value in screening genetically diverse mice for both physical and social behaviours. The strains were chosen for their importance in genomic and genetic studies (Silva *et al.*, 1997). B6 mice were previously selected for genome sequencing and 129 mice are widely used for targeted mutagenesis in ES cells; both strains are recommended for behavioural phenotyping (Paigen & Eppig, 2000, Silva *et al.*, 1997). The mixed B6129 background is the most commonly used background for the generation of transgenic mice; we chose B6129F1 since F1 mice provide both genetic and phenotypic uniformity, as well as hybrid vigor (Dierssen *et al.*, 2002). Importantly, the goal of this report was not to characterize the strains themselves but to explore the interaction of test conditions and discrimination power.

2.2 Methods and materials

2.2.1 Mouse facility

All mice were born, reared, and tested in the pathogen-free behaviour suite under reverse L/D cycle (light 23:00-11:00 h at 320 lux), at the Centre for Molecular Medicine & Therapeutics, Vancouver, Canada. The three-room behaviour suite consists of a breeding room and a dedicated testing room, separated by an anteroom. The lighting in all three rooms was synchronized. Care was taken not to expose the mice to any inappropriate light, even during testing. When light was needed by the investigator during experiments in the dark phase, a dim red light (8 lux) was used. Since limited color vision renders mice insensitive to red light at wavelengths >630 nm (Jacobs *et al.*, 1999), phase was not disturbed (Crawley, 2000). The mice were maintained at $20 \pm 2°C$ with relative humidity of $50 \pm 5\%$ and had food and water ad libitum.

2.2.2 Mice

Behavioural testing was started at 12 weeks of age on 168 test mice (24 for home cage activity and 72 each for experiment 1 and 2). The 168 mice represented 56 from each strain (C57BL/6J (JAX®00664) (B6), 129S1/SvImJ (JAX®02448) (129), and B6129F1 (F1)). An additional 24 mice, 8 from each strain (12 female and 12 male, 8 months old ± 1 week) were used as target animals in the social interaction test (experiment 1). All test mice and target mice were weaned at 18 days of age and then individually housed in polycarbonate cages (28x17x12 cm). A further 99 prewean pups B6129F2 at 11-17 days old were used as the stimulus "same" (n=31) or "different" (n=68) animal in the social recognition test (experiment 2). Handling of all mice was minimized.

2.2.3 Testing procedures

To test the phase conditions, home cage activity was measured in 24 mice (4 females and 4 males from each strain) for 24 hours. Eight individually housed mice were tested at a time.

In experiment 1, 72 mice were divided into two sets: 36 mice always tested in a 3-hour period (6:00-9:00 h) in the light phase (18 each in groups 1 and 3) and 36 mice always tested in a 3-hour period (18:00-21:00 h) in the dark phase (18 each in groups 2 and 4). All four groups were matched for strain and sex. Groups 1 and 2 underwent open-field testing and SHIRPA primary screening on day 1 (Fig. 2.1). Groups 3 and 4 underwent the same testing on day 2. The social interaction test was performed on groups 1, 2 and groups 3, 4 on days 3 and 4, respectively. The rotarod test was performed on day 5 for all four groups. The tail-flick test was conducted on day 7. The testing order for strain and sex was based on a

constrained randomized sequence. The order of tests was chosen such that the procedures most likely to be affected by prior handling were conducted first. All mice were handled by the tail. A single investigator conducted all tests.
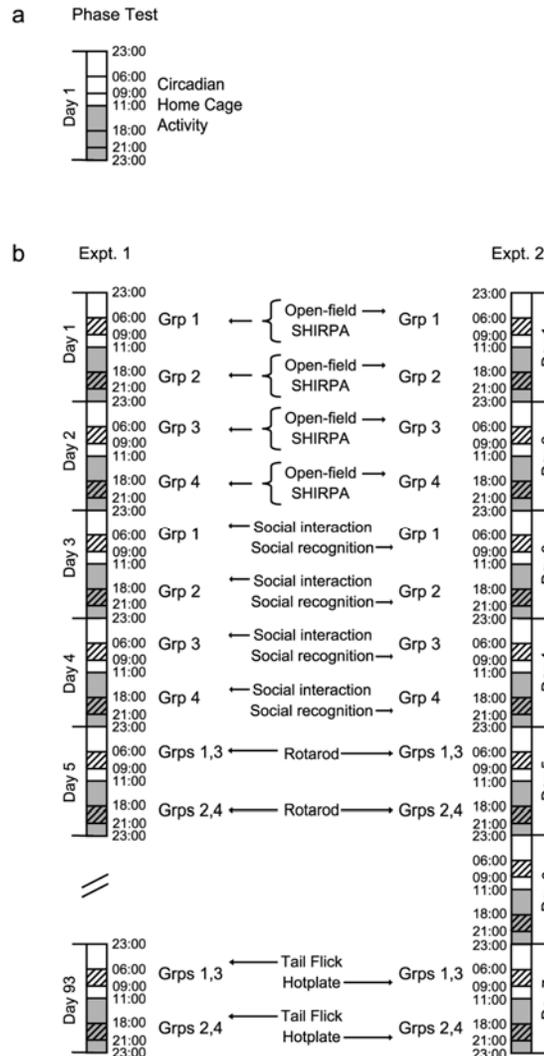
Figure 2.1 One room, two test times

Protocol for comparing L/D cycle effects under reverse light cycle (lights on at 2300 hr. and off at 1100 hr.). a) The phase test was designed to validate the testing conditions used. b) Experiments 1 and 2 were a similar battery of tests conducted on different sets of mice. Groups were tested during the same relative 3-hour period, 7 hrs after a lighting change and 2 hrs before the next lighting change. The light phase is indicated in white, dark phase in grey; the test periods are hatched.

In experiment 2, the experimental design from experiment 1 was repeated with a different set of 72 mice and a modified set of tests. The open-field test was repeated with a modified protocol but the SHIRPA was not repeated. The social interaction test was replaced by the social recognition test, the rotarod test was repeated with a modified protocol, and the tail-flick test was replaced with the hot-plate analgesia test.

Each behaviour-testing session began at 6:00 h (for light-phase mice) and 18:00 h (for dark-phase mice). Thus, the tests were conducted during a 3-hour period beginning 7 h after the onset of a new lighting phase and completed 2 h before the onset of the next phase (Figs. 2.1 and 2.2). At the start of each test session, an assistant transported all required mice from the breeding room to the anteroom at one time on a mobile cart. Mice stayed in their home cages in the anteroom with food and water available at all times until they were tested so as not be exposed to other mice being tested. After testing, each mouse was immediately returned to the anteroom. Before each mouse, all equipment was cleaned with 70% ethanol except for the SHIRPA primary screen, where Clidox (Pharmacal Research Laboratory Inc., Naugatuck, CT) was used.

2.2.4 Home cage activity

Home cage activity was measured using eight identical Cage Rack Systems (San Diego Instruments, San Diego, CA). Each mouse home cage is placed in the center of a metal cage rack frame that generates a uniformly spaced 8 x 4 photobeam grid. The mice were provided with food and water and spontaneous locomotor activity was measured by counting the total number of beam breaks each hour during the 24-hour period (Kopp, 2001).

2.2.5 Open-field test

Spontaneous exploratory locomotor activity was measured by the open-field test (Slow *et al.*, 2003) using a digiscan photocell-equipped automated open-field apparatus (Med Associates, St. Albans, VT). In experiment 1, all mice were tested in the same open field apparatus 27.5L x 27.5W x 20H cm with lower and upper beams at 1.5 cm and 5.5 cm from floor, respectively. In experiment 2, half the mice were tested in a second open field apparatus 27.3L x 27.3W x 20H cm with lower and upper beams at 1.5 cm and 3.6 cm from floor, respectively. Computer software was used to define two zones: the center 16 x 16 cm (center zone), and the surrounding periphery (residual zone). Each mouse was placed in the center zone of the novel arena and allowed to explore for 3 min while the software tallied spatially identified beam breaks. The following parameters were derived separately for the central and residual zones: distance traveled, ambulatory counts (consecutive interruption of at least four beams within 0.5 sec), time of ambulation, stereotypic counts (number of beam breaks within a virtual 'box' of a 4 x 4 beam), time of stereotypic counts, time of rest, vertical counts, and vertical time. The number of jumps in either zone was also recorded.

Since our aim was to examine spontaneous exploratory locomotor activity, and not to subject the mice to a strongly anxiogenic situation, standard room illumination was used during the open-field test in experiment 1 in the light phase. However, to test the hypothesis that a strong anxiogenic situation such as open field with an illuminated center would increase the strain discrimination in the light phase, we added a 60-w bulb 30 cm above the arena in experiment 2. The lighting conditions in the dark phase were the same in experiments 1 and 2.

2.2.6 SHIRPA primary screen

The SHIRPA primary screen is a battery of high throughput tests that provides a behavioural and functional profile based on 40 separate parameters observed for each mouse. The SHIRPA screen was conducted 5 minutes after the open-field test, one mouse at a time. The tests followed the SHIRPA protocol primary screen as described by the mouse mutagenesis consortium partners including observations of defecation and urination, but excluding the measure of body length (Rogers *et al.*, 1997).

2.2.7 Social interaction test

The social interaction test evaluates the ethological response of a test mouse to natural conflicts experienced during an encounter with a target mouse in a neutral arena. All encounters occurred in the arena of the open-field apparatus and were recorded by low-light video camera (Panasonic, model AG-5710). Recordings were scored using video analysis software (Observer Video Pro, Noldus, The Netherlands). A test mouse, and then a target mouse, was placed in the centre zone of the arena. Partners only met at the time of testing. The number of social events towards an introduced target mouse was recorded for 3 min. Each target mouse was used for three consecutive tests and then retired. The behavioural responses to the target mouse were classified as either social or non-social, based on ethological profiles (Calamandrei *et al.*, 2000). Social responses were sniffing (sniffing the anogenital region, head, or snout of the partner), following the partner around the cage, without any quick or sudden movement, push under (pushing the snout or the whole anterior part of the body under the partner's body, and then resting), and crawl over (crawling over the partner's back, crossing it transversally from one side to the other). Non-social responses were exploring (moving around, rearing, sniffing the air and the walls), and self-grooming

(wiping, licking, combing or scratching any part of own body). The non-social response of immobility (laying flat, sitting, or standing still) was also measured.

2.2.8 Social recognition test

The social recognition test measures the ability of the test mouse to recognize a familiar mouse as measured by a reduction in social investigation time between the first and second encounters. Using a modification of the procedure described by Engelmann *et. al* (Engelmann *et al.*, 1995), the test consisted of a 5-min learning trial during which a novel pup was introduced into the home cage of the test mouse, and the time spent by the test mouse on investigating the pup was measured. Social investigation was defined as the tip of the nose being within approximately 10 mm of the pup and accompanied by sniffing or anogenital investigation. The number of aggressive behaviours towards the pup (tail rattle, attack, biting) was also recorded. The pups were then isolated in individual small plastic cages with paper towel. After a 30-min interval, the test mouse is exposed to either the same or novel pup for 5 min. Observations were recorded by low-light video camera (Panasonic, model AG-5710, Matsuhita Electric Co. of America, Los Angeles, CA). Recordings were scored using video analysis software (Observer Video Pro, Noldus, The Netherlands).

2.2.9 Rotarod test

Motor coordination and balance, and motor learning were measured with the rotarod test as previously described (Slow *et al.*, 2003). The rotating drum (San Diego Instruments, San Diego, CA) accelerated at a constant rate from 0 to 45 rpm over 2 minutes (experiment 1) or 1 minute (experiment 2). Mice were tested in squads of four. Mice were submitted to stationary training (non-moving rod) for 60 sec to adapt to the environment before receiving

four consecutive trials with a 3-minute interval between each trial. After a 1-hour rest, a final test was given. In each trial and test, the latency to fall off the rotarod was recorded. Mice clinging on to the rod and rotating for three consecutive rotations were scored as a fall. Motor coordination and balance was scored as the mean latency of the four trials. Motor learning was defined as the test score minus trial 1 score.

2.2.10 Tail-flick test

Pain sensitivity in mice was measured with the tail-flick test (Crawley *et al.*, 2003) using an automated tail-flick analgesia meter (Columbus Instruments, Columbus, OH). Mice were placed in a clear restraining tube (Model 33033, Columbus Instruments) and the tail was placed freely on a level surface between two photo detector panels. Immediately after a 90-sec habituation, radiant heat from a 20-V beam of light was focused on the ventral surface of the tail and the time for the mouse to flick its tail away from the surface was automatically recorded. A 10 sec cut-off time was employed to prevent tissue damage. The average of two consecutive trials, separated by 1 min interval, was calculated.

2.2.11 Hot-plate test

The thermal nociceptive threshold in mice was assessed using a hot plate apparatus (Columbus Instruments, Columbus, OH). Mice were placed on a hot plate thermostatically set at $55.0 \pm 0.5 \,°C$ (Crawley *et al.*, 2003). The latency of first licking or kicking of the fore or hind paws was recorded. A cut-off time of 60 sec was employed to avoid tissue damage. The average of two consecutive trials, separated by 1 min interval, was calculated.

2.2.12 Statistical analysis

All data were analyzed using SPSS® statistical package (SPSS, Chicago, IL). Data from the home cage activity were analyzed by repeated measures ANOVA.

Data from the SHIRPA, open field, and social interaction tests were subjected to discriminant analysis separately for the light and dark phases. Discriminant functions, which are linear composites of the original parameters, were defined by Eigenvalues > 1 and Wilk's lambda $p<0.05$ in the classification matrix. These functions were used to discriminate between the strains. The ability of a test to discriminate between strains was evaluated by the spread in the data and the relative position of and the distances between group centroids. Data were validated with the "leave one out" cross validation procedure.

The home cage activity, social interaction, social recognition, rotarod, hot-plate, and tail-flick data were analyzed with a multifactorial ANOVA for sex, phase, and strain. For all tests, no effect of sex was found so this factor was dropped from the analyses. Multivariate analyses found no effect of which apparatus was used in open field testing for experiment 2 and no effect of which of the 24 target mice was used in the social interaction test in experiment 1. Discrimination was defined as a significant difference between strains within a phase using multifactorial post hoc analyses.

2.3 Results

2.3.1 Home cage activity showed expected diurnal patterns in response to reverse L/D cycle

As expected, the home cage activity of the three strains showed a typical diurnal pattern of increased activity levels during the dark phase (Whishaw *et al.*, 1999) (Fig. 2.2a). The sum of beam breaks during the 3-hour period chosen for behaviour testing showed a significant increase in activity level during the dark phase for all three strains (Fig. 2.2b). Thus, we conclude that the mice were responding appropriately to the reverse L/D cycle.
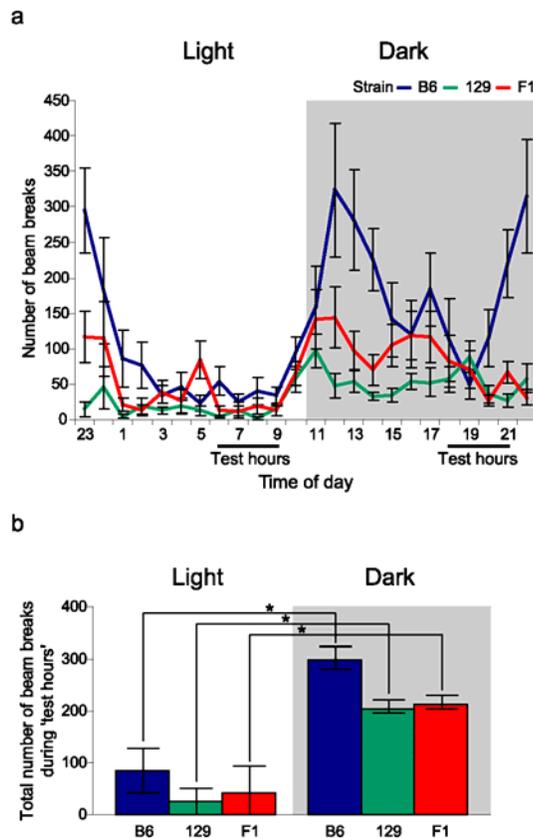
Figure 2.2 Home cage activity is affected by L/D cycle

a) More beam breaks occur in the dark phase than in the light phase as summed every hour over 24 hours. b) Sum of beam breaks during the 3-hour test period confirms higher activity in the dark phase for all three strains, thus validating the test conditions. *p<0.004. N = 4 per strain/sex.

2.3.2 Open-field test discriminates better in the dark phase

Discriminant analysis included all seventeen parameters measured by the open field to define two significant functions for the dark phase data (Function 1 (F1), Eigenvalue 23.72, Wilks' lambda significance <0.001; F2, Eigenvalue 8.2, Wilks' lambda significance <0.001), but only one function for the light phase data in experiment 1 (light phase = room lighting) (F1, Eigenvalue 12.53, Wilks' lambda significance <0.001) (Fig. 2.3, experiment 1). Furthermore, the cross validation of parameters led to 100 % reclassification of original grouped cases in the dark phase, whereas in the light phase the reclassification was 94.4%. Thus, the dark phase provided better discrimination between strains than the light phase, as is demonstrated by the relative position of and distance between centroids on discriminant function plots (Fig. 2.4, experiment 1).

| | Experiment 1 | | | | Experiment 2 | | | |
| | Light | | Dark | | Light | | Dark | |
	F1	F2	F1	F2	F1	F2	F1	F2
Eigenvalues	12.53	1.07	23.72	8.2	28.41	0.97	15.26	2.79
Canonical correlation	0.962	0.720	0.980	0.944	0.983	0.702	0.969	0.858
Wilks' Lambda	0.036	0.482	0.004	0.109	0.017	0.507	0.016	0.264
Wilks' Lambda Significance	<0.001	0.311	<0.001	<0.001	<0.001	0.387	<0.001	0.007
Ambulatory Count (Center)	*0.484*	0.038	*0.604*	0.169	*0.453*	0.243	*0.674*	0.036
Distance Traveled (Center)	*0.420*	0.017	*0.555*	0.097	*0.395*	0.201	*0.506*	0.003
Jump Count	*0.639*	0.324	*0.496*	-0.219	*0.297*	0.088	*0.331*	-0.276
Time of Ambulation (Center)	*0.446*	-0.005	*0.447*	0.348	-0.249	*0.315*	*0.565*	0.153
Time of Rest (Residual)	0.143	*0.311*	*0.309*	-0.238	0.196	*0.494*	*0.208*	-0.204
Vertical Count (Residual)	*0.478*	-0.153	*0.304*	0.081	-0.062	*0.343*	*0.168*	-0.092
Stereotypic Count (Center)	-0.184	*0.252*	*0.278*	0.229	-0.213	*0.351*	0.209	*0.246*
Vertical Count (Center)	*0.401*	-0.127	*0.244*	0.071	-0.088	*0.194*	*0.162*	-0.045
Vertical Time (Residual)	*0.414*	-0.189	*0.239*	0.085	-0.102	*0.382*	*0.230*	-0.066
Ambulatory Count (Residual)	*0.239*	0.190	*0.212*	-0.039	-0.149	*0.157*	*0.392*	-0.235
Vertical Time (Center)	-0.331	*0.366*	*0.185*	0.061	-0.097	*0.139*	*0.163*	-0.048
Distance Traveled (Residual)	-0.187	*0.219*	*0.141*	-0.052	-0.126	*0.133*	*0.345*	0.061
Time of Stereotypic Counts (Residual)	-0.006	*0.246*	*0.127*	-0.117	*0.085*	-0.036	-0.022	*0.041*
Time of Ambulation (Residual)	*0.170*	0.169	*0.058*	-0.049	-0.096	*0.181*	*0.171*	-0.057
Time of Stereotypic Counts (Center)	-0.083	*0.297*	-0.217	*0.268*	-0.165	*0.394*	0.150	*0.254*
Time of Rest (Center)	0.127	*0.370*	-0.060	*0.201*	-0.047	*0.337*	0.001	*0.162*
Stereotypic Count (Residual)	-0.054	*0.232*	0.085	*0.114*	*0.044*	0.012	0.019	*0.036*

Figure 2.3 The open-field test discriminates better in the dark phase
Discriminant analysis performed on the 17 parameters measured by the open field defined two significant functions for the dark phase data, but only one significant function for the light phase data in both experiment 1 (light phase = room light) and experiment 2 (light phase = bright light) based on Eigenvalues > 1 and p<0.05 for Wilk's lambda. Correlation coefficients for parameters used to define function 1 (F1) and function 2 (F2) are shown in bold italic text. The functions are defined by all 17 parameters measured. N = 6 per strain/sex/phase for each experiment.

To test the possibility of improving the strain discrimination in the light phase, the open-field test was repeated in experiment 2 using the stronger anxiogenic situation of brighter illumination during light-phase testing. However, discriminant analysis again defined two significant functions for the dark phase data (F1, Eigenvalue 15.26, Wilks' lambda significance <0.001; F2, Eigenvalue 2.79, Wilks' lambda significance 0.007), but only one function for the light phase data (F1, Eigenvalue 28.41, Wilks' lambda significance <0.001) (Fig. 2.3, experiment 2). Furthermore, the cross validation of parameters led to 100

% reclassification of original grouped cases in the dark phase versus 86.1% in the light phase. Thus, increased illumination of the open field did not improve strain discrimination in the light phase as is demonstrated by the relative position of and distance between centroids on discriminant function plots (Fig. 2.4, experiment 2). We conclude that open-field testing discriminates strains better in the dark phase.
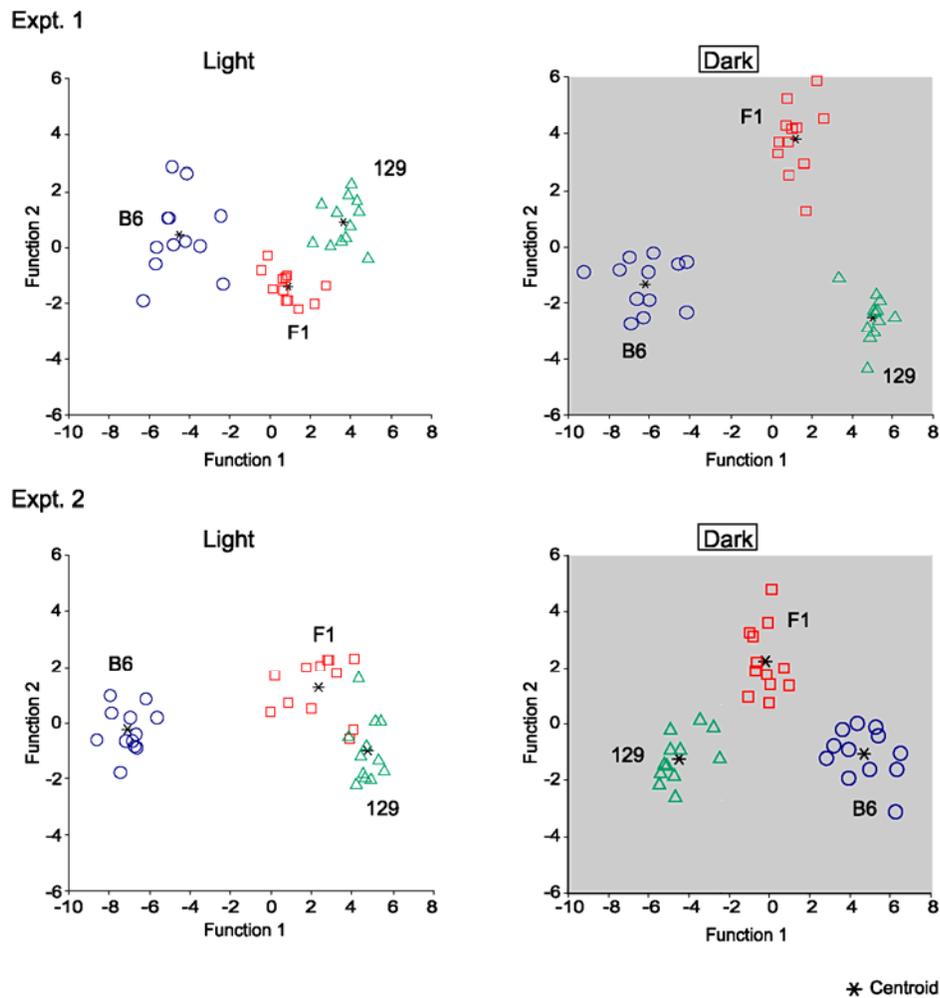
Figure 2.4 Discriminant function plots of open-field data show improved strain discrimination in the dark phase

Experiment 1: discrimination between strains for function 1 and 2 is better in the dark phase, as demonstrated by the relative position of and distances between group centroids.
Experiment 2: The bright lighting conditions used during the light phase of experiment 2 did not significantly improve discrimination in the light phase. The better phase is indicated by a box. N = 6 per strain/sex/phase for each experiment.

2.3.3 SHIRPA primary screen discriminates better in the dark phase

Discriminant analysis performed on the 41 SHIRPA parameters successfully defined two significant functions for both the dark-phase (F1, Eigenvalue 87.037, Wilks' lambda significance <0.001; F2, Eigenvalue 10.954, Wilks' lambda significance <0.001) and light-phase data (F1, Eigenvalue 25.07, Wilks' lambda significance <0.001; F2, Eigenvalue 7.895, Wilks' lambda significance 0.002) (Fig. 2.5). However, the cross validation of parameters led to 91.7 % reclassification of original grouped cases in the dark phase versus only 63.9% in the light phase. In addition, the relative position of and distance between centroids on discriminant function plots showed improved discrimination in the dark phase (Fig. 2.6). Furthermore, the dark phase only required 21 parameters versus 24 for the light phase to define discriminant functions. Thus, we conclude that SHIRPA data discriminate strains better in the dark phase. Interestingly, in either phase, only approximately half the parameters measured were used.

| | Experiment 1 | | | |
| | Light | | Dark | |
	F1	F2	F1	F2
Eigenvalue	25.07	7.895	87.037	10.954
Canonical Correlation	0.981	0.942	0.994	0.957
Wilks' Lambda	0.004	0.112	0.001	0.084
Wilks' Lambda Significance	<0.001	0.002	<0.001	<0.001
Spontaneous Activity	*0.281*	0.048	*-0.246*	-0.036
Fear	*-0.349*	0.189	*0.154*	0.113
Locomotor Activity	*0.199*	-0.090	*-0.144*	0.029
Transfer Arousal	*0.173*	-0.075	*-0.142*	0.071
Toe Pinch	*0.126*	0.080	*-0.138*	0.039
Grip Strength	0.138	*-0.209*	*-0.126*	0.117
Touch Escape	0.130	*-0.248*	*-0.125*	0.006
Positional Passivity	*-0.217*	-0.204	*0.120*	-0.052
Provoked Biting	*0.108*	0.099	*-0.115*	-0.109
Startle Response	0.071	*-0.115*	*-0.075*	-0.068
Limb Tone	*0.147*	0.129	*-0.075*	-0.068
Visual Placing	-0.046	*-0.113*	*0.062*	-0.017
Tail Elevation	0.119	*0.199*	-0.236	*0.477*
Aggression	*0.107*	-0.027	-0.142	*0.240*
Irritability	*0.107*	-0.027	-0.112	*0.228*
Body Weight	0.033	*-0.127*	-0.005	*-0.092*
Catalepsy	-0.017	*-0.028*	0.015	*-0.091*
Urination	*0.070*	0.061	-0.019	*0.085*
Defecation	0.053	*0.103*	-0.049	*-0.079*
Vocalization	*0.024*	-0.013	0.003	*0.074*
Body Temperature	0.010	*-0.100*	0.022	*-0.052*
Wire Maneuver	*-0.070*	0.038		
Tremor	-0.003	*0.147*		
Body Position	0.036	*0.060*		

Figure 2.5 The SHIRPA primary screen discriminates better in the dark phase

Discriminant analysis performed on the 41 parameters measured by the SHIRPA data defined two significant functions in both the light and dark phases based on Eigenvalues > 1 and p<0.05 for Wilk's lambda. Correlation coefficients for parameters used to define function 1 (F1) and function 2 (F2) are shown in bold italic text. The functions are defined by 24 parameters in the light phase but only 21 in the dark phase. N = 6 per strain/sex/phase for each experiment.
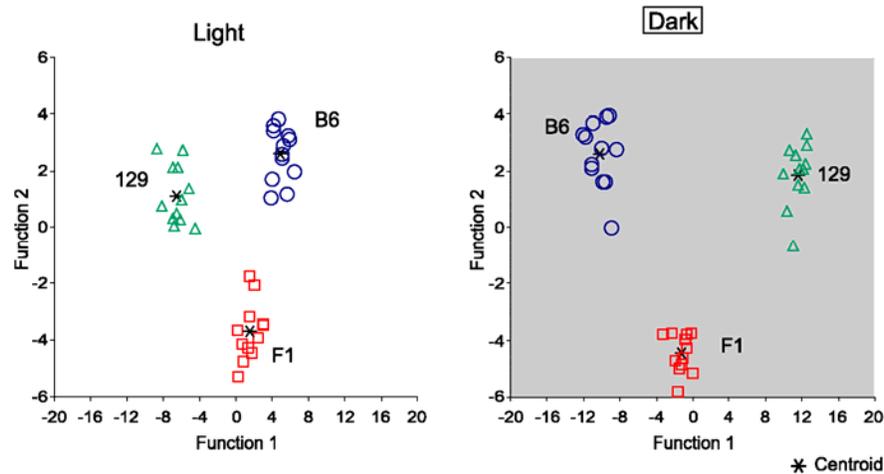
Figure 2.6 Discriminant function plots of SHIRPA data show improved strain discrimination in the dark phase

Discrimination between strains for both functions is better in the dark phase, as demonstrated by the relative position of and distances between group centroids. The better phase is indicated by a box. N = 6 per strain/sex/phase.

2.3.4 Social interaction test is not improved by the dark phase

Discriminant analysis of the social interaction data failed to define any significant functions. However, the multifactorial ANOVA indicated significant effects of phase for self grooming ($p<0.04$), sniffing ($p<0.04$), and immobility ($p<0.001$); and effects of strain for self grooming ($p<0.006$), sniffing ($p=0.001$), immobility ($p<0.03$), and exploring ($p<0.001$). No significant effects on push under were found. Three parameters for B6 mice (self grooming, crawl over, and immobility), and two parameters for 129 mice (sniffing and immobility), gave significantly different results between the light and dark phases; these mice showed more self grooming, more social interactions, and less immobility in the dark phase (Fig. 2.7). F1 mice were not significantly affected by phase. Discrimination between strains did not show a clear benefit to either phase. Three of the parameters (self grooming, crawl over, and exploring) showed better discrimination in the dark phase and three parameters (sniffing,

following, and immobility) showed better discrimination in the light phase. Thus, although

the social interaction test is affected by L/D cycle, there is no clear advantage to dark-phase

testing.
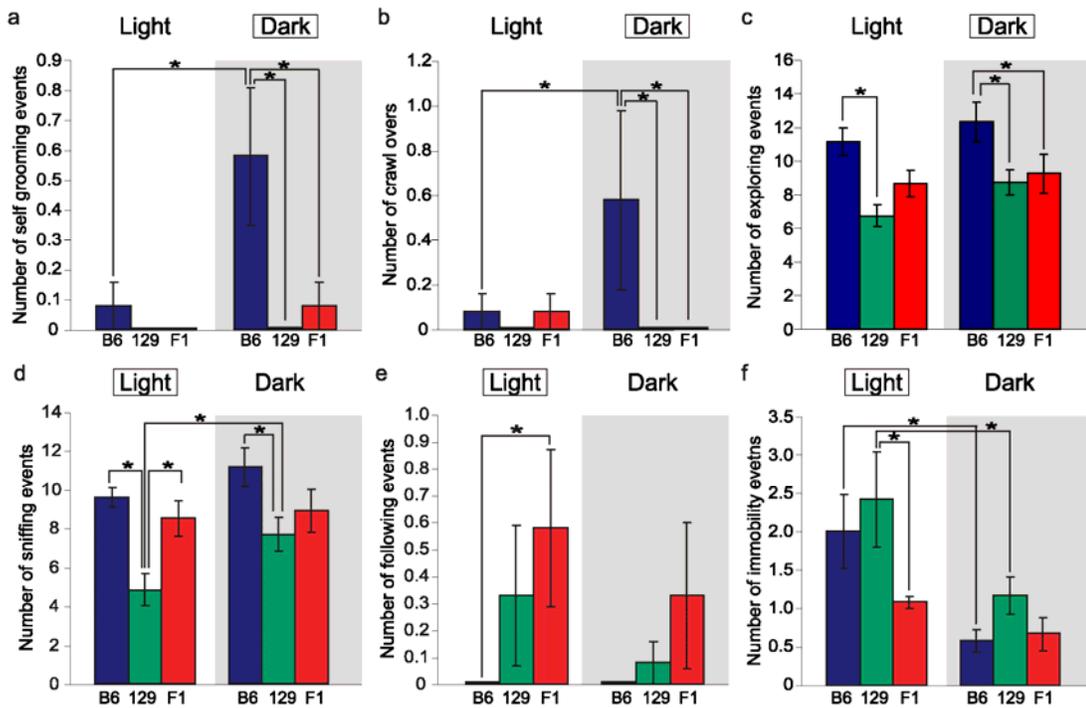
Figure 2.7 The social interaction test was affected by L/D cycle but discrimination was not clearly better in one phase than the other

The six of the seven parameters measured that showed significant effect of phase or strain are shown here. Phase was a significant effect for a, b, d, and f. Three parameters for B6 mice (a,b,f) and two parameters for 129 mice (d,f) gave significantly different results between the light and dark phases; these mice showed more self grooming, more social interactions, and less immobility in the dark phase. The F1 mice were not significantly affected by phase. Discrimination between strains did not show a clear benefit to either phase. Three parameters showed better discrimination in the dark phase (a-c) but three showed better discrimination in the light phase (d-f). The better phase is indicated by a box. $*p<0.04$. N = 6 per strain/sex/phase.

59

2.3.5 Social Recognition test is not improved by the dark phase

Because the social interaction test failed to show a clear advantage to testing in either phase, we examined the effects of dark-phase testing on a second high throughput test for social behaviour, the social recognition test. This test assesses a mouse's ability to recognize a familiar pup upon a second encounter as measured by a reduction in time spent investigating it. The multifactorial ANOVA found no effect of phase or strain. However, since the difference in investigation time between the first and second encounter for the 'same' pup failed to reach statistical significance for all three strains for both phases (data not shown), we conclude that the test did not work. Therefore, no conclusions can be drawn about the effects of phase. We hypothesize the test failure may be due to the age of the pups used, which may have been too old (11-17 days) and thus perceived by the test mice as intruders. In fact, we did note a significant difference in frequency ($p < 0.05$) and duration ($p < 0.05$) of aggressive behaviours between strains in the dark phase by Kruskal-Wallis ranked sums test and noted the highest score means for the F1 mice.

2.3.6 The rotarod test discriminates better in the dark phase

In experiment 1, no differences in performance (motor coordination and balance), as assessed by the mean latency to fall from the rod during four trials, were observed between the light and dark phases for any of the three strains (Fig. 2.8a). A multifactorial ANOVA found an effect of strain ($p < 0.001$) but not phase. Performance was significantly different between all three strains in both light and dark phases.

Motor learning, as assessed by the difference between the final test score minus the first trial, also showed an effect of strain ($p < 0.009$) but not of phase. However, dark phase

testing did improve the test's ability to discriminate between strains; the 129 mice tested in

the dark phase showed significantly better learning than both B6 and F1 mice (Fig. 2.8b).
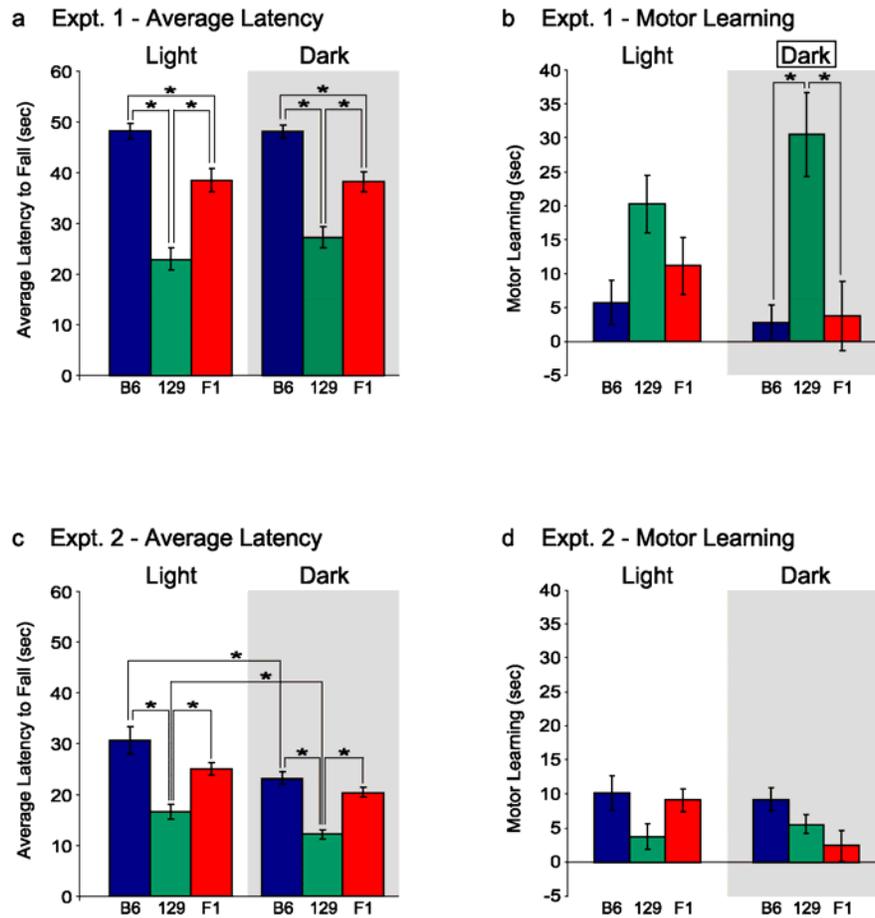
Figure 2.8 The rotarod test discriminates better in the dark phase
a) In experiment 1 (0-45 rpm over 2 min), all three strains showed no difference in average latency to fall from the rotarod between phases. Furthermore, discrimination between the strains worked well in both phases. b) Motor learning was not different between phases but showed improved strain discrimination in the dark phase. c) In experiment 2 (0-45 rpm over 1 min), B6 and 129 mice demonstrated improved performance in the light phase and again, discrimination between the strains worked equally in both phases. d) Motor learning was not affected by phase under these conditions. The better phase is indicated by a box. *p<0.02. Since performance, strain discrimination, and learning were all better in experiment 1 than in experiment 2, we conclude that the slower acceleration time was more appropriate. Only under these conditions did dark phase testing result in improved strain discrimination for motor learning. N = 6 per strain/sex/phase for each experiment.

To further optimize the rotarod test by reducing throughput time, we repeated it in experiment 2 using a shorter test time (1 min rather than 2 min) and a faster acceleration. Under these more challenging conditions, B6 and 129 mice showed longer latency to fall in the light phase than in the dark phase (Fig. 2.8c). However, in both phases, the test could not discriminate differences between B6 and F1 mice as had been achieved in experiment 1, but rather, only between 129 and the other two strains. Motor learning in experiment 2 showed no effect of phase or strain (Fig. 2.8d).

2.3.7 The tail-flick test discriminates only in the light phase

The multivariate ANOVA found significant effects of phase ($p<0.002$) and strain ($p<0.001$). The 129 mice showed significantly longer latency to flick their tails in the light phase than in the dark phase (Fig. 2.9). This accounted for discrimination between the strains in the light phase that was not possible in the dark phase. B6 and F1 mice were unaffected by phase for this test. Thus, we conclude that, when 129 mice are being tested, the tail-flick test discriminates better in the light phase.
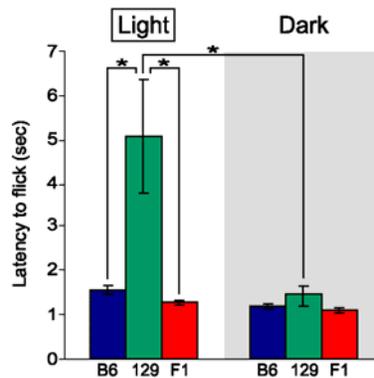
Figure 2.9 The tail-flick test does not discriminate better in the dark phase

The 129 mice show a longer latency to remove their tails in the light phase - a response that differentiated them from the other strains in the light phase only. B6 and F1 mice were unaffected by phase. The better phase is indicated by a box. *$p<0.001$. N = 6 per strain/sex/phase.

2.3.8 The hot-plate test does not discriminate better in the dark phase

As an alternative to the tail-flick test for pain sensitivity, for which phase could have been affected by the light beam used to generate the heat source, we assessed pain response with the hot-plate test. The multivariate ANOVA found significant effects of phase ($p<0.001$) and strain ($p<0.001$). The latency to lick or kick a paw was shorter in the dark phase than in the light phase for B6 mice (Fig. 2.10). However, the test could discriminate 129 mice, who had significantly longer latency than the other two strains, equally well in both phases.
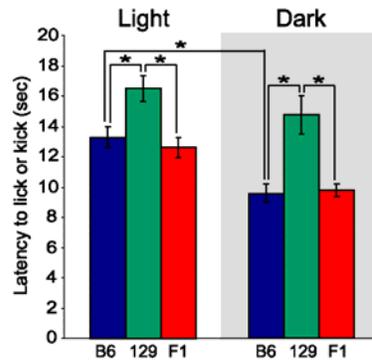
Figure 2.10 The hot-plate test does not discriminate better in the dark phase
The latency to lick or kick a paw was shorter in the dark phase than in the light phase for B6 mice. However, the ability to discriminate 129 mice, which had significantly longer latency than the other two strains, was not different between the phases. The better phase is indicated by a box. *p<0.04. N = 6 per strain/sex/phase.

2.4 Discussion

The present study demonstrates that dark-phase testing affects the outcome of high throughput behavioural phenotyping. Six of the seven tests showed significant phase differences for at least one parameter in at least one strain. Generally, where significant differences existed, activity levels were higher in the dark phase. For example, in the social interaction test, mice tested in the dark phase demonstrated increased self grooming (B6), crawl overs (B6), sniffing (129), and decreased immobility (B6 and 129). Similarly, in each test of pain sensitivity, a shorter latency to move was present in the dark phase: tail flick (129), and hotplate (B6). The only exception to this was in the second rotarod experiment for which the test conditions were too challenging and thus, inappropriate. Importantly, an overall examination of the data does not show the results from a single strain drove the light dark differences, but rather that both B6 and 129 are affected by phase, whereas F1 is generally not.

Dark-phase testing provided improved discrimination between strains using the SHIRPA primary screen. Although the discriminant analysis was able to discriminate between the strains in the light phase as others have shown (Rogers *et al.*, 1999), the dark phase was clearly more sensitive. Since discrimination between genetically different mice is the ultimate goal of a behavioural screen such as SHIRPA, we must conclude that in our test conditions, dark-phase testing is superior. Dark-phase testing also provided better strain discrimination using the open-field test. Since the open-field test is an assessment of spontaneous exploratory behaviour, and exploration is naturally a dark-phase behaviour for mice, the improved ability to discriminate strains in the dark supports our hypothesis for ethologically correct testing.

In contrast, we were surprised to find that social interaction did not consistently discriminate strains better in the dark phase, but rather that the significantly different parameters split evenly, in their discriminate ability, between the light and dark phases. A likely explanation is that the test mouse was so focused on the target mouse during the brief interaction time (3 min.), that effects of L/D cycle were less important to the response. However, the significant effects of strain and phase we did find are supported by the work of previous investigators (Lister & Hilakivi, 1988, Paterson & Vickers, 1984, Pieper *et al.*, 1997).

Similarly, performance on the rotarod may be so driven by the strong stimulus of the rotating rod, that there is little or no affect of phase. However, despite this strong stimulus, the motor learning ability of the 129 mice in the dark phase was still enhanced sufficiently that strain discrimination was achieved only in this phase.

Interestingly, even in the competing presence of a strong pain stimulus, the 129 mice were so affected by phase that strain discrimination occurred in only one phase. Because our goal was to interpret results in terms of strain discrimination, it is the light phase that we score as better. However, a likely explanation for this result is that the 129 mice are 'frozen' in the light, a common behaviour in this strain, and so appear differentially more resistant to pain than B6 and F1, whereas in the dark they don't freeze and thus are indistinguishable from the other strains.

The practicalities of working in the dark phase must also be considered. We found the challenges of reverse light cycle to be easily overcome using the methodology we have described; reverse light cycle, dim red light, and low-light level camera. However, not all tests were easily amenable to the dark-phase. For example, the SHIRPA parameter, skin color, was difficult to assess in the dark. In addition, the researcher may have been less coordinated and had slower movements in the dark. Furthermore, the researcher was less likely to be blinded to sex or strain (as indicated by coat color) in the light phase. Thus, we conclude that these unavoidable differences may have contributed, along with the intended differences in diurnal cycle and illumination, to the effect of phase.

Should high throughput behaviour testing be done in the dark phase? Since the preponderance of our data shows dark-phase testing improves, or does not affect strain discrimination, we conclude that for these strains and tests, dark-phase testing provided superior outcomes. If discrimination is not achieved in the dark phase, or if the test is known a priori to have a strong test stimulus, then light phase testing would be undertaken.

2.5 References

Brown, R.E., Stanford, L. & Schellinck, H.M. (2000) Developing standardized behavioral tests for knockout and mutant mice. *ILAR J,* 41, 163-174.

Calamandrei, G., Venerosi, A., Branchi, I., Valanzano, A. & Alleva, E. (2000) Prenatal exposure to anti-HIV drugs. long-term neurobehavioral effects of lamivudine (3TC) in CD-1 mice. *Neurotoxicol Teratol,* 22, 369-379.

Crabbe, J.C., Wahlsten, D. & Dudek, B.C. (1999) Genetics of mouse behavior: interactions with laboratory environment. *Science,* 284, 1670-1672.

Crawley, J.N. (2000) *What's wrong with my mouse?: behavioural phenotyping of transgenic and knockout mice,* A John Wiley and Sons, Inc., New York.

Crawley, J.N., Gerfen, C.R., Rogawski, M.A., Sibley, D.A., Skolnick, P. & Wray, S. (2003) Current Protocols in Neuroscience. In Taylor, G.P. (ed), John Wiley & Sons, Inc.

Crawley, J.N. & Paylor, R. (1997) A proposed test battery and constellations of specific behavioral paradigms to investigate the behavioral phenotypes of transgenic and knockout mice. *Horm Behav,* 31, 197-211.

Dierssen, M., Fotaki, V., Martinez de Lagran, M., Gratacos, M., Arbones, M., Fillat, C. & Estivill, X. (2002) Neurobehavioral development of two mouse lines commonly used in transgenic studies. *Pharmacol Biochem Behav,* 73, 19-25.

Engelmann, M., Wotjak, C.T. & Landgraf, R. (1995) Social discrimination procedure: an alternative method to investigate juvenile recognition abilities in rats. *Physiol Behav,* 58, 315-321.

Jacobs, G.H., Fenwick, J.C., Calderone, J.B. & Deeb, S.S. (1999) Human cone pigment
expressed in transgenic mice yields altered vision. *J Neurosci,* 19, 3258-3265.

Kopp, C. (2001) Locomotor activity rhythm in inbred strains of mice: implications for
behavioural studies. *Behav Brain Res,* 125, 93-96.

Kriegsfeld, L.J., Eliasson, M.J., Demas, G.E., Blackshaw, S., Dawson, T.M., Nelson, R.J.
& Snyder, S.H. (1999) Nocturnal motor coordination deficits in neuronal nitric
oxide synthase knock-out mice. *Neuroscience,* 89, 311-315.

Lister, R.G. & Hilakivi, L.A. (1988) The effects of novelty, isolation, light and ethanol on
the social behavior of mice. *Psychopharmacology (Berl),* 96, 181-187.

Marques, M.D. & Waterhouse, J.M. (1994) Masking and the evolution of circadian
rhythmicity. *Chronobiol Int,* 11, 146-155.

Nejdi, A., Guastavino, J.M. & Lalonde, R. (1996) Effects of the light--dark cycle on a
water tank social interaction test in mice. *Physiol Behav,* 59, 45-47.

Paigen, K. & Eppig, J.T. (2000) A mouse phenome project. *Mamm Genome,* 11, 715-717.

Paterson, A.T. & Vickers, C. (1984) Saline drinking and naloxone: lightcycle dependent
effects on social behaviour in male mice. *Pharmacol Biochem Behav,* 21, 495-
499.

Pieper, J.O., Forester, D.C. & Elmer, G.I. (1997) Mice show strain differences in social
affiliation. Implications for open field behavior. *Ann N Y Acad Sci,* 807, 552-555.

Rogers, D.C., Fisher, E.M., Brown, S.D., Peters, J., Hunter, A.J. & Martin, J.E. (1997)
Behavioral and functional analysis of mouse phenotype: SHIRPA, a proposed
protocol for comprehensive phenotype assessment. *Mamm Genome,* 8, 711-713.

Rogers, D.C., Jones, D.N., Nelson, P.R., Jones, C.M., Quilter, C.A., Robinson, T.L. & Hagan, J.J. (1999) Use of SHIRPA and discriminant analysis to characterise marked differences in the behavioural phenotype of six inbred mouse strains. *Behavioural Brain Research,* 105, 207-217.

Silva, A., Simpson, E.M., Takahashi, J.S., Lipp, H.-P., Nakanishi, S., Wehner, J.M., Giese, K.P., Tully, T., Abel, T., Chapman, P.F., Fox, K., Grant, S., Itohara, S., Lathe, R., Mayford, M., McNamara, J.O., Morris, R.J., Picciotto, M., Roder, J., Shin, H.-S., Slesinger, P.A., Storm, D.R., Stryker, M.P., Tonegawa, S., Wang, Y. & Wolfer, D.P. (1997) Mutant mice and neuroscience: recommendations concerning genetic background. *Neuron,* 19, 755-759.

Slow, E.J., van Raamsdonk, J., Rogers, D., Coleman, S.H., Graham, R.K., Deng, Y., Oh, R., Bissada, N., Hossain, S.M., Yang, Y.Z., Li, X.J., Simpson, E.M., Gutekunst, C.A., Leavitt, B.R. & Hayden, M.R. (2003) Selective striatal neuronal loss in a YAC128 mouse model of Huntington disease. *Human Molecular Genetics,* 12, 1555-1567.

Valentinuzzi, V.S., Buxton, O.M., Chang, A.M., Scarbrough, K., Ferrari, E.A., Takahashi, J.S. & Turek, F.W. (2000) Locomotor response to an open field during C57BL/6J active and inactive phases: differences dependent on conditions of illumination. *Physiol Behav,* 69, 269-275.

van der Staay, F.J. & Steckler, T. (2002) The fallacy of behavioral phenotyping without standardisation. *Genes, Brain and Behavior,* 1, 9-13.

Wahlsten, D. (2001) Standardizing tests of mouse behavior: reasons, recommendations, and reality. *Physiol Behav,* 73, 695-704.

Whishaw, I.Q., Haun, F. & Kolb, B. (1999) Analysis of Behavior in Laboratory Rodents. In Windhorst, U. & Johansson, H. (eds), *Modern Techniques in Neuroscience.* Springer-Verlag, Berlin, pp. 1243-1275.

Würbel, H. (2002) Behavioral phenotyping enhanced - beyond (environmental) standardization. *Genes, Brain and Behavior,* 1, 3-8.

Chapter 3: Hyperactivity, startle reactivity and cell-proliferation deficits are lithium resistant in $Nr2e1^{frc/frc}$ mice[2]

3.1 Introduction

Although bipolar disorder (BP) is a multifactorial psychiatric disorder that is highly heritable (60-85%) (Burmeister *et al.*, 2008), and the 6q chromosomal region has repeatedly shown evidence for genetic linkage to BP and other neurological disorders (Dick *et al.*, 2003, Hayden & Nurnberger, 2006, Kohn & Lerer, 2005, Mcqueen *et al.*, 2005, Middleton *et al.*, 2004, Pato *et al.*, 2004, Schulze *et al.*, 2004), the causative genes for BP are just beginning to be identified (Craddock & Sklar, 2009, Martinowich *et al.*, 2009, Ogden *et al.*, 2004). The largest meta-analysis of BP to date, found the strongest genome-wide linkage at 6q21-22 (108.5 Mb), with the highest LOD score (4.19) specifically for bipolar I disorder (BPI), the more manic subtype (Mcqueen *et al.*, 2005). One of the genes in the 6q21-22 region is *NR2E1*. A role for *NR2E1* in BP has also been supported by a significant association after correction between *NR2E1* and BPI, and candidate mutations in *NR2E1* in BP patients (Kumar *et al.*, 2008).

Mice lacking orphan nuclear receptor *Nr2e1*, the mammalian homolog of the *Drosophila Tlx* (*tailless*) gene, have been developed in several laboratories (aka *Tlx*^{-/-}, *Nr2e1*[frc/frc]) and are generally referred to as *Nr2e1*-null mice. Unlike the *Nr2e1* heterozygous mice that have no significant behavioural and neurological phenotypes (Young *et al.*, 2002), the *Nr2e1*-null mice have a wide range of neurological

---

[2] A version of this chapter has been submitted for publication. Wong, B.K.Y., Hossain, S.M., Trinh, E., Ottmann, G.A., Budaghzadeh, S., Zheng, Q.Y., and Simpson, E.M.. Hyperactivity, startle reactivity and cell-proliferation deficits are lithium resistant in *Nr2e1*[frc/frc] mice.

abnormalities, of particular interest are those similar to abnormalities seen in some patients with BP, including: increased lateral ventricular volume; reduced volume of the hippocampus, cerebral cortex, corpus callosum, amygdala, and cortical layers II and III; olfactory abnormality and dysfunction; altered cell cycling, cell morphology and plasticity in the hippocampus; reduced neurogenesis; impairment in GABAergic interneurons; and cognitive deficits (Anand & Shekhar, 2003, Brambilla *et al.*, 2003, Christie *et al.*, 2006, Goldberg & Chengappa, 2009, Kruger *et al.*, 2006, Land & Monaghan, 2003, Mccurdy *et al.*, 2006, Monaghan *et al.*, 1997, Roy *et al.*, 2004, Roy *et al.*, 2002, Shi *et al.*, 2004, Stenman *et al.*, 2003, Swayze *et al.*, 1990, Tian *et al.*, 2007, Young *et al.*, 2002, Zhang *et al.*, 2008). These neurological similarities, as well as linkage and association evidences, provide strong support for *NR2E1* as a candidate for BP, especially BPI.

Despite the support for *NR2E1* in BP, *Nr2e1*-null mice have not been fully characterized for anomalies similar to those seen in some patients with BP. Here, we examine *Nr2e1^{frc/frc}* mice carrying a spontaneous deletion of *Nr2e1* (Kumar *et al.*, 2004) for abnormalities in activity level, cognition, information processing, and cell proliferation in neurogenic regions. To further evaluate the similarity of *Nr2e1^{frc/frc}* mice and BP, we tested the effect of lithium treatment on these parameters. Lithium is the standard treatment for BP and it has been shown to attenuate psychostimulus-induced hyperactivity in rodent models of mania (O'donnell K & Gould, 2007) and to promote cell proliferation in the dentate gyrus (DG) (Son *et al.*, 2003). Considering that *Nr2e1*-null neural stem/progenitor cells (NSCs) showed reduced proliferation that could be rescued by reintroducing *Nr2e1 in vitro* (Shi *et al.*, 2004), we tested whether lithium

could allow reengagement of the cell cycle in these quiescent NSCs and whether any behavioural amelioration would accompany.

3.2 Methods and materials

3.2.1 Mice

The B6129F1-*Nr2e1* mice used for experimental analysis were all first generation offspring resulting from mating C57BL/6J.129-*Nr2e1^{frc}* (B6-*Nr2e1$^{frc/+}$*) females (backcross generation N17-22) to 129S1/SvImJ.Cg-*Nr2e1^{frc}* (129-*Nr2e1$^{frc/+}$*) males (N15-20). The *Nr2e1^{frc}* allele is a 44 kb spontaneous deletion of all 9 exons of *Nr2e1* that does not affect transcription of neighboring genes (Kumar *et al.*, 2004). In accordance with Mendelian inheritance, approximately 25% of the offspring were homozygous *Nr2e1$^{frc/frc}$* mice and 25% were *Nr2e1$^{+/+}$* (Wt) littermates; the latter were used as controls. All mice were weaned at postnatal day (P)18 - 21, housed with same-sex littermates, and then individually housed by 4 weeks to avoid aggressive incidence with *Nr2e1$^{frc/frc}$* mice and to be consistent for all mice. Mice were provided with food and water *ad libitum* and were provided standard care according to University of British Columbia animal care policies. Handling of all mice was minimized.

3.2.2 Genotyping

All mice were analyzed by two separate polymerase chain reaction (PCR) assays. Wild-type allele of *Nr2e1* was amplified using oEMS1859 (5′-CTGGGCCCTGCAGATACTC-3′) and oEMS1860 (5′-GGTGGCATGATGGGTAACTC-3′), and the fierce deletion allele of *Nr2e1* was detected using oEMS650 (5′-GGCGGAGGGAGCTTAAATAG-3′) and oEMS1368 (5′-

GATTCATCCTATTCCACAAAGTCA-3′). Cycling conditions were as follow: 2 min at 92°C, 30 cycles of 30 s at 94°C, 30 s at 58°C, and 55 s at 72°C; and a final extension of 5 min at 72°C.

3.2.3 Testing procedure

All mice were tested in the pathogen-free behaviour suite under reverse L/D cycle (light 23:00-11:00 h at 320 lux), at the Centre for Molecular Medicine and Therapeutics, Vancouver, Canada, as previously described (Hossain *et al.*, 2004). The multi-room behaviour suite consists of a breeding room and dedicated testing rooms, separated by corridors. The lighting in all areas was synchronized. Care was taken not to expose the mice to any inappropriate light, even during testing. When light was needed by the investigator during experiments in the dark phase, a dim red light (8 lux) was used. All adult mice tested were males between the ages of 2 – 6 months. The testing chambers and equipment were thoroughly cleaned between each test subject, using Clidox (Pharmacal Research Laboratories Inc., Naugatuck, CT) and 70% ethanol.

3.2.4 Pup body weight and milk consumption

The body weights of 15 Wt and 14 *Nr2e1$^{frc/frc}$* pups were measured at P0, 7, 14, and 21. Pups were individually placed on a clean plastic weigh boat and body weight was measured on a bench-top balance. The amount of milk consumption was similarly measured in a different cohort of 11 Wt and 12 *Nr2e1$^{frc/frc}$* pups. Pups were removed from their mother and weighed, then kept separate from their mother for 2 h after which the pups were returned to their mother and given 15 min for feeding and were weighed again.

3.2.5 Pup open field activity

Spontaneous exploratory locomotor activity was measured on 10 Wt and 12 *Nr2e1^{frc/frc}* pups at P9, 14, and 18 using a digiscan photocell-equipped automated open field apparatus 27.5 cm (L) x 27.5 cm (W) x 20.0 cm (H) with lower and upper beams at 1.5 cm and 5.5 cm from the floor, respectively (Med Associates Inc., St. Albans, VT). Each pup was placed in the center of the novel arena and allowed to explore for 3 min while the software tallied spatially identified beam breaks.

3.2.6 Home cage activity

Home cage activity was measured on a total of 8 Wt and 8 *Nr2e1^{frc/frc}* mice during a 48-h period using identical Cage Rack Systems (San Diego Instruments, San Diego, CA). Each mouse home cage was placed in the center of a metal cage rack frame that generates a uniformly spaced 8×4 photobeam grid. The mice were provided with food and water *ad libitum* throughout the testing period and spontaneous locomotor activity was measured by counting the total number of beam breaks each hour during the 48-h period (Kopp, 2001).

3.2.7 Open field activity and habituation

Activity and habituation in the open field of 12 Wt and 9 *Nr2e1^{frc/frc}* mice were measured using the open field apparatus described above (Pup open field activity). Mice were introduced to the open field apparatus for three consecutive days and tested for 10 min each time. The numbers of beam breaks were recorded for all trials.

3.2.8 Tail suspension

Struggling during the 3 min tail suspension test was measured on 8 Wt and 4 *Nr2e1$^{frc/frc}$* mice using a PHM-300TSS mouse tail suspension system (Med Associates, St. Albans, VT), as previously described (Abrahams *et al.*, 2005). The apparatus was calibrated to normalize for body weight before testing of each animal and the settings for struggle and gain were 15 and 4, respectively. Percent time struggle was calculated as time spent struggling during which force exceeded the struggle threshold (set to 15) divided by the total testing time (3 min).

3.2.9 Hot plate and tail flick

Thermal nociception and pain sensitivity of 8 Wt and 8 *Nr2e1$^{frc/frc}$* mice was measured for each mouse using the hot plate and tail flick tests, respectively, as previously described (Hossain *et al.*, 2004). Mice were placed on the hot plate apparatus (Columbus Instruments, Columbus, OH) thermostatically set at 55.0 ± 0.5 °C. The latency of first licking or kicking of the fore or hind paw was recorded. A cut-off time of 60 s was employed to avoid tissue damage.

For the tail flick test, mice were placed in a clear restraining tube (Model 33033, Columbus Instruments, Columbus, OH) and the tail was placed freely on a level surface between two photo detector panels of the automated tail flick analgesia meter (Columbus Instruments, Columbus, OH). Immediately after a 90-s habituation period, radiant heat from a 20-V beam of light was focused on the ventral surface of the tail and the time for the mouse to flick its tail was automatically recorded by the apparatus. A 10-s cut-off time was employed to prevent tissue damage.

For both tests, the average of two consecutive trials, separated by a 1-min interval, was calculated for each animal.

3.2.10 Auditory brainstem response

Auditory functions of 5 Wt and 4 $Nr2e1^{frc/frc}$ mice were tested using the auditory brainstem response (ABR) procedure, as previously described (Zheng *et al.*, 1999). Briefly, electrodes were placed under the scalp and recordings taken as different sound intensities were presented to anesthetized mice.

3.2.11 Passive avoidance

Learning and memory of 9 Wt and 6 $Nr2e1^{frc/frc}$ mice was tested in the passive avoidance test using the GEMINI^{TM} Avoidance System (San Diego Instruments, San Diego, CA). The equipment has two chambers separated by a sliding door. Mice were introduced to the first chamber in the presence of an auditory stimulus. After 30 s in the first chamber, the door separating the two chambers opened and the mouse was allowed to enter into the second chamber without the auditory stimulus. The time it took for the mouse to enter the second chamber after the door opened was recorded. The maximum time allowed to enter the second chamber was 180 s. Once the mouse entered the second chamber it received a mild electrical shock. The mouse was again tested 24 h later and the latency of entering the second chamber was recorded.

3.2.12 Acoustic startle reactivity

Acoustic startle reactivity was tested using the SR-LAB system (San Diego Instruments, San Diego, CA). Two separate groups of male mice were used: Group 1 (12 Wt, 9 $Nr2e1^{frc/frc}$) and Group 2 (7 Wt, 7 $Nr2e1^{frc/frc}$). After a 5-min acclimatization period,

each mouse was subjected to 90 acoustic startle stimuli (10 at each of nine intensities ranging from 75 to 125 dB) in a semi-randomized sequence. The startles had a fixed duration of 50 ms and were separated by a variable inter-stimulus interval (ISI) ranging from 20 to 30 s, while the recording window was set at 100 ms. Startle response was measured at each stimulus as well as at 10 no-stimulus trials.

3.2.13 Lithium administration and testing procedure

3 Wt and 5 $Nr2e1^{frc/frc}$ male mice received lithium chloride (LiCl) diets, while 4 Wt and 4 $Nr2e1^{frc/frc}$ male mice received control diets. Mice on the control diet were fed with untreated purified diet with Teklad Vitamin Mix (Harlan Teklad, Madison, WI). Mice on the lithium diet were fed with 1.7 g LiCl/kg added to the untreated purified diet with Teklad Vitamin Mix (Harlan Teklad, Madison, WI) for 4 weeks, and then switched to 2.55 g LiCl/kg added to the untreated purified diet with Teklad Vitamin Mix (Harlan Teklad, Madison, WI) for 2 additional weeks, before behaviour testing. These mice remained on the 2.55 g LiCl/kg of chow diet throughout the testing period. All mice were also given water *ad libitum* and a water bottle of 450 mM sodium chloride solution. Each mouse was subjected to behaviour tests in the following order: home cage activity, open field activity and habituation, and startle reactivity. The start of each test was performed one week after the end of the previous test. Tests were performed as described in the above sections. At the end of behaviour testing all animals were sacrificed and bled for serum analysis of lithium level, and brains were harvested for immunohistochemical analysis.

3.2.14 Serum analysis

Mice from the lithium-treatment experiment were given a lethal injection of 2,2,2-tribromoethanol in tert amyl alcohol (Sigma-Aldrich, St. Louis, MO) (aka avertin) and blood was collected via cardiac puncture using a 25-gauge needle. Blood samples were allowed to separate for 30 min at room temperature (RT). Samples were then centrifuged for 10 min at RT at 3000 RPM for separation of serum. The serum was then isolated and kept at $-20°C$ until lithium levels analyses. The Department of Pathology and Laboratory Medicine at Vancouver General Hospital, blinded to the experimental conditions, analyzed serum lithium level. 0.2 mmol/L was the minimum detection limit of lithium serum assay.

3.2.15 Brain harvesting and immunohistochemistry

Brains of mice from the lithium-treatment experiment were dissected out intact and placed into 4% paraformaldehyde in $1\times$ PBS at 4°C for 48 h, then transferred to a 20% sucrose solution at 4°C until saturated. Brains were then sectioned at 25 µm using the Cryo-Star HM 560 cryostat (MICROM International, Walldorf, Germany) and representative sections (every 24th) starting from the most rostral aspect of the ventricles to the most caudal aspect of the hippocampus were analyzed by immunofluorescence.

Sections were blocked with 5% normal goat serum (NGS) + 5% bovine serum albumin (BSA) in 0.1% Triton-X100 in PBS, incubated overnight at RT with rabbit anti-Ki67 polyclonal antibody (1:1000 dil, Cat. #ab15580; Abcam Inc., Cambridge, MA), and further incubated with Alexa Fluor[®] 594 goat anti-rabbit IgG (H+L) (Cat. #A31631; Invitrogen, Carlsbad, CA). Sections were mounted onto Superfrost[®] Plus slides (Cat.

#12-550-15; Fisher Scientific, Ottawa, ON) and coverslipped using Vectashield Hard Set™ (Cat. #H-1400; Vector Laboratories, Inc., Burlingame, CA). Images were captured on an Olympus BX61 motorized fluorescence microscope (Olympus America Inc., Center Valley, PA) and proliferating cells in the SVZ and DG were analyzed using the ImageJ software.

3.2.16 Statistical analysis

All data were analyzed using STATISTICA$^©$ 6 (StatSoft, Inc., Tulsa, OK). Body weight, milk consumption, tail suspension, hot plate, tail flick, auditory brainstem response, and passive avoidance data were analyzed by *t*-test on genotype. The remaining behavioural data were analyzed using repeated measures ANOVA for genotype and trials. In all repeated measures ANOVAs the Greenhouse-Geisser correction factor (ε) was used to adjust the degrees of freedom (Vasey & Thayer, 1987). *Post-hoc* tests with Bonferroni correction were performed for repeated between-subject comparisons.

Behavioural data pertaining to the lithium experiment were analyzed using repeated measures ANOVA for interaction between genotype and drug treatment. The same corrections as above were performed for these analyses. Cell proliferation data were analyzed using factorial ANOVA for genotype and drug treatment. All data are reported as mean values ± standard error of the mean (SEM).

3.3 Results

3.3.1 Young *Nr2e1$^{frc/frc}$* mice show early hyperactivity

Previously, we showed that *Nr2e1$^{frc/frc}$* pups on a C57BL/6J (B6) background failed to gain weight at the rate of their Wt littermates between postnatal weeks 2 and 3

(Young *et al.*, 2002). For the current study, we retested this phenotype at postnatal (P) 0,

7, 14, and 21 on the B6129F1 background. We showed that B6129F1-*Nr2e1*$^{frc/frc}$ mice

were also significantly smaller than their Wt siblings at P21 (Fig. 3.1a; Wt = 14.1 ± 0.2 g,

Nr2e1$^{frc/frc}$ = 12.7 ± 0.2 g, *P* < 0.001), but not at P0, 7, or 14. Therefore, small size at

wean is a stable phenotype across two genetic backgrounds.
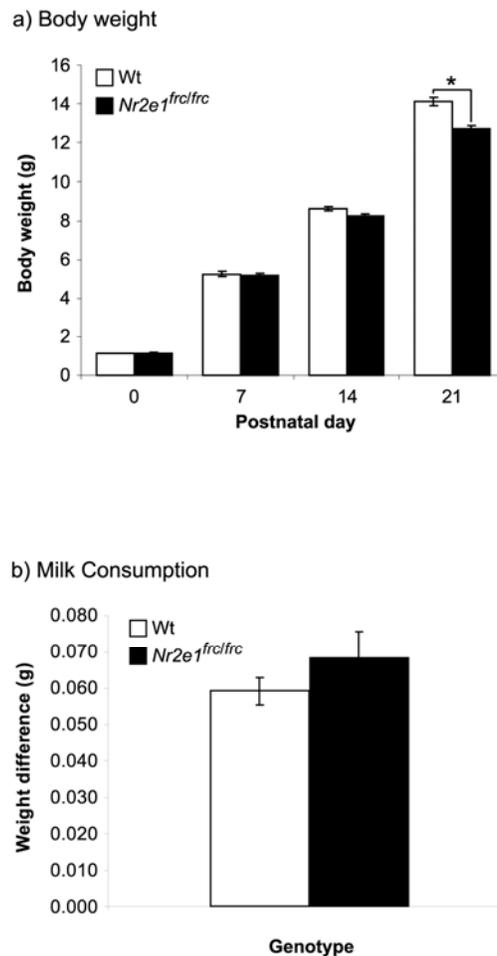
Figure 3.1 Reduced body weight of *Nr2e1*$^{frc/frc}$ pups not explained by milk consumption
(a) *Nr2e1*$^{frc/frc}$ pups weighed significantly less than Wt pups by postnatal day 21. * *P* <
0.001. N = 15 Wt and 14 *Nr2e1*$^{frc/frc}$ pups. (b) Pups were weighed before and after
feeding to determine their amount of milk consumption. No significant difference in milk
intake was seen between Wt and *Nr2e1*$^{frc/frc}$ pups (*P* > 0.1). N = 11 Wt and 12 *Nr2e1*$^{frc/frc}$
pups.

We measured milk consumption in pre-wean pups to test the hypothesis that the failure of *Nr2e1$^{frc/frc}$* mice to gain weight normally may depend on a reduction in milk consumption. This hypothesis was not supported by the milk consumption data, where no significant differences were found between the two genotypes (Fig. 3.1b; Wt = 0.059 ± 0.004 g, *Nr2e1$^{frc/frc}$* = 0.07 ± 0.01 g, $P > 0.1$). We then measured activity level in the same group of pre-wean pups at P9, 14, and 18 using the open field apparatus. Activity level was significantly higher in *Nr2e1$^{frc/frc}$* mice than Wt controls at P18 (Fig. 3.2; Beam breaks: Wt = 186 ± 15.0, *Nr2e1$^{frc/frc}$* = 325 ± 39.9, $P < 0.01$), but not at P9 and 14 ($P > 0.1$). Therefore, the post-wean size reduction of *Nr2e1$^{frc/frc}$* mice was not apparently the result of a feeding abnormality but may be a secondary effect of hyperactivity.
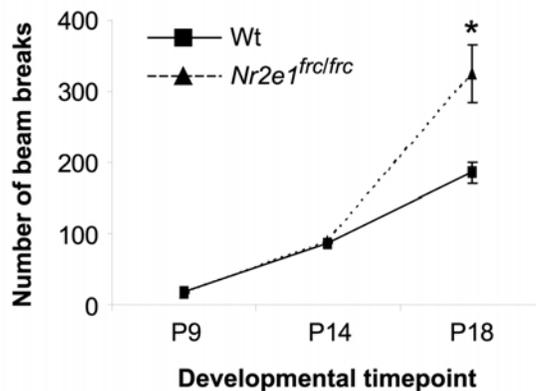
Figure 3.2 *Nr2e1$^{frc/frc}$* mice showed hyperactivity as early as postnatal day (P)18
A 3-min open field test showed that *Nr2e1$^{frc/frc}$* mice were significantly more active at P18, but not at younger ages. * $P < 0.01$. N = 10 Wt and 12 *Nr2e1$^{frc/frc}$* pups.

3.3.2 Adult *Nr2e1$^{frc/frc}$* mice show hyperactivity in three behavioural tests

To fully characterize the extent of the hyperactivity phenotype in *Nr2e1$^{frc/frc}$* mice we used the home cage activity monitor, a powerful and ethological test that assesses movement of mice in their home cage. This test showed that *Nr2e1$^{frc/frc}$* mice are extremely hyperactive (Fig. 3.3a; genotype effect $F(1,11) = 10.6$, $P < 0.01$). The mean number of beam breaks per hour was ~8-fold higher in *Nr2e1$^{frc/frc}$* mice than in Wt controls for both light and dark phases (Fig. 3.3b; Beam breaks: Light: Wt = 189 ± 19.0, *Nr2e1$^{frc/frc}$* = 1304 ± 118.9, $P < 0.001$; Dark: Wt = 313 ± 21.6, *Nr2e1$^{frc/frc}$* = 2403 ± 148.6, $P < 0.001$).
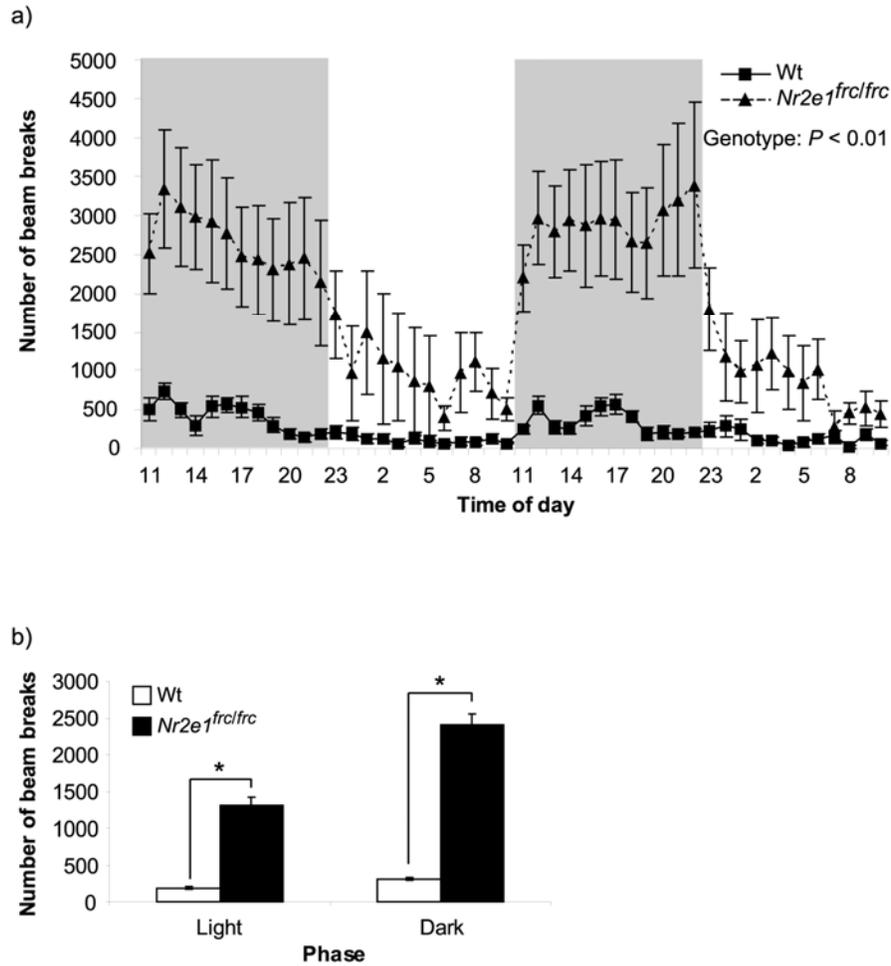
Figure 3.3 *Nr2e1^frc/frc* mice showed hyperactivity in the home cage
(a) *Nr2e1^frc/frc* mice broke more beams than their Wt littermates over 48 h. (b) *Nr2e1^frc/frc* mice are significantly more active than Wt controls in both light and dark phases. * $P <$ 0.001. N = 8 Wt and 8 *Nr2e1^frc/frc* mice.

Hyperactivity in *Nr2e1^frc/frc* mice was also seen in the open field test. Throughout the three days of open field habituation testing there was a significant effect of genotype on distance traveled (Fig. 3.4; $F(1,57) = 80.0$, $P < 0.001$).
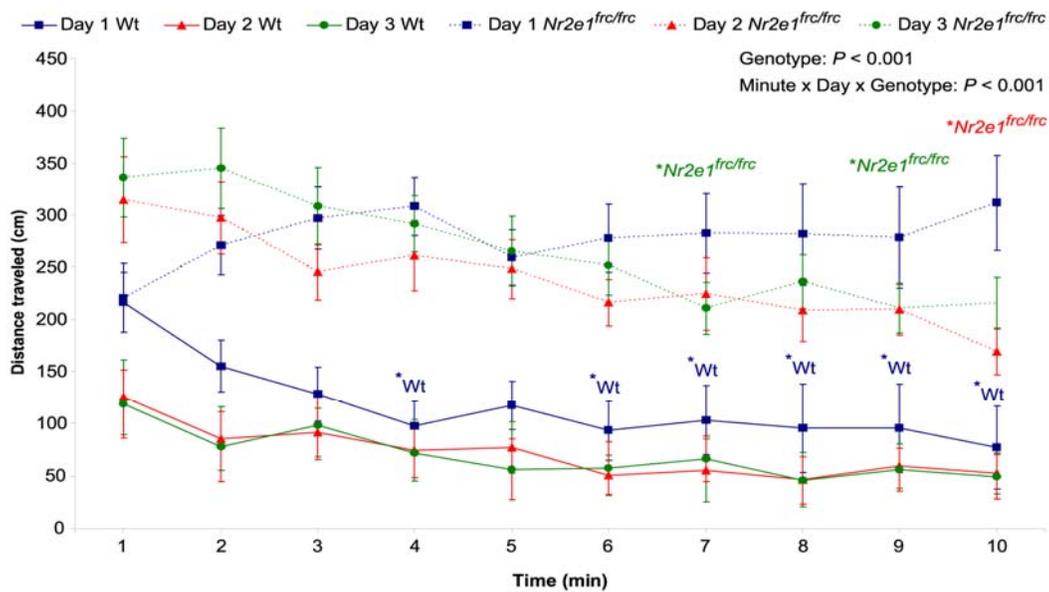
Figure 3.4 *Nr2e1^{frc/frc}* mice showed hyperactivity and habituation deficiency in the open field

Distance traveled was measured in the open field on 3 consecutive days for 10 min each day. *Nr2e1^{frc/frc}* mice were significantly more active than Wt mice on all 3 days. Wt mice showed habituation on day 1 (solid blue). *Wt: $P < 0.05$. *Nr2e1^{frc/frc}* mice did not show habituation on day 1 (dotted blue), but showed habituation on days 2 (dotted red) and 3 (dotted green). **Nr2e1^{frc/frc}*: $P < 0.05$. N = 12 Wt and 9 *Nr2e1^{frc/frc}* mice.

Finally, in the tail suspension test we found that *Nr2e1^{frc/frc}* mice spent significantly more time struggling than Wt mice (Fig. 3.5; Wt = 8.49 ± 1.60 % time struggle, *Nr2e1^{frc/frc}* = 33.3 ± 3.30 % time struggle, $F(1,10) = 2.13$, $P < 0.001$). This observation is consistent with a similar study testing mice lacking *Nr2e1* (Abrahams *et al.*, 2005). Therefore, increased struggle of *Nr2e1^{frc/frc}* mice in the tail suspension test is a stable phenotype across studies.
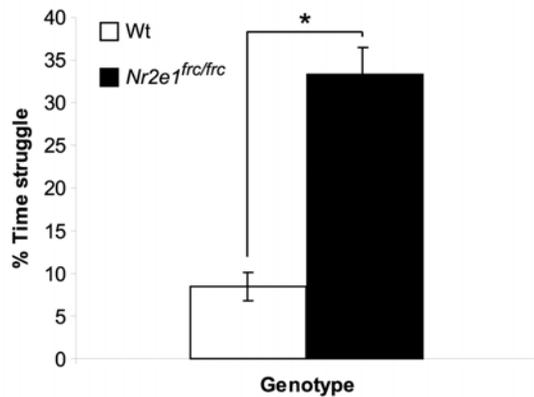
Figure 3.5 *Nr2e1$^{frc/frc}$* mice struggled more during the tail suspension test
The *Nr2e1$^{frc/frc}$* mice spent significantly more time struggling compared to their Wt
controls. * $P < 0.001$. N = 8 Wt and 4 *Nr2e1$^{frc/frc}$* mice.

3.3.3 Nr2e1$^{frc/frc}$ mice showed a deficit in two different learning and memory tasks

To characterize the behavioural manifestation of hippocampal and cortical
hypoplasia, hallmarks of the *Nr2e1$^{frc/frc}$* brain, we tested our mice for deficits in learning
and memory tasks. Since *Nr2e1$^{frc/frc}$* mice have reduced vision and showed deficits in the
hidden cookie test, which could result from abnormal olfaction because of hypoplasia of
olfactory bulbs (Young *et al.*, 2002), we used two tests that do not rely primarily on
visual or olfactory cues.

The ability of mice to habituate in the open field is measured by a decrease in
exploratory activity over time. We demonstrate here that although *Nr2e1$^{frc/frc}$* mice were
able to habituate to the open field arena, they required significantly more time than the
Wt controls. Throughout the three days of testing the two genotypes showed different
activity patterns depending on the day, as shown by a significant effect of minute, day,
and genotype interaction (Fig. 3.4; $F(18, 513) = 3.02$, $P < 0.001$, $\varepsilon = 0.46$). More

specifically, during day 1 of testing Wt mice already showed habituation by the 4th min of testing ($P < 0.05$), whereas *Nr2e1*[*frc/frc*] mice did not habituate during the 10 min on day 1 ($P > 0.7$). *Nr2e1*[*frc/frc*] mice did eventually show habituation on test days 2 and 3, at 10 ($P < 0.01$) and 7 ($P < 0.05$) min, respectively. Similarly, Wt mice showed inter-session habituation such that exploratory activity during days 2 and 3 was significantly reduced when compared to day 1 ($P < 0.05$), whereas *Nr2e1*[*frc/frc*] mice did not show a significant decrease in activity across days ($P > 0.05$).

The passive avoidance test depends on the ability of the mouse to react to pain, and therefore prior to this test, we examined our mice for pain sensitivity using the hot plate and tail flick tests. *Nr2e1*[*frc/frc*] mice began licking their paws in significantly less time compared to Wt mice, indicating increased pain sensitivity in the hot plate test (Fig. 3.6a; Wt = 16.2 ± 1.71 s, *Nr2e1*[*frc/frc*] = 11.3 ± 1.05 s, $P < 0.05$). In the tail flick test there was no difference in the time required to remove the tail between *Nr2e1*[*frc/frc*] and Wt mice (Fig. 3.6b; Wt = 1.75 ± 0.15 s; *Nr2e1*[*frc/frc*] = 1.90 ± 0.11 s; $P > 0.1$). Despite the discordance in the results of these two tests we have reason to favor the finding of increased pain sensitivity when *Nr2e1*[*frc/frc*] mice are not restrained (see Discussion). More importantly, both tests showed the ability of *Nr2e1*[*frc/frc*] mice to respond to pain, thus supporting the use of the passive avoidance test.
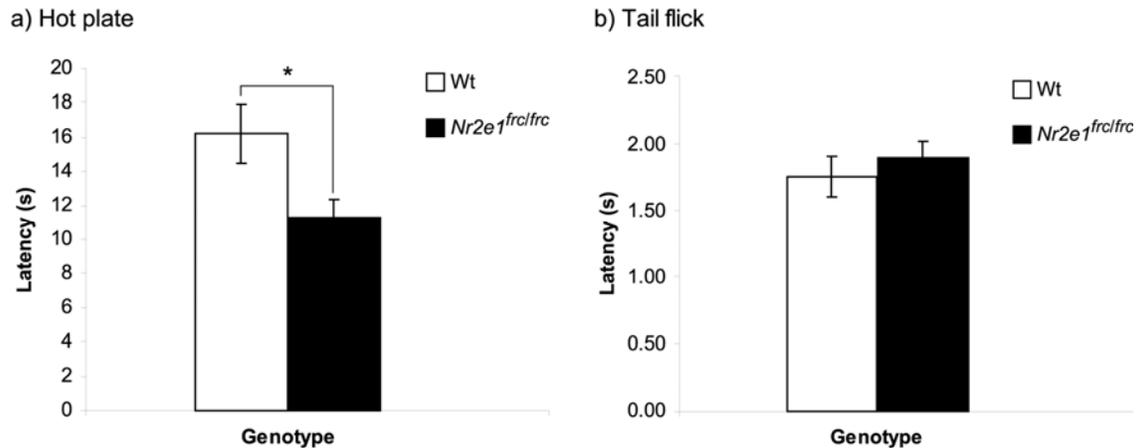
Figure 3.6 $Nr2e1^{frc/frc}$ mice showed increased pain sensitivity
(a) The latency to lick paws as a sign of discomfort from heat is measured in the hot plate test. $Nr2e1^{frc/frc}$ mice took significantly less time to lick their paws compared to the Wt controls. * $P < 0.05$. (b) The tail flick test was also used to test pain sensitivity in these mice; however, there was no significant difference found between the two genotypes ($P > 0.1$). N = 8 Wt and 8 $Nr2e1^{frc/frc}$ mice for each test.

The standard protocol for passive avoidance testing is to use light as an adverse stimulus to encourage the animal to cross into the second chamber. However, since $Nr2e1^{frc/frc}$ mice have impaired vision, we decided to use sound as the adverse stimulus. We have previously tested 4-month-old $Nr2e1^{frc/frc}$ mice on a B6 background and showed that they have normal hearing as measured by auditory brainstem response (ABR) (Young *et al.*, 2002). However, since our current mice are on a B6129F1 hybrid background, we retested them for ABR. $Nr2e1^{frc/frc}$ mice did not show any significant differences from Wt controls (Fig. 3.7; Click: Wt = 50.0 ± 2.89 dB, $Nr2e1^{frc/frc} = 45.0 \pm 2.74$ dB, $P > 0.5$, 16 kHz: Wt = 22.5 ± 4.33 dB, $Nr2e1^{frc/frc} = 17.0 \pm 2.00$ dB, $P > 0.5$). Therefore, normal ABR in $Nr2e1^{frc/frc}$ mice is a stable phenotype across two genetic backgrounds.
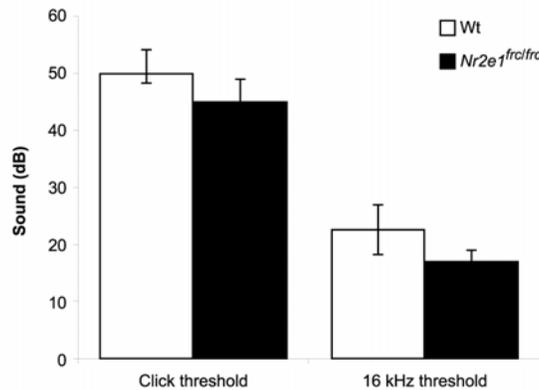
Figure 3.7 *Nr2e1$^{frc/frc}$* mice showed normal hearing

Auditory brainstem response was used to assess hearing ability in the mice. No significant differences in click and 16 kHz thresholds were seen between Wt and *Nr2e1$^{frc/frc}$* mice ($P > 0.1$). N = 5 Wt and 4 *Nr2e1$^{frc/frc}$* mice.

Since we confirmed that B6129F1-*Nr2e1$^{frc/frc}$* mice are able to respond to pain and that their hearing is normal, we used sound to test these mice for passive avoidance. Wt mice demonstrated the expected learning response, showing an average >3-fold increase in latency to re-enter the second chamber upon the second exposure to the condition stimulus (Fig. 3.8; Day 1 = 41.7 ± 3.32 s, Day 2 = 150 ± 12.1 s, $P < 0.001$). Although *Nr2e1$^{frc/frc}$* mice also showed an increase in latency to re-enter, this change was much less than that seen in Wt mice, and did not reach statistical significance (Day 1 = 29.3 ± 7.21 s, Day 2 = 71.0 ± 23.1 s, $P > 0.05$), demonstrating that they did not perform this learning task as well as Wt mice.

89
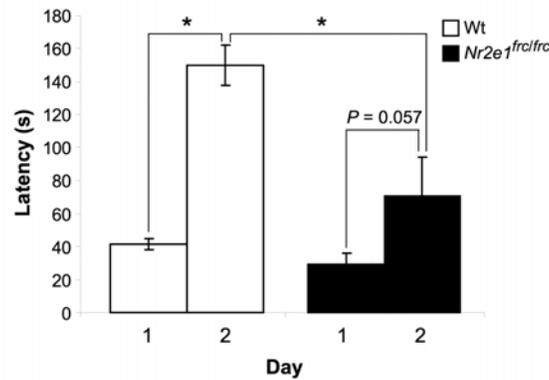
Figure 3.8 *Nr2e1^{frc/frc}* mice showed impaired performance in the passive avoidance test
Learning is measured by the increase in latency to enter the chamber where the mouse
received a mild shock the day before. Although *Nr2e1^{frc/frc}* mice did show an increase in
latency to enter the 2nd chamber, this was much less than that seen in Wt mice (* $P <$
0.001), and did not reach statistical significance ($P = 0.057$). N = 9 Wt and 6 *Nr2e1^{frc/frc}*
mice.

3.3.4 *Nr2e1^{frc/frc}* mice lack startle reactivity

Hippocampal lesions in rodent models have been well documented to show

impairments in prepulse inhibition (PPI), a measure of sensorimotor gating (Kamath *et*

al., 2008, Pouzet *et al.*, 1999). Prior to evaluating PPI, acoustic startle reactivity (ASR)

must be tested to establish a startle threshold, as defined as the lowest startle intensity that

produces a startle reaction significantly different than at the no-stimulus condition.

Nr2e1^{frc/frc} mice showed less acoustic startle reactivity than Wt controls, as shown by a

significant main effect of genotype (Fig. 3.9; $F(1,19) = 17.5$, $P < 0.001$) and a significant

interaction between intensity and genotype ($F(9,171) = 29.9$, $P < 0.001$, $\varepsilon = 0.27$). *Post-*

hoc analysis indicated that the startle threshold for Wt mice was at 105 dB ($P < 0.001$);

interestingly, there was no startle threshold for *Nr2e1^{frc/frc}* mice ($P > 0.05$). This

surprising result was confirmed with a new group of mice (data not shown). Therefore,

90

we conclude that *Nr2e1^{frc/frc}* mice show a lack of normal startle reaction. When we

compared the startle magnitudes of *Nr2e1^{frc/frc}* and Wt mice at each startle intensity, there

were significant differences at no stimulus, 85, 90, 95, 110, 115, and 120 dB ($P < 0.005$).

Significant genotype differences below the Wt startle threshold (105 dB) are indicative of

hyperactivity in *Nr2e1^{frc/frc}* mice. This test becomes the fourth test demonstrating

hyperactivity in *Nr2e1^{frc/frc}* mice. Furthermore, as PPI tests are based on the startle

response, PPI results for these mice would be uninformative.
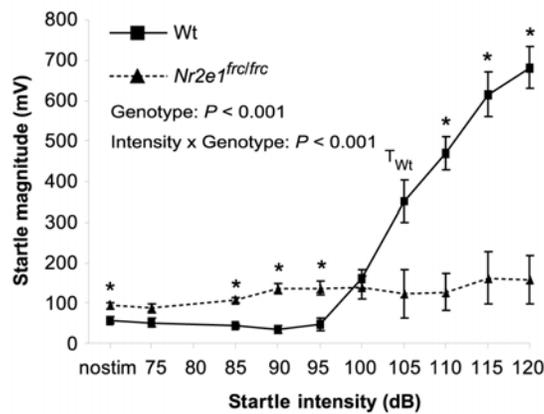
Figure 3.9 *Nr2e1^{frc/frc}* mice showed no startle reactivity to auditory stimuli
Wt controls showed a normal pattern of increasing startle responses as startle stimuli
became louder. However, *Nr2e1^{frc/frc}* mice showed no increase in their startle responses at
any decibel level tested. T_{Wt}, startle threshold for Wt ($P < 0.001$). * $P < 0.005$, between
genotype comparison at each individual startle intensity. N = 12 Wt and 9 *Nr2e1^{frc/frc}*
mice.

3.3.5 *Nr2e1$^{frc/frc}$* hyperactivity resistant to lithium treatment

Lithium chloride is the most effective drug for treatment of mania in patients with BPI, with human therapeutic plasma lithium level between 0.6-1.2 mmol/L (equivalent to mouse plasma lithium level 0.77-1.17 mmol/L), which can attenuate psychostimulus-induced hyperactivity and increase cell proliferation in the dentate gyrus in rodent models (Chen *et al.*, 2000). Using a dietary source of lithium, Wt and *Nr2e1$^{frc/frc}$* mice showed therapeutic levels of lithium in their serum (Fig. 3.10; Wt, control diet = below detection limit, Wt, lithium diet = 0.9 ± 0.1 mmol/L, *Nr2e1$^{frc/frc}$*, control diet = below detection limit, *Nr2e1$^{frc/frc}$*, lithium diet = 0.8 ± 0.1 mmol/L, significant main effect of diet $F(1,14)$ = 78.1, $P < 0.001$).
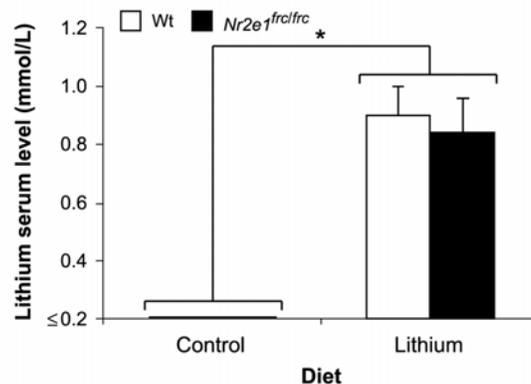
Figure 3.10 Lithium-treated mice showed therapeutic levels of lithium in their serum
Mice fed with a lithium diet showed significant, and importantly, therapeutic levels of lithium in their serum compared to mice fed control diet (* $P < 0.001$). There was no significant difference in lithium serum level between genotypes on the same diet ($P >$ 0.1). N = 4 Wt and 4 *Nr2e1$^{frc/frc}$* mice on control diet; 3 Wt and 5 *Nr2e1$^{frc/frc}$* mice on lithium diet.

We showed that lithium treatment was unable to alleviate the hyperactivity seen in *Nr2e1*[frc/frc] mice in the 24-h home cage activity test, as demonstrated by the significant effect of genotype (Fig. 3.11a; $F(1,12) = 37.7$, $P < 0.001$), but no significant effect of diet ($F(1,12) = 0.15$, $P > 0.5$), nor a significant interaction between genotype and diet ($F(1,12) = 0.004$, $P > 0.5$). The mean number of beam breaks in both light and dark phases was significantly higher in *Nr2e1*[frc/frc] mice compared to Wt controls, regardless of lithium treatment (Fig. 3.11b; Light: Wt, normal diet = 78.9 ± 10.8, Wt, lithium diet = 110.2 ± 21.6, *Nr2e1*[frc/frc] normal diet = 285.5 ± 46.0, *Nr2e1*[frc/frc] lithium diet = 321.4 ± 55.8; Dark: Wt, normal diet = 158.5 ± 16.7, Wt, lithium diet = 197.2 ± 24.4, *Nr2e1*[frc/frc] normal diet = 997.4 ± 65.1, *Nr2e1*[frc/frc] lithium diet = 1005.7 ± 79.4; for all comparisons between Wt and *Nr2e1*[frc/frc] regardless of diet $P < 0.05$).
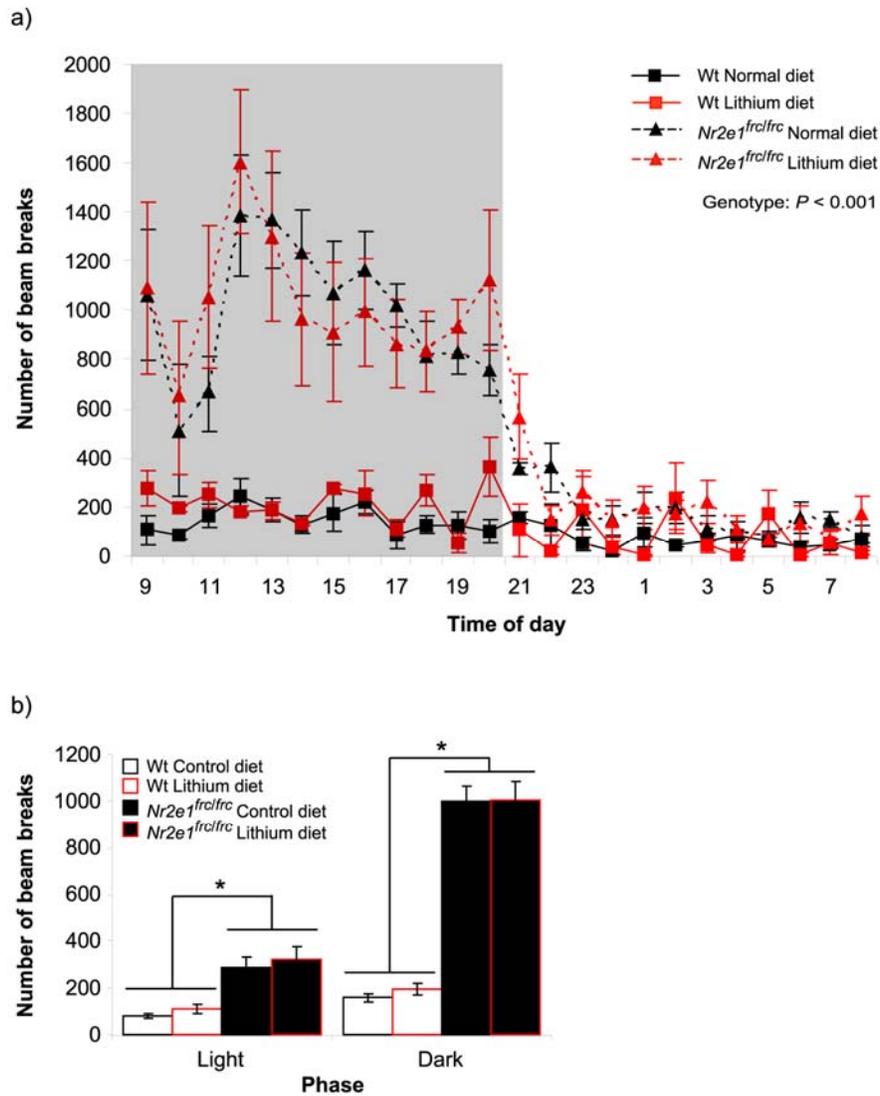
Figure 3.11 *Nr2e1^{frc/frc}*-induced hyperactivity in the home cage was unaffected by lithium treatment

(a) *Nr2e1^{frc/frc}* mice, on control and lithium diet, broke more beams than their Wt littermates over 24 h. (b) *Nr2e1^{frc/frc}* mice, regardless of diet, were significantly more active than Wt controls in both light and dark phases. * $P < 0.05$. N = 4 Wt and 4 *Nr2e1^{frc/frc}* mice on control diet; 3 Wt and 5 *Nr2e1^{frc/frc}* mice on lithium diet.

$Nr2e1^{frc/frc}$ mice hyperactivity in the open field test was similarly unaffected by lithium treatment, where there was a significant effect of genotype on distance traveled (Fig. 3.12; $F(1,36) = 44.9$, $P < 0.001$) with no significant effect of diet ($F(1,36) = 3.42$, $P > 0.05$), and no significant interaction between genotype and diet ($F(1,36) = 0.31$, $P > 0.5$).
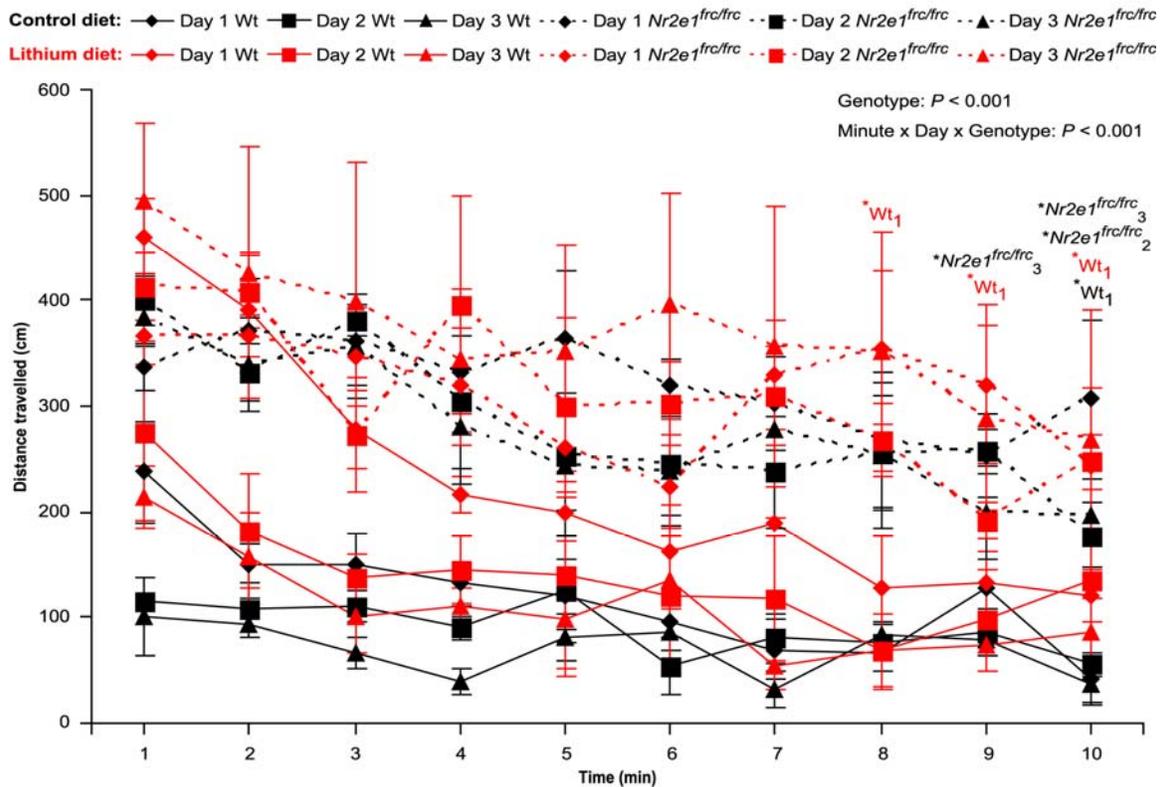
Figure 3.12 Hyperactivity and habituation deficits in $Nr2e1^{frc/frc}$ mice unaffected by lithium treatment

$Nr2e1^{frc/frc}$ mice, regardless of diet, showed significantly higher activity than Wt mice on all 3 days. Wt mice on a normal diet showed habituation on day 1 (solid black line with diamond; Black *Wt_1: $P < 0.05$), as did lithium-treated Wt mice (solid red line with diamond; Red *Wt_1: $P < 0.05$). $Nr2e1^{frc/frc}$ mice on a normal diet did not show habituation on day 1 (dotted black line with diamond), but showed habituation on days 2 (dotted black line with square; Black *$Nr2e1^{frc/frc}{}_2$: $P < 0.05$) and 3 (dotted black line with triangle; Black *$Nr2e1^{frc/frc}{}_3$: $P < 0.05$). Lithium-treated $Nr2e1^{frc/frc}$ mice did not show habituation on any of the 3 days. N = 4 Wt and 4 $Nr2e1^{frc/frc}$ mice on control diet; 3 Wt and 5 $Nr2e1^{frc/frc}$ mice on lithium diet.

3.3.6 *Nr2e1$^{frc/frc}$* open field habituation deficit is unaffected by lithium treatment

To evaluate the effect of lithium treatment on the habituation deficit in *Nr2e1$^{frc/frc}$*

mice, mice fed control and lithium diets were assayed in the open field habituation test.

As before (Fig. 3.4), there was a significant effect of minutes, day, and genotype

interaction (Fig. 3.12; $F(18,324) = 1.96$, $P < 0.05$, $\varepsilon = 0.59$), indicating that *Nr2e1$^{frc/frc}$*

mice showed different activity patterns on the different test days compared to Wt

controls. Lithium treatment was unable to improve habituation in *Nr2e1$^{frc/frc}$* mice, as

indicated by the lack of significant interaction between minute, day, genotype, and diet

($F(18, 324) = 0.77$, $P > 0.7$, $\varepsilon = 0.59$).

3.3.7 Lithium-treated *Nr2e1$^{frc/frc}$* mice show no improvement in startle reactivity

The lack of startle reactivity was one of the most striking phenotypes shown in

Nr2e1$^{frc/frc}$ mice. To assess the effect of lithium on this behavioural phenotype, control

and lithium-treated Wt and *Nr2e1$^{frc/frc}$* mice were assayed in the startle reactivity test.

Similar to our previous experiments (Fig. 3.9), the two genotype groups responded

differently to the varying acoustic startle stimuli as evidenced by the significant

interaction between intensity and genotype (Fig. 3.13; $F(9,126) = 9.32$, $P < 0.001$). We

showed that lithium treatment did not significantly correct the deficient acoustic startle

response in *Nr2e1$^{frc/frc}$* mice compared to that shown by Wt mice, as there was no

significant effect of diet ($F(1,14) = 0.87$, $P > 0.5$), and there were no significant

interactions between: genotype and diet ($F(1,14) = 0.92$, $P > 0.5$); intensity and diet

($F(9,126) = 0.32$, $P > 0.5$); nor genotype, intensity, and diet ($F(9,126) = 0.47$, $P > 0.5$).

Wt mice showed startle thresholds on control and lithium diets at 110 and 115 dB,

respectively ($P < 0.05$), while control or lithium-treated $Nr2e1^{frc/frc}$ mice lacked a startle

threshold at any startle intensity ($P > 0.05$), paralleling results shown in Fig. 9 and

demonstrating the lack of a lithium effect on startle reactivity. As seen previously, when

we compared the startle magnitudes of $Nr2e1^{frc/frc}$ and Wt mice on control diet at each

startle intensity, there were significant differences at many stimulus levels: no stimulus,

75, 85, 90, 95, and 120 dB ($P < 0.05$), indicative of $Nr2e1^{frc/frc}$ hyperactivity. $Nr2e1^{frc/frc}$

and Wt mice on a lithium diet also showed significant differences in startle reactivity at

90 and 120 dB ($P < 0.05$). The reduction in differences was attributable to increase in

variability with drug treatment.
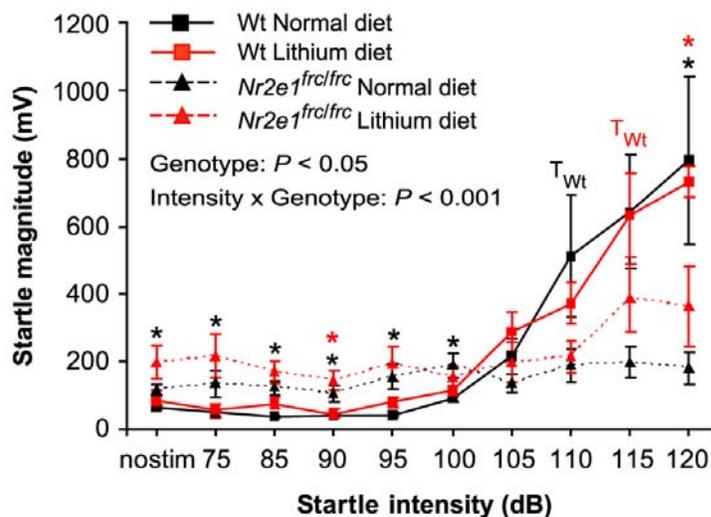
Figure 3.13 Lithium treatment did not significantly improve startle reactivity deficit in
$Nr2e1^{frc/frc}$ mice

Wt controls showed startle thresholds on control (Black T_{Wt}: $P < 0.05$) and lithium (Red
T_{Wt}: $P < 0.05$) diets. However, $Nr2e1^{frc/frc}$ mice lacked a startle threshold at any intensity,
regardless of diet. Between genotype comparison at each individual startle intensity for
mice on control diet (Black * $P < 0.05$). Between genotype comparison at each individual
startle intensity for mice on lithium diet (Red * $P < 0.05$). N = 4 Wt and 4 $Nr2e1^{frc/frc}$
mice on control diet; 3 Wt and 5 $Nr2e1^{frc/frc}$ mice on lithium diet.

3.3.8 Cell proliferation in subventricular zone and dentate gyrus is unaffected by lithium treatment

Reduced neural stem/progenitor cell proliferation has been shown in *Nr2e1*-knockout mice when compared to their Wt littermates (Shi *et al.*, 2004). Here we show for the first time, using Ki67 staining of proliferating cells, a significant genotype effect (Fig. 3.14a & b; $F_{(2,10)} = 44.46$, $P < 0.001$), indicating that mice carrying the $Nr2e1^{frc/frc}$ alleles also show the same reduction in cell proliferation when compared to Wt mice. Since lithium has been shown to act through multiple pathways to increase cell proliferation *in vivo* (Jope, 1999, Wada *et al.*, 2005), we also analyzed its effect on cell proliferation in $Nr2e1^{frc/frc}$ mice. We showed that lithium treatment was unable to alter cell proliferation, as evident by no significant effect of diet ($F_{(2,10)} = 0.13$, $P > 0.5$) and no significant interaction between genotype and diet ($F_{(2,10)} = 0.04$, $P > 0.9$). Cell proliferation in normal and lithium-treated $Nr2e1^{frc/frc}$ mice is not significantly different in either the subventricular zone (SVZ) (Fig. 3.14a; $Nr2e1^{frc/frc}$ normal diet = 14.4 ± 3.1 Ki67+ cells/count area, $Nr2e1^{frc/frc}$ lithium diet = 10.6 ± 1.4 Ki67+ cells/count area, $P > 0.5$) or in the dentate gyrus (DG) (Fig. 3.14b; $Nr2e1^{frc/frc}$ normal diet = 2.3 ± 0.8 Ki67+ cells/count area, $Nr2e1^{frc/frc}$ lithium diet = 1.6 ± 0.5 Ki67+ cells/count area, $P > 0.5$). Lithium treatment also did not affect cell proliferation of WT mice in the SVZ (Fig. 3.14a; WT normal diet = 129.3 ± 21.8 Ki67+ cells/count area, WT lithium diet = 129.7 ± 2.2 Ki67+ cells/count area, $P > 0.5$) and in the DG (Fig. 3.14b; WT normal diet = 13.8 ± 2.8 Ki67+ cells/count area, WT lithium diet = 12.5 ± 1.7 Ki67+ cells/count area, $P > 0.5$).
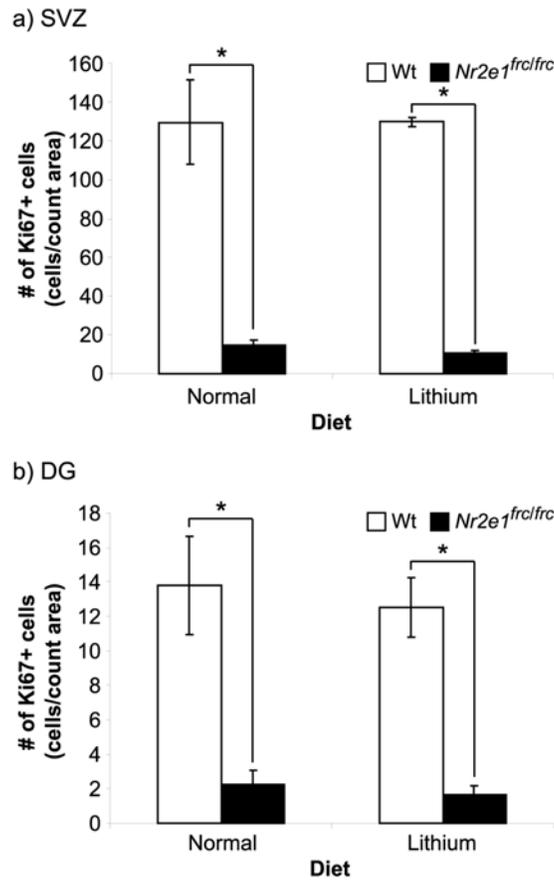
Figure 3.14 Lithium treatment did not increase cell proliferation in *Nr2e1frc/frc* mice
(a) In the subventricular zone (SVZ), there were significantly less Ki67+ cells in
Nr2e1frc/frc mice compared to Wt mice, regardless of diet (* $P < 0.001$). (b) In the dentate
gyrus (DG), there were significantly less Ki67+ cells in *Nr2e1frc/frc* mice compared to Wt
mice, regardless of diet (* $P < 0.01$). N = 4 Wt and 4 *Nr2e1frc/frc* mice on control diet; 3
Wt and 5 *Nr2e1frc/frc* mice on lithium diet.

3.4 Discussion

This study was the first to characterize a spectrum of phenotypes in $Nr2e1^{frc/frc}$ mice, which have been used in the literature to model aspects of BP (Arban *et al.*, 2005, Cao & Peng, 1993, Decker *et al.*, 2000, Einat, 2006a, Einat, 2006b, Einat *et al.*, 2003, El-Mallakh *et al.*, 2003, Gessa *et al.*, 1995, Ralph-Williams *et al.*, 2003). In addition, it is the first to evaluate the effect of any drug treatment on *Nr2e1*-null mice. Results from this study showed new important behavioural phenotypes in $Nr2e1^{frc/frc}$ mice including extreme hyperactivity and deficits in habituation and startle reactivity. The presence of reduced cellular proliferation in the SVZ and DG was a novel finding for $Nr2e1^{frc/frc}$ mice and the resistance of these behavioural and proliferative phenotypes to lithium treatment is a novel finding amongst all *Nr2e1*-null mice.

In the present study, the extreme hyperactivity phenotype of the $Nr2e1^{frc/frc}$ animals was documented in four different tests: home cage activity, tail suspension, open field habituation, and startle reactivity. Of these tests, the tail suspension was originally chosen to evaluate depressive behaviour in this study, but because of the overwhelming hyperactivity phenotype, the results were not indicative of depressive behaviour. Currently, the most frequently used model of mania is psychostimulant-induced hyperactivity (Einat, 2006a, Machado-Vieira et al., 2004). Interestingly, hyperactivity seen in $Nr2e1^{frc/frc}$ mice was approximately 8-fold higher than basal activity level in the home cage, while administration of psychostimulant commonly increases activity by 2- to 4-fold over non-induced mice (Arban et al., 2005). As far as we are aware, $Nr2e1^{frc/frc}$ mice show the most extreme hyperactivity phenotype currently documented.

Nr2e1-null mice have previously been shown to have hypoplasia of the hippocampus and decreased adult neurogenesis in the granular layer of the DG, regions important for learning and memory (Mainen & Sejnowski, 1996, Shi et al., 2004, Young et al., 2002). Our group also demonstrated that not only is the dendritic branching structure of granule cells in *Nr2e1^frc/frc^* mice reminiscent of immature neurons in the DG, they also lack synaptic plasticity, as demonstrated by the absence of long-term potentiation (LTP) in their dentate gyrus (Christie et al., 2006). LTP is thought by some to be an electrophysiological measure of learning and memory (Howland & Wang, 2008, Kinney et al., 2009). Therefore, in an attempt to reveal impairments in cognitive function as seen in some patients with BP (Green, 2006), we showed, using two distinct tests of learning and memory, that *Nr2e1^frc/frc^* mice perform poorly on these tasks compared to Wt mice. Since *Nr2e1^frc/frc^* mice have reduced vision and may also have abnormal olfaction, many conventional behavioural paradigms of learning and memory were not appropriate. The two different tests used in this study were chosen and designed specifically to assess learning and memory with minimal use of visual or olfactory cues. Both tests provide an internal control for activity level since they consider the change in activity between the same groups of mice on different days, thus normalizing for activity levels. The increased time required to habituate in the open field test and the lack of significant increase in latency to re-enter in the passive avoidance test are suggestive of reduced learning. Yet, we cannot completely exclude the possibility that a slowness to acquire environmental cues due to sensory deficits or an inability to control hyperactivity contributes to their deficits in performance in these tasks. Despite these caveats, we conclude that abnormal habituation and conditioned avoidance, along with the significant neuropathological

101

phenotypes in *Nr2e1frc/frc* mice (Christie et al., 2006, Young et al., 2002) are all evidence indicative of cognitive deficits in these mice.

This study was also the first to test for acoustic startle reactivity (ASR) in *Nr2e1*-null mice. Our novel finding of complete lack of startle was unexpected, since previously there has not been a case of hearing mice not showing ASR. ASR was done in preparation for evaluating PPI; however, we are unable to test PPI since PPI requires startle reactivity greater than movements seen at background noise and *Nr2e1frc/frc* mice showed no startle threshold. This result, along with normal response for the tail flick test, was surprising since our previous results, and those of others (Roy et al., 2002), led us to anticipate a hyper-responsive phenotype. However, we note that the lack of hyperresponsiveness in these instances correlates with the use of restraint, an extreme stressor in mice (Bain et al., 2004). Brain regions shown to contribute to stress-related response include the amygdala and hippocampus (Liberzon & Martis, 2006, Vermetten & Bremner, 2002). Regions suggested to be involved in modulation of ASR, include nucleus accumbens, basolateral amygdala, and prefrontal cortex (Stevenson & Gratton, 2004, Storozheva et al., 2003). All of these regions are structurally abnormal in the *Nr2e1frc/frc* mice and may underlie the lack of hyperresponsiveness to pain, as well as the lack of ASR. Based on the hot plate test where *Nr2e1frc/frc* mice were not tested under restraint and showed a significant reduction in time to lick their paws, we concluded that *Nr2e1frc/frc* mice had increased pain sensitivity. However, in the tail flick test, *Nr2e1frc/frc* mice were placed in a restrainer and, we concluded that under this stressor, the expected hyper-responsive phenotype of *Nr2e1frc/frc* mice was masked by the atypical stress response caused by restraint.

We chose to evaluate the effect of lithium treatment on $Nr2e1^{frc/frc}$ mice for four reasons: (1) lithium has been shown to attenuate symptoms of mania in patients with BP (Shastry, 2005); (2) lithium reduces amphetamine-induced hyperactivity in rodent models of mania (Gould et al., 2001); (3) lithium has shown neuroprotective effects by inducing neural stem cell proliferation in the mouse DG both in vitro and in vivo assays (Wada et al., 2005); and (4) lithium is thought to act through multiple key neurological pathways (Jope, 1999), thus increasing the probability that lithium would effect $Nr2e1^{frc/frc}$ behavioural phenotypes compared to drugs with restricted modes of action.

In this study, we showed that adult lithium treatment was ineffective in attenuating any of the abnormal behavioural phenotypes observed in $Nr2e1^{frc/frc}$ mice including the extreme hyperactivity in the home cage, the habituation deficit in the open field test, and the lack of acoustic startle reactivity. Despite the fact that lithium can induce cell cycle *in vitro* and *in vivo* (Wada et al., 2005) and that the introduction of Nr2e1 can "rescue" quiescent stem cells from *Nr2e1*-null brains in vitro (Shi et al., 2004), here we showed that lithium administration to adult $Nr2e1^{frc/frc}$ mice was unable to trigger an increase in cell proliferation in the SVZ and DG.

The lack of significant lithium effect could be interpreted as a result of the low number of mice examined in the lithium experiment. However based on the literature of other genetic and psychostimulant-induced mouse models of mania, lithium treatment, was able to reduced the hyperactivity phenotype by at least half, if not returning activity level to that seen in wild-type controls (Gould et al., 2007, Gould et al., 2001, Roybal et al., 2007). Therefore, since $Nr2e1^{frc/frc}$ mice exhibit ~8-fold increase in locomotor activity compared to Wt controls, the number of mice tested in the lithium experiment had

sufficient power to detect lithium effect given the anticipated reduction in locomotor activity.

The development of an all-encompassing mouse model for complex diseases, such as mental illness, is challenging for reasons of environmental factors, minor multiple gene effects, and appropriate pharmacological responsiveness. However, many single gene mouse models, such as *Gsk3b* overexpressing mice, nitric oxide synthase (NOS-III) and nNOS knockout mice, and *DISC1* mutant mice (Flint & Shifman, 2008, Kato et al., 2007, Prickaerts et al., 2006, Reif et al., 2006, Tanda et al., 2009) have proven valuable as they exhibit aspects of complex disorders. We have now added *Nr2e1^{frc/frc}* mice to this group. We have shown here that *Nr2e1^{frc/frc}* mice, although complicated by sensory defects, demonstrate the behavioural traits of hyperactivity and deficit in habituation and learning tasks, which are commonly used in genetic models of BP.

However, since *Nr2e1^{frc/frc}* mice failed to respond to lithium treatment, they do not meet the criteria of pharmacological validity as a model for BP (Kato et al., 2007). We hypothesize for future consideration that *in utero* or perinatal administration of lithium might further elucidate the effectiveness of lithium treatment. We also acknowledge that the genetic components of BP are likely to be mutations of minor effect; furthermore, the phenotype of the *Nr2e1* heterozygous mouse is too weak for behavioural detection (Roy et al., 2002). Therefore, we hypothesize that mice carrying subtle mutations, or patient variants, *in trans* with *Nr2e1* deletion might more closely represent the human condition.

3.5 References

Abrahams, B.S., Kwok, M.C., Trinh, E., Budaghzadeh, S., Hossain, S.M. & Simpson, E.M. (2005) Pathological aggression in "fierce" mice corrected by human nuclear receptor 2E1. *J Neurosci,* **25,** 6263-6270.

Anand, A. & Shekhar, A. (2003) Brain imaging studies in mood and anxiety disorders: special emphasis on the amygdala. *Ann N Y Acad Sci,* **985,** 370-388.

Arban, R., Maraia, G., Brackenborough, K., Winyard, L., Wilson, A., Gerrard, P. & Large, C. (2005) Evaluation of the effects of lamotrigine, valproate and carbamazepine in a rodent model of mania. *Behav Brain Res,* **158,** 123-132.

Bain, M.J., Dwyer, S.M. & Rusak, B. (2004) Restraint stress affects hippocampal cell proliferation differently in rats and mice. *Neurosci Lett,* **368,** 7-10.

Brambilla, P., Perez, J., Barale, F., Schettini, G. & Soares, J.C. (2003) GABAergic dysfunction in mood disorders. *Mol Psychiatry,* **8,** 721-737, 715.

Burmeister, M., McInnis, M.G. & Zollner, S. (2008) Psychiatric genetics: progress amid controversy. *Nat Rev Genet,* **9,** 527-540.

Cao, B.J. & Peng, N.A. (1993) Magnesium valproate attenuates hyperactivity induced by dexamphetamine-chlordiazepoxide mixture in rodents. *Eur J Pharmacol,* **237,** 177-181.

Chen, G., Rajkowska, G., Du, F., Seraji-Bozorgzad, N. & Manji, H.K. (2000) Enhancement of hippocampal neurogenesis by lithium. *J Neurochem,* **75,** 1729-1734.

Christie, B.R., Li, A.M., Redila, V.A., Booth, H., Wong, B.K., Eadie, B.D., Ernst, C. & Simpson, E.M. (2006) Deletion of the nuclear receptor Nr2e1 impairs synaptic plasticity and dendritic structure in the mouse dentate gyrus. *Neuroscience,* **137,** 1031-1037.

Craddock, N. & Sklar, P. (2009) Genetics of bipolar disorder: successful start to a long journey. *Trends Genet, 25,* 99-105.

Decker, S., Grider, G., Cobb, M., Li, X.P., Huff, M.O., El-Mallakh, R.S. & Levy, R.S. (2000) Open field is more sensitive than automated activity monitor in documenting ouabain-induced hyperlocomotion in the development of an animal model for bipolar illness. *Prog Neuropsychopharmacol Biol Psychiatry, 24,* 455-462.

Dick, D.M., Foroud, T., Flury, L., Bowman, E.S., Miller, M.J., Rau, N.L., Moe, P.R., Samavedy, N., El-Mallakh, R., Manji, H., Glitz, D.A., Meyer, E.T., Smiley, C., Hahn, R., Widmark, C., McKinney, R., Sutton, L., Ballas, C., Grice, D., Berrettini, W., Byerley, W., Coryell, W., DePaulo, R., MacKinnon, D.F., Gershon, E.S., Kelsoe, J.R., McMahon, F.J., McInnis, M., Murphy, D.L., Reich, T., Scheftner, W. & Nurnberger, J.I., Jr. (2003) Genomewide linkage analyses of bipolar disorder: a new sample of 250 pedigrees from the National Institute of Mental Health Genetics Initiative. *Am J Hum Genet, 73,* 107-114.

Einat, H. (2006a) Establishment of a Battery of Simple Models for Facets of Bipolar Disorder: A Practical Approach to Achieve Increased Validity, Better Screening and Possible Insights into Endophenotypes of Disease. *Behav Genet*.

Einat, H. (2006b) Modelling facets of mania - new directions related to the notion of endophenotypes. *J Psychopharmacol*.

Einat, H., Manji, H.K., Gould, T.D., Du, J. & Chen, G. (2003) Possible involvement of the ERK signaling cascade in bipolar disorder: behavioral leads from the study of mutant mice. *Drug News Perspect, 16,* 453-463.

El-Mallakh, R.S., El-Masri, M.A., Huff, M.O., Li, X.P., Decker, S. & Levy, R.S. (2003) Intracerebroventricular administration of ouabain as a model of mania in rats. *Bipolar Disord,* **5,** 362-365.

Flint, J. & Shifman, S. (2008) Animal models of psychiatric disease. *Curr Opin Genet Dev,* **18,** 235-240.

Gessa, G.L., Pani, L., Fadda, P. & Fratta, W. (1995) Sleep deprivation in the rat: an animal model of mania. *Eur Neuropsychopharmacol,* **5 Suppl,** 89-93.

Goldberg, J.F. & Chengappa, K.N. (2009) Identifying and treating cognitive impairment in bipolar disorder. *Bipolar Disord,* **11 Suppl 2,** 123-137.

Gould, T.D., O'Donnell, K.C., Picchini, A.M. & Manji, H.K. (2007) Strain differences in lithium attenuation of d-amphetamine-induced hyperlocomotion: a mouse model for the genetics of clinical response to lithium. *Neuropsychopharmacology,* **32,** 1321-1333.

Gould, T.J., Keith, R.A. & Bhat, R.V. (2001) Differential sensitivity to lithium's reversal of amphetamine-induced open-field activity in two inbred strains of mice. *Behav Brain Res,* **118,** 95-105.

Green, M.F. (2006) Cognitive impairment and functional outcome in schizophrenia and bipolar disorder. *J Clin Psychiatry,* **67 Suppl 9,** 3-8; discussion 36-42.

Hayden, E.P. & Nurnberger, J.I., Jr. (2006) Molecular genetics of bipolar disorder. *Genes Brain Behav,* **5,** 85-95.

Hossain, S.M., Wong, B.K. & Simpson, E.M. (2004) The dark phase improves genetic discrimination for some high throughput mouse behavioral phenotyping. *Genes Brain Behav,* **3,** 167-177.

Howland, J.G. & Wang, Y.T. (2008) Synaptic plasticity in learning and memory: stress effects in the hippocampus. *Prog Brain Res,* **169,** 145-158.

Jope, R.S. (1999) Anti-bipolar therapy: mechanism of action of lithium. *Mol Psychiatry,* **4,** 117-128.

Kamath, A., Al-Khairi, I., Bhardwaj, S. & Srivastava, L.K. (2008) Enhanced alpha1 adrenergic sensitivity in sensorimotor gating deficits in neonatal ventral hippocampus-lesioned rats. *Int J Neuropsychopharmacol,* **11,** 1085-1096.

Kato, T., Kubota, M. & Kasahara, T. (2007) Animal models of bipolar disorder. *Neurosci Biobehav Rev,* **31,** 832-842.

Kinney, J.W., Sanchez-Alavez, M., Barr, A.M., Criado, J.R., Crawley, J.N., Behrens, M.M., Henriksen, S.J. & Bartfai, T. (2009) Impairment of memory consolidation by galanin correlates with in vivo inhibition of both LTP and CREB phosphorylation. *Neurobiol Learn Mem*.

Kohn, Y. & Lerer, B. (2005) Excitement and confusion on chromosome 6q: the challenges of neuropsychiatric genetics in microcosm. *Mol Psychiatry,* **10,** 1062-1073.

Kopp, C. (2001) Locomotor activity rhythm in inbred strains of mice: implications for behavioural studies. *Behav Brain Res,* **125,** 93-96.

Kruger, S., Frasnelli, J., Braunig, P. & Hummel, T. (2006) Increased olfactory sensitivity in euthymic patients with bipolar disorder with event-related episodes compared with patients with bipolar disorder without such episodes. *J Psychiatry Neurosci,* **31,** 263-270.

Kumar, R.A., Chan, K.L., Wong, A.H., Little, K.Q., Rajcan-Separovic, E., Abrahams, B.S. & Simpson, E.M. (2004) Unexpected embryonic stem (ES) cell mutations represent a concern in gene targeting: lessons from "fierce" mice. *Genesis,* **38,** 51-57.

Kumar, R.A., McGhee, K.A., Leach, S., Bonaguro, R., Maclean, A., Aguirre-Hernandez, R., Abrahams, B.S., Coccaro, E.F., Hodgins, S., Turecki, G., Condon, A., Muir, W.J., Brooks-Wilson, A.R., Blackwood, D.H. & Simpson, E.M. (2008) Initial association of NR2E1 with bipolar disorder and identification of candidate mutations in bipolar disorder, schizophrenia, and aggression through resequencing. *Am J Med Genet B Neuropsychiatr Genet,* **147B,** 880-889.

Land, P.W. & Monaghan, A.P. (2003) Expression of the transcription factor, tailless, is required for formation of superficial cortical layers. *Cereb Cortex,* **13,** 921-931.

Liberzon, I. & Martis, B. (2006) Neuroimaging studies of emotional responses in PTSD. *Ann N Y Acad Sci,* **1071,** 87-109.

Machado-Vieira, R., Kapczinski, F. & Soares, J.C. (2004) Perspectives for the development of animal models of bipolar disorder. *Prog Neuropsychopharmacol Biol Psychiatry,* **28,** 209-224.

Mainen, Z.F. & Sejnowski, T.J. (1996) Influence of dendritic structure on firing pattern in model neocortical neurons. *Nature,* **382,** 363-366.

Martinowich, K., Schloesser, R.J. & Manji, H.K. (2009) Bipolar disorder: from genes to behavior pathways. *J Clin Invest,* **119,** 726-736.

McCurdy, R.D., Feron, F., Perry, C., Chant, D.C., McLean, D., Matigian, N., Hayward, N.K., McGrath, J.J. & Mackay-Sim, A. (2006) Cell cycle alterations in biopsied olfactory neuroepithelium in schizophrenia and bipolar I disorder using cell culture and gene expression analyses. *Schizophr Res,* **82,** 163-173.

McQueen, M.B., Devlin, B., Faraone, S.V., Nimgaonkar, V.L., Sklar, P., Smoller, J.W., Abou Jamra, R., Albus, M., Bacanu, S.A., Baron, M., Barrett, T.B., Berrettini, W., Blacker, D.,

Byerley, W., Cichon, S., Coryell, W., Craddock, N., Daly, M.J., Depaulo, J.R., Edenberg, H.J., Foroud, T., Gill, M., Gilliam, T.C., Hamshere, M., Jones, I., Jones, L., Juo, S.H., Kelsoe, J.R., Lambert, D., Lange, C., Lerer, B., Liu, J., Maier, W., Mackinnon, J.D., McInnis, M.G., McMahon, F.J., Murphy, D.L., Nothen, M.M., Nurnberger, J.I., Pato, C.N., Pato, M.T., Potash, J.B., Propping, P., Pulver, A.E., Rice, J.P., Rietschel, M., Scheftner, W., Schumacher, J., Segurado, R., Van Steen, K., Xie, W., Zandi, P.P. & Laird, N.M. (2005) Combined analysis from eleven linkage studies of bipolar disorder provides strong evidence of susceptibility loci on chromosomes 6q and 8q. *Am J Hum Genet,* **77,** 582-595.

Middleton, F.A., Pato, M.T., Gentile, K.L., Morley, C.P., Zhao, X., Eisener, A.F., Brown, A., Petryshen, T.L., Kirby, A.N., Medeiros, H., Carvalho, C., Macedo, A., Dourado, A., Coelho, I., Valente, J., Soares, M.J., Ferreira, C.P., Lei, M., Azevedo, M.H., Kennedy, J.L., Daly, M.J., Sklar, P. & Pato, C.N. (2004) Genomewide linkage analysis of bipolar disorder by use of a high-density single-nucleotide-polymorphism (SNP) genotyping assay: a comparison with microsatellite marker assays and finding of significant linkage to chromosome 6q22. *Am J Hum Genet,* **74,** 886-897.

Monaghan, A.P., Bock, D., Gass, P., Schwager, A., Wolfer, D.P., Lipp, H.P. & Schutz, G. (1997) Defective limbic system in mice lacking the tailless gene. *Nature,* **390,** 515-517.

O'Donnell K, C. & Gould, T.D. (2007) The behavioral actions of lithium in rodent models: Leads to develop novel therapeutics. *Neurosci Biobehav Rev*.

Ogden, C.A., Rich, M.E., Schork, N.J., Paulus, M.P., Geyer, M.A., Lohr, J.B., Kuczenski, R. & Niculescu, A.B. (2004) Candidate genes, pathways and mechanisms for bipolar (manic-

depressive) and related disorders: an expanded convergent functional genomics approach. *Mol Psychiatry, ***9,** 1007-1029.

Pato, C.N., Pato, M.T., Kirby, A., Petryshen, T.L., Medeiros, H., Carvalho, C., Macedo, A., Dourado, A., Coelho, I., Valente, J., Soares, M.J., Ferreira, C.P., Lei, M., Verner, A., Hudson, T.J., Morley, C.P., Kennedy, J.L., Azevedo, M.H., Daly, M.J. & Sklar, P. (2004) Genome-wide scan in Portuguese Island families implicates multiple loci in bipolar disorder: fine mapping adds support on chromosomes 6 and 11. *Am J Med Genet B Neuropsychiatr Genet,* **127,** 30-34.

Pouzet, B., Feldon, J., Veenman, C.L., Yee, B.K., Richmond, M., Nicholas, J., Rawlins, P. & Weiner, I. (1999) The effects of hippocampal and fimbria-fornix lesions on prepulse inhibition. *Behav Neurosci,* **113,** 968-981.

Prickaerts, J., Moechars, D., Cryns, K., Lenaerts, I., van Craenendonck, H., Goris, I., Daneels, G., Bouwknecht, J.A. & Steckler, T. (2006) Transgenic mice overexpressing glycogen synthase kinase 3beta: a putative model of hyperactivity and mania. *J Neurosci,* **26,** 9022-9029.

Ralph-Williams, R.J., Paulus, M.P., Zhuang, X., Hen, R. & Geyer, M.A. (2003) Valproate attenuates hyperactive and perseverative behaviors in mutant mice with a dysregulated dopamine system. *Biol Psychiatry,* **53,** 352-359.

Reif, A., Strobel, A., Jacob, C.P., Herterich, S., Freitag, C.M., Topner, T., Mossner, R., Fritzen, S., Schmitt, A. & Lesch, K.P. (2006) A NOS-III haplotype that includes functional polymorphisms is associated with bipolar disorder. *Int J Neuropsychopharmacol,* **9,** 13-20.

Roy, K., Kuznicki, K., Wu, Q., Sun, Z., Bock, D., Schutz, G., Vranich, N. & Monaghan, A.P. (2004) The Tlx gene regulates the timing of neurogenesis in the cortex. *J Neurosci,* **24,** 8333-8345.

Roy, K., Thiels, E. & Monaghan, A.P. (2002) Loss of the tailless gene affects forebrain development and emotional behavior. *Physiol Behav,* **77,** 595-600.

Roybal, K., Theobold, D., Graham, A., DiNieri, J.A., Russo, S.J., Krishnan, V., Chakravarty, S., Peevey, J., Oehrlein, N., Birnbaum, S., Vitaterna, M.H., Orsulak, P., Takahashi, J.S., Nestler, E.J., Carlezon, W.A., Jr. & McClung, C.A. (2007) Mania-like behavior induced by disruption of CLOCK. *Proc Natl Acad Sci U S A,* **104,** 6406-6411.

Schulze, T.G., Buervenich, S., Badner, J.A., Steele, C.J., Detera-Wadleigh, S.D., Dick, D., Foroud, T., Cox, N.J., MacKinnon, D.F., Potash, J.B., Berrettini, W.H., Byerley, W., Coryell, W., DePaulo, J.R., Jr., Gershon, E.S., Kelsoe, J.R., McInnis, M.G., Murphy, D.L., Reich, T., Scheftner, W., Nurnberger, J.I., Jr. & McMahon, F.J. (2004) Loci on chromosomes 6q and 6p interact to increase susceptibility to bipolar affective disorder in the national institute of mental health genetics initiative pedigrees. *Biol Psychiatry,* **56,** 18-23.

Shastry, B.S. (2005) Bipolar disorder: an update. *Neurochem Int,* **46,** 273-279.

Shi, Y., Chichung Lie, D., Taupin, P., Nakashima, K., Ray, J., Yu, R.T., Gage, F.H. & Evans, R.M. (2004) Expression and function of orphan nuclear receptor TLX in adult neural stem cells. *Nature,* **427,** 78-83.

Son, H., Yu, I.T., Hwang, S.J., Kim, J.S., Lee, S.H., Lee, Y.S. & Kaang, B.K. (2003) Lithium enhances long-term potentiation independently of hippocampal neurogenesis in the rat dentate gyrus. *J Neurochem,* **85,** 872-881.

Stenman, J.M., Wang, B. & Campbell, K. (2003) Tlx controls proliferation and patterning of lateral telencephalic progenitor domains. *J Neurosci,* **23,** 10568-10576.

Stevenson, C.W. & Gratton, A. (2004) Basolateral amygdala dopamine receptor antagonism modulates initial reactivity to but not habituation of the acoustic startle response. *Behav Brain Res,* **153,** 383-387.

Storozheva, Z.I., Afanas'ev, II, Proshin, A.T. & Kudrin, V.S. (2003) Dynamics of intracellular dopamine contents in the rat brain during the formation of conditioned contextual fear and extinction of an acoustic startle reaction. *Neurosci Behav Physiol,* **33,** 307-312.

Swayze, V.W., 2nd, Andreasen, N.C., Alliger, R.J., Ehrhardt, J.C. & Yuh, W.T. (1990) Structural brain abnormalities in bipolar affective disorder. Ventricular enlargement and focal signal hyperintensities. *Arch Gen Psychiatry,* **47,** 1054-1059.

Tanda, K., Nishi, A., Matsuo, N., Nakanishi, K., Yamasaki, N., Sugimoto, T., Toyama, K., Takao, K. & Miyakawa, T. (2009) Abnormal social behavior, hyperactivity, impaired remote spatial memory, and increased D1-mediated dopaminergic signaling in neuronal nitric oxide synthase knockout mice. *Mol Brain,* **2,** 19.

Tian, S.Y., Wang, J.F., Bezchlibnyk, Y.B. & Young, L.T. (2007) Immunoreactivity of 43 kDa growth-associated protein is decreased in post mortem hippocampus of bipolar disorder and schizophrenia. *Neurosci Lett,* **411,** 123-127.

Vasey, M.W. & Thayer, J.F. (1987) The continuing problem of false positives in repeated measures ANOVA in psychophysiology: a multivariate solution. *Psychophysiology,* **24,** 479-486.

Vermetten, E. & Bremner, J.D. (2002) Circuits and systems in stress. II. Applications to neurobiology and treatment in posttraumatic stress disorder. *Depress Anxiety,* **16,** 14-38.

Wada, A., Yokoo, H., Yanagita, T. & Kobayashi, H. (2005) Lithium: potential therapeutics against acute brain injuries and chronic neurodegenerative diseases. *J Pharmacol Sci,* **99,** 307-321.

Young, K.A., Berry, M.L., Mahaffey, C.L., Saionz, J.R., Hawes, N.L., Chang, B., Zheng, Q.Y., Smith, R.S., Bronson, R.T., Nelson, R.J. & Simpson, E.M. (2002) Fierce: a new mouse deletion of Nr2e1; violent behaviour and ocular abnormalities are background-dependent. *Behav Brain Res,* **132,** 145-158.

Zhang, C.L., Zou, Y., He, W., Gage, F.H. & Evans, R.M. (2008) A role for adult TLX-positive neural stem cells in learning and behaviour. *Nature,* **451,** 1004-1007.

Zheng, Q.Y., Johnson, K.R. & Erway, L.C. (1999) Assessment of hearing in 80 inbred strains of mice by ABR threshold analyses. *Hear Res,* **130,** 94-107.

Chapter 4: Increased *Nr2e1* transcription affects gene regulation, cell proliferation, and brain and eye morphology in mice[3]

4.1 Introduction

Nr2e1 is an orphan nuclear receptor, with no known ligand, expressed in the developing and adult brain and eye (Land & Monaghan, 2003, Liu *et al.*, 2008, Miyawaki *et al.*, 2004, Monaghan *et al.*, 1995, Roy *et al.*, 2004, Rudolph *et al.*, 1997). *Nr2e1* controls proliferation and differentiation of neural and retinal stem/progenitor cells by regulating gene expression important in these cellular processes (Hollemann *et al.*, 1998, Kobayashi *et al.*, 2000, Li *et al.*, 2008, Liu *et al.*, 2008, Miyawaki *et al.*, 2004, Shi *et al.*, 2004, Sun *et al.*, 2007, Yokoyama *et al.*, 2008, Yu *et al.*, 2000). In particular, *Nr2e1* acts as a transcriptional repressor by binding to the promoters of *Pten*, *Gfap*, *S100b*, and *Aqp4* (Shi *et al.*, 2004, Yu *et al.*, 2000, Zhang *et al.*, 2006) that further affects downstream molecules important for cell cycle progression, such as CyclinD1 and p27^{Kip1} (Miyawaki *et al.*, 2004, Zhang *et al.*, 2006). *Nr2e1*-null mice (also known as *Tlx$^{-/-}$*, *Nr2e1$^{-/-}$*, *Nr2e1$^{frc/frc}$*) display numerous neurological and ocular phenotypes including: hypoplasia of the cerebral cortex and olfactory bulbs; increased exposure of the colliculi; enlarged ventricles; reduced proliferation in the subventricular zone (SVZ) and the dentate gyrus (DG) of the hippocampus; hypoplasia of the optic nerve; retinal degeneration especially the inner nuclear layer (INL) and the outer nuclear layer (ONL); enhanced S-cone generation; thinning of the inner plexiform layer (IPL), outer plexiform layer (OPL), and

---

[3] This chapter is in preparation for submission for publication. Wong, B.K.Y., Borrie, A.E., Tam, C., Cheng, J.C.Y., Sze, J., Yang, W.H.W., Ottmann, G.A., Abrahams, B.S., Wallace, V. and Simpson, E.M.. Increased *Nr2e1* transcription affects gene regulation, cell proliferation, and brain and eye morphology in mice.

the photoreceptor outer segment (OS); and reduced to flat electroretinogram (Christie *et al.*, 2006, Land & Monaghan, 2003, Li *et al.*, 2008, Liu *et al.*, 2008, Miyawaki *et al.*, 2004, Monaghan *et al.*, 1997, Monaghan *et al.*, 1995, Roy *et al.*, 2004, Roy *et al.*, 2002, Shi *et al.*, 2004, Stenman *et al.*, 2003a, Stenman *et al.*, 2003b, Young *et al.*, 2002, Yu *et al.*, 2000, Zhang *et al.*, 2006).

The role of *NR2E1* in human neurological diseases is also starting to become evident. The 6q21-22 region, where *NR2E1* is located, has been shown by a meta-analysis of original data from 11 genome-wide linkage studies to have the highest LOD score (4.19) for bipolar I disorder (BPI), a psychiatric disorder characterized by mood fluctuations ranging from mania to depression (Mcqueen *et al.*, 2005). Recent work from our laboratory identified novel candidate-regulatory mutations in *NR2E1* in patients with either severe cortical malformations or BPI, as well as a significant association between *NR2E1* and BPI (Kumar *et al.*, 2007, Kumar *et al.*, 2008).

Although *NR2E1* has not yet been studied in human eye disorders, numerous mutations in *NR2E3*, the closest relative of *NR2E1*, have been characterized in enhanced S-cone syndrome (ESCS), Goldmann-Favre syndrome (GFS), clumped pigmentary retinal degeneration (CPRD), and retinitis pigmentosa (RP) (Bandah *et al.*, 2009, Pachydaki *et al.*, 2009, Schorderet & Escher, 2009). Mouse mutants carrying patient variants of *Nr2e3* have also displayed phenotypes similar to those seen in patients (Haider *et al.*, 2006, Wang *et al.*, 2009). Functional changes caused by patient-specific variants in *NR2E3* have not been fully characterized; however, it appears that the mutations do not always result in a loss of inhibitory function (Fradot *et al.*, 2007).

Since *NR2E1* is essential to normal neural and retinal development, variants identified from patients with BPI, and potential future variants from eye disorders, are highly unlikely to be null mutations. *NR2E1* variants, especially those found in regulatory and untranslated regions (Kumar *et al.*, 2007, Kumar *et al.*, 2008), may exude their effects by altering *NR2E1* transcript levels or stability, which makes it imperative to study the effects of varying *Nr2e1* levels.

The bulk of our knowledge has come from studying the phenotypes of *Nr2e1*-null mice; however, the effects of *Nr2e1* overexpression have not yet been examined. This study aims to evaluate the transcriptional, morphological, and cellular phenotypes resulting from *Nr2e1* overexpression in mice. This new set of data will further our understanding of the pathways in which *Nr2e1* functions.

4.2 Methods and materials

4.2.1 Mice

Random insertion transgenic mice carrying mouse and human *NR2E1* examined here have been previously published (Abrahams *et al.*, 2003, Abrahams *et al.*, 2005). Briefly, founders carrying a BAC clone containing the mouse *Nr2e1* genomic locus were generated on a C57BL/6J × 129S1/SvImJ hybrid background (B6129F1) and backcrossed to C57BL/6J to generate C57BL/6J.Cg-Tg(*Nr2e1*bacEMS4A)5Ems and C57BL/6J.Cg-Tg(*Nr2e1*bacEMS4B)6Ems strains, abbreviated to B6-bacEMS4A and B6-bacEMS4B respectively (Abrahams *et al.*, 2003). Similarly, two mouse strains carrying a PAC clone spanning human *NR2E1* were backcrossed to C57BL/6J to generate C57BL/6J.Cg-Tg(*NR2E1*pacEMS1B)10Ems and C57BL/6J.Cg-Tg(*NR2E1*pacEMS1D)11Ems,

abbreviated to B6-pacEMS1B and B6-pacEMS1D respectively (Abrahams *et al.*, 2005).

All mice were full congenics by backcrossing to C57BL/6J for more than 10 generation

before analysis. All mice were weaned at postnatal day (P)18 – 21 and housed with same-

sex littermates. Mice were provided with food and water *ad libitum* and standard care

according to University of British Columbia animal care policies. Handling of all mice

was minimized. Timed pregnancies were set up for collecting embryos of different

developmental timepoints. Mice (2 – 6 months old) were used for adult analysis.

4.2.2 Genotyping

Three PCR assays were used to genotype individuals before and after each

experiment. A common assay used for both BAC and PAC mice detects the presence of

the endogenous mouse *Nr2e1* gene using oEMS1859 (5′-

CTGGGCCCTGCAGATACTC-3′) and oEMS1860 (5′-

GGTGGCATGATGGGTAACTC-3′) (Abrahams *et al.*, 2005). A BAC-specific assay

detects the presence of the pBeloBAC11 vector using oEMS1753 (5′-

CTGGCGAAAGGGGGATGT-3′) and oEMS1755 (5′-

GCTGGAGGGGAATGGAAAAC-3′) (Abrahams *et al.*, 2003). A PAC-specific assay

detects the presence of the human *NR2E1* using oEMS800 (5′-

CCCAGCAGCTGCGGTTTTGC-3′) and oEMS801 (5′-

GCAGCGCTCCAGGCAGGAC-3′) (Abrahams *et al.*, 2005). The PCR conditions were

92°C for 2 min, 30 cycles of 94°C for 30 sec, 58°C for 30 sec, and 72°C for 55 sec, and

72°C for 5 min.

4.2.3 Interphase and metaphase FISH

Detailed methods for performing interphase and metaphase fluorescence *in situ* hybridization (FISH) have previously been published (Abrahams *et al.*, 2003). Briefly, interphase chromosomes were prepared from interphase nuclei obtained from peripheral blood smears. Interphase chromosomes were probed with bEMS4 DNA labeled with biotin-14-dCTP and pEMS1 DNA labeled with biotin-14-dCTP for detection of mouse *Nr2e1* and PAC clone spanning the human *NR2E1*, respectively. Metaphase chromosomes were prepared from lung tissue cultures. Metaphase chromosomes were probed with pEMS1 DNA labeled with dig-14-dUTP for detection of PAC clone spanning human *NR2E1* and chromosome-specific probes (Incyte Genomics, St. Louis, MO).

4.2.4 Quantitative reverse transcriptase PCR

RNA from embryonic day (E)12.5 whole brain, adult forebrain, and adult eyes were extracted using Qiagen RNA Mini Plus Kit (Cat#74134; Qiagen Inc., Mississauga, ON). RNA was cleaned with Qiagen DNase kit (Cat#79254; Qiagen Inc., Mississauga, ON) and cDNA generated using SuperScript III Master Mix kit (Cat#11752-050; Invitrogen, Carlsbad, CA). cDNA quantification was performed using ABI TaqMan® assays specifically designed for *Aqp4*, *Ccnd1*, *Dcx*, *Gfap, Gsk3β*, *Nes*, *Nr2e1*, *NR2E1*, *Nr2e3*, *Nr4a2*, *Opsin1sw*, *Pax6*, *Pten*, and *S100β*. The 7500 Fast real-time PCR system and TaqMan® Fast Universal PCR Master Mix (Cat#4352042; Applied Biosystems Inc., Foster City, CA) was used for all the qRT-PCR runs. The cycle threshold (Ct) value was

defined as the number of cycles required for the fluorescent signal to cross a threshold above background signals and is inversely proportional to the amount of target cDNA.

4.2.5 Brain and eye harvesting

4.2.5.1 Tissue for RNA extraction

Adult brains were freshly dissected from the skull; a coronal cut was made at the caudal end of the cortical lobes and the anterior portion of the cut brains were used for RNA extraction. Embryos were collected at E12.5 in cold saline and whole heads were removed. Eyes were also freshly extracted from adult mice. All tissues harvested for qRT-PCR were flash frozen in liquid nitrogen.

4.2.5.2 Tissue for immunofluorescence

Mice for brain harvesting were injected intraperitoneally (i.p.) with heparin and perfused intracardially with 4% paraformaldehyde, 30 min following the heparin injection. Whole brains were dissected from the skull intact and placed into 4% paraformaldehyde in 1× PBS at 4°C for 48 h, then transferred to a 20% sucrose solution at 4°C until saturated. Prior to sectioning, images of brains were taken on the Leica MZ6 (Leica Microsystems Inc., Bannockburn, IL). These images were traced using Image-Pro Express (Media Cybernetics Inc., Bethesda, MD) for quantification of brain regions. Brains were then sectioned at 25 μm using the Cryo-Star HM 560 cryostat (MICROM International, Walldorf, Germany) and every 24th section starting from the most rostral aspect of the ventricles to the most caudal aspect of the hippocampus was analyzed by immunofluorescence.

For eye harvesting, mice were sacrificed by cervical dislocation and eyes were removed. Eyes were placed into 4% paraformaldehyde in 1× PBS at 4°C for 24 h, then transferred to a 20% sucrose solution at 4°C until saturated. Eyes were then sectioned at 14 μm using the Cryo-Star HM 560 cryostat (MICROM International, Walldorf, Germany) and every 30th section was analyzed by immunofluorescence.

4.2.6 Immunofluorescence

Free-floating brain sections and mounted eye sections were blocked with 5% normal goat serum (NGS) + 5% bovine serum albumin (BSA) in 0.1% Triton-X100 in PBS. Brain sections were incubated overnight at room temperature (RT) with rabbit anti-Ki67 polyclonal antibody (1:1000 dil, Cat. #ab15580, Abcam Inc., Cambridge, MA), and further incubated with Alexa Fluor® 594 goat anti-rabbit IgG (H+L) (Cat. #A31631, Invitrogen, Carlsbad, CA). Eye sections were incubated overnight at RT with: mouse anti-CRALBP (1:1000 dil, Cat. #sc-48354, Santa Cruz Biotech., Santa Cruz, CA); mouse anti-GFAP (1:1000 dil, Cat. #VP-G805, Vector Laboratories., Burlingame, CA); rabbit anti-Pax6 (1:1000 dil, Cat. #sc-11357, Santa Cruz Biotech., Santa Cruz, CA); mouse anti-rhodopsin (clone B630, 1:150 dil, gift from Dr. Valarie Wallace); and mouse anti-syntaxin (clone HPC-1, 1:1000 dil, Cat. #S0664, Sigma-Aldrich Ltd., Oakville, ON), and further incubated with either Alexa Fluor® 488 goat anti-mouse IgG (H+L) (Cat. #A11001, Invitrogen, Carlsbad, CA) or Alexa Fluor® 594 goat anti-rabbit IgG (H+L) (Cat. #A31631, Invitrogen, Carlsbad, CA). Hoechst 33342 was used for nuclear staining for all sections. All sections were mounted onto Superfrost® Plus slides (Cat. #12-550-15, Fisher Scientific, Ottawa, ON) and coverslipped using Vectashield Hard Set™ (Cat. #H-1400, Vector Laboratories, Inc., Burlingame, CA). Images were captured on an Olympus

BX61 motorized fluorescence microscope (Olympus America Inc., Center Valley, PA). Proliferating cells in the SVZ and DG were counted using the ImageJ software (Rasband, 1997-2009).

4.2.7 Statistical analysis

All data were analyzed using STATISTICA$^©$ 6 (StatSoft, Inc., Tulsa, OK). QRT-PCR and brain morphological data were analyzed by factorial ANOVA for strain and genotype effects. When significant effects were found, *post-hoc* tests with Tukey correction were performed for multiple comparisons to reveal the underlying differences within the main effects. Data are reported as mean values ± 1 standard error of the mean (SEM).

4.3 Results

4.3.1 High copy integration of B6-pacEMS into mouse genome

The generation of B6-bacEMS4 and B6-pacEMS1 mice and the mapping of the BAC inserts have been described in detail in Abrahams *et al*. (2003, 2005); however, the mapping of the 141-kb PAC in the two strains of B6-pacEMS1 mice has not been shown. Interphase fluorescence *in situ* hybridization (FISH) showed an intense signal from the human specific probe at Chromosome 6 (band A2) and Chromosome 4 (band A2) in B6-pacEMS1B and B6-pacEMS1D mice, respectively (Fig. 4.1). The intensity of the signals compared to the endogenous locus probed with mouse specific bEMS4 DNA suggested high copy of PAC integration.
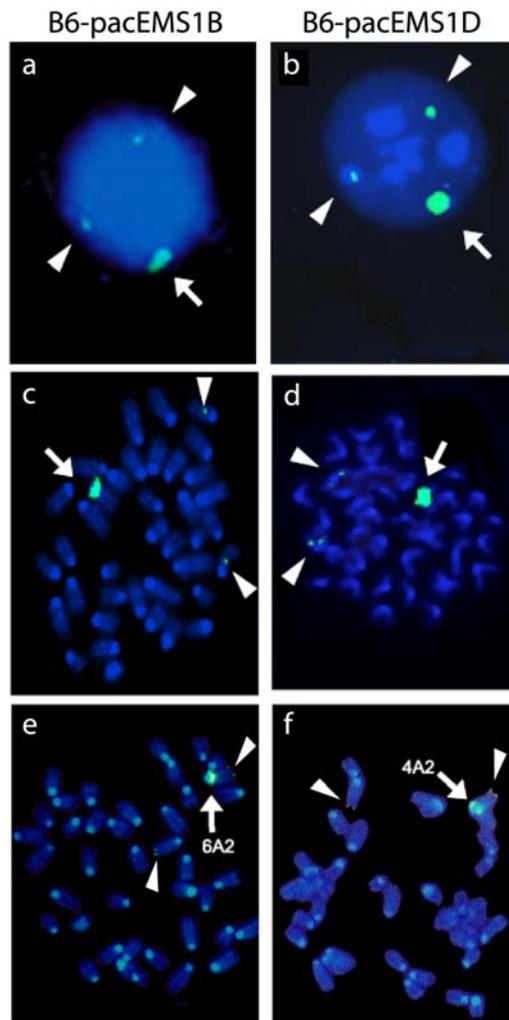
Figure 4.1 FISH mapping of pacEMS1 transgenes

(a & b) Interphase and (c & d) metaphase FISH using probes specific for mouse and human *NR2E1* of pacEMS1B and pacEMS1D, respectively. Both pacEMS1B and 1D show two single copy endogenous signals of mouse *Nr2e1* (arrowheads) and a more intense signal indicative of transgene (arrow). (e & f) Metaphase FISH using mapping probes and probe specific for human *NR2E1* of pacEMS1B and pacEMS1D, respectively. Both pacEMS1B and 1D show two signals from chromosome 6 and 4 mapping probes (arrowheads) respectively, and an intense signal indicative of the transgene (arrow). Further banding localized the human transgene to chromosome 6A2 and 4A2 for pacEMS1B and pacEMS1D respectively.

4.3.2 B6-bacEMS4A mice show increased *Nr2e1* transcription

Transcription of mouse *Nr2e1* and human *NR2E1* from the high copy inserts of BAC and PAC, respectively, were examined. Mouse *Nr2e1* transcript levels from whole head of embryonic day (E)12.5 embryos of B6-bacEMS4A, B6-bacEMS4B, B6-pacEMS1B, and B6-pacEMS1D were examined using a mouse-specific *Nr2e1* TaqMan assay. B6-bacEMS4A transgenic E12.5 heads showed a significant increase in the level of *Nr2e1* transcripts (Fig. 4.2a; Wt = 1.00 ± 0.15-fold change, Tg = 2.07 ± 0.26-fold change, $P < 0.05$), while there were no significant differences in embryonic heads of B6-bacEMS4B (Fig. 4.2a; Wt = 1.00 ± 0.18-fold change, Tg = 1.01 ± 0.19-fold change, $P > 0.05$), B6-pacEMS1B (Fig. 4.2a; Wt = 1.00 ± 0.26-fold change, Tg = 0.73 ± 0.14-fold change, $P > 0.05$), and B6-pacEMS1D (Fig. 4.2a; Wt = 1.00 ± 0.21-fold change, Tg = 0.88 ± 0.19-fold change, $P > 0.05$) transgenics compared to their Wt counterparts.

Similarly, the anterior portion of the adult brain transcript level of *Nr2e1* was only significantly higher in B6-bacEMS4A Tg (Fig. 4.2b; Wt = 1.00 ± 0.19-fold change, Tg = 4.79 ± 0.76-fold change, $P < 0.05$), and not in B6-bacEMS4B (Fig. 4.2b; Wt = 1.00 ± 0.20-fold change, Tg = 1.02 ± 0.19-fold change, $P > 0.05$), B6-pacEMS1B (Fig. 4.2b; Wt = 1.00 ± 0.19-fold change, Tg = 0.73 ± 0.18-fold change, $P > 0.05$), and B6-pacEMS1D (Fig. 4.2b; Wt = 1.00 ± 0.19-fold change, Tg = 1.02 ± 0.19-fold change, $P > 0.05$) when compared to Wt. These results indicate that high copy number of BAC inserts in B6-bacEMS4A results in increased transcription of mouse *Nr2e1*.

a) E12.5 whole head

b) Anterior portion of adult brain
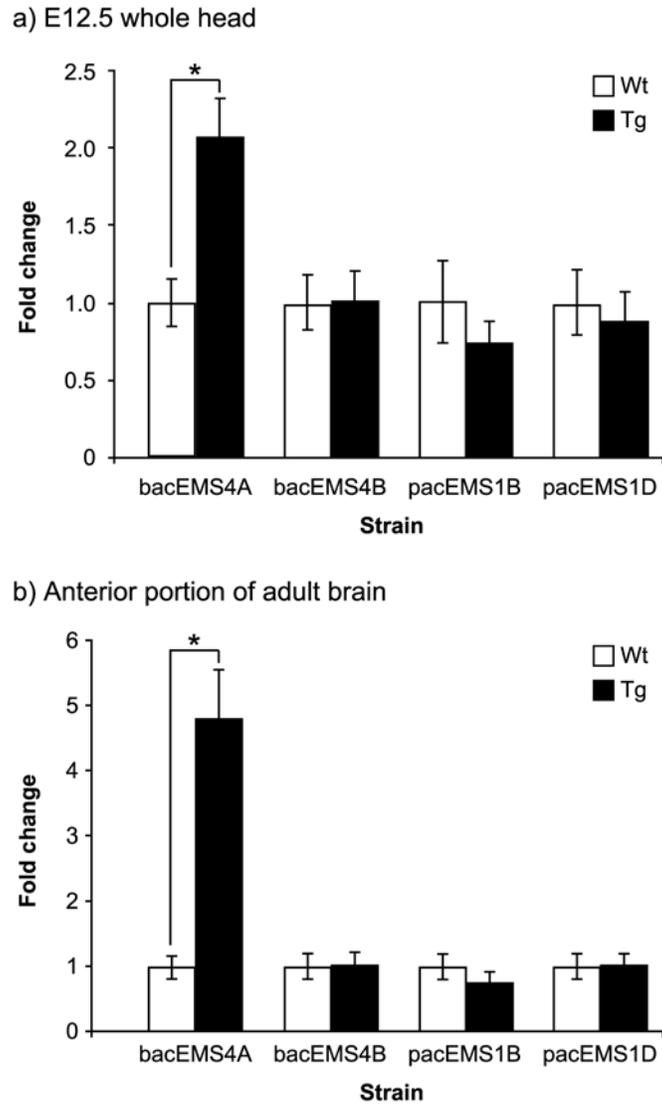
Figure 4.2 B6-bacEMS4A show increased *Nr2e1* expression in E12.5 whole head and adult brain

B6-bacEMS4A was the only strain that showed significant fold increase of *Nr2e1* expression in (a) E12.5 whole head and (b) anterior portion of adult brain. * $P < 0.05$. N = 5 per strain/genotype/age.

4.3.3 PAC mice show overexpression of human *NR2E1*

A human-specific *NR2E1* TaqMan assay only detected transcripts in human whole brain, B6-pacEMS1B, B6-pacEMS1D, and rescue transgenic mice and not in Wt B6 mice (Table 4.1), corresponding to qRT-PCR results previously demonstrated in Abrahams *et al*. (2003).

Table 4.1 Ct values obtained from human-specific *NR2E1* TaqMan assay

Genotype	Ct
Human RNA	31.4 $\pm$ 0.13
B6-pacEMS1B	32.4 $\pm$ 0.26
B6-pacEMS1D	38.0 $\pm$ 1.42
Rescue	31.0 $\pm$ 0.10
B6	Not detectable
Water	Not detectable

Expression level of human *NR2E1* in both pacEMS1 transgenic strains was compared to the endogenous levels of mouse *Nr2e1* in Wt controls. Human *NR2E1* levels were significantly higher than endogenous level of mouse *Nr2e1* in E12.5 B6-pacEMS1B (Fig. 4.3a; Wt mouse *Nr2e1* = 1.00 $\pm$ 0.34-fold change, Tg human *NR2E1* = 3.91 $\pm$ 0.98-fold change, $P < 0.05$), E12.5 B6-pacEMS1D (Fig. 4.3a; Wt mouse *Nr2e1* = 1.00 $\pm$ 0.21-fold change, Tg human *NR2E1* = 30.7 $\pm$ 6.13-fold change, $P < 0.05$), adult B6-pacEMS1B (Fig. 4.3b; Wt mouse *Nr2e1* = 1.00 $\pm$ 0.19-fold change, Tg human *NR2E1* = 4.97 $\pm$ 1.14-fold change, $P < 0.05$), and adult B6-pacEMS1D (Fig. 4.3b; Wt mouse *Nr2e1* = 1.00 $\pm$ 0.19-fold change, Tg human *NR2E1* = 7.36 $\pm$ 1.48-fold change, $P < 0.05$) indicating that high copy number of PAC inserts results in increased transcription of the

human *NR2E1* gene, similar to increased transcription of the mouse *Nr2e1* gene in B6-

bacEMS4A mice.

a) E12.5 whole head

b) Anterior portion of adult brain
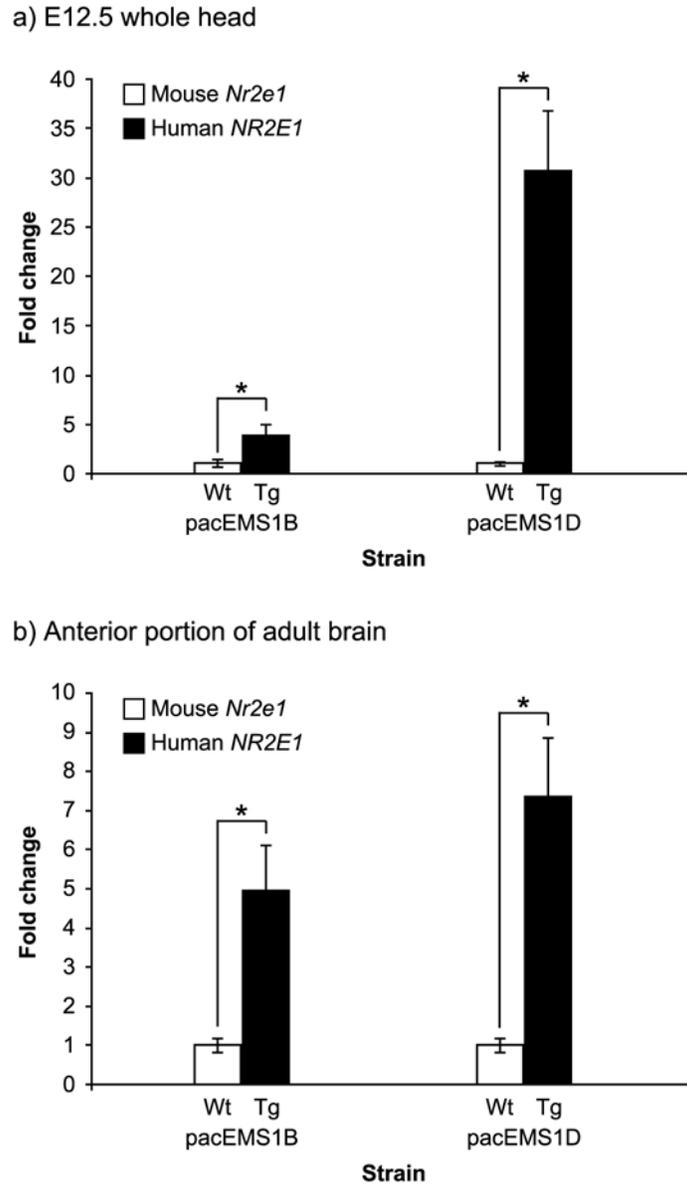
Figure 4.3 B6-pacEMS1B and 1D showed significant increase in level of human *NR2E1*
Level of human *NR2E1* transcript from B6-pacEMS1B and 1D transgenic (a) E12.5
whole head and (b) anterior portion of adult brain showed significant fold increase when
compared to the level of mouse *Nr2e1* from equivalent Wt regions. * $P < 0.05$. N = 5 per
strain/genotype/age.

4.3.4 Characterization of gross brain and eye morphology of four transgenic strains

Hypoplasia of the olfactory bulbs and frontal lobes and gross neuroanatomical differences are well documented in mice lacking *Nr2e1*, therefore we obtained detailed measurements of various brain regions to document effects of increased *Nr2e1* transcription on brain morphology. B6-bacEMS4A transgenic mice showed significantly reduced brain weight when compared to Wt mice (Table 4.2). However, this weight reduction was not observed in the other strains. All four transgenic strains of mice were also examined for eye phenotypes including: corneal opacity, microphthalmia, and anophthalmia. B6-bacEMS4A Tg mice showed increased frequency of eye phenotypes compared to Wt mice, while the other three Tg strains did not (Table 4.2). B6-bacEMS4A also showed bilateral and unilateral optic nerve hypoplasia (data not shown). These eye abnormalities are grossly reminiscent of those seen in $Pax6^{+/Sey}$ mice (Hill *et al.*, 1991, Ramaesh *et al.*, 2003).

Table 4.2 Gross phenotypic description of the four transgenic strains

	bacEMS4A			bacEMS4B		
	Wt (n = 6)	Tg (n = 6)	*P*	Wt (n = 6)	Tg (n = 7)	*P*
Transgene location	N/A	Chr 16[1]	N/A	N/A	Chr 13[1]	N/A
Body weight (g)	24.8 ± 1.14	24.5 ± 1.13	0.46	24.2 ± 2.01	22.0 ± 1.29	0.19
Brain weight (g)	0.61 ± 0.01	0.57 ± 0.01	0.04*	0.59 ± 0.01	0.60 ± 0.01	0.34
Eye phenotype	0 affected	6 affected	<0.001*	0 affected	2 affected	0.15
	pacEMS1B			pacEMS1D		
	Wt (n = 6)	Tg (n = 6)	*P*	Wt (n = 6)	Tg (n = 7)	*P*
Transgene location	N/A	Chr 6	N/A	N/A	Chr 4	N/A
Body weight (g)	25.4 ± 2.03	26.0 ± 2.26	0.69	30.1 ± 2.83	31.7 ± 1.25	0.48
Brain weight (g)	0.46 ± 0.01	0.45 ± 0.01	0.69	0.53 ± 0.01	0.54 ± 0.01	0.66
Eye phenotype	0 affected	0 affected	1.00	1 affected	2 affected	0.50

[1] Abrahams *et al.* (2003)
* statistical significance

A multifactorial ANOVA was performed on all brain measurements of all four transgenic strains. From this analysis, significant main effects of strain ($F(3,39) = 10.4$, $P < 0.001$) and genotype ($F(1,13) = 3.49$, $P < 0.01$), and a significant interaction between strain and genotype ($F(3,39) = 2.72$, $P < 0.001$) were observed. These results indicate that there were inter-strain differences in brain morphology that was genotype-dependent and that the four strains are significantly different from each other. However, *post-hoc* analysis did not identify any significant genotype effect in any brain measurements in the four strains (Table 4.3). Since *post-hoc* analysis did not reveal the underlying source of the significant strain and genotype effects, we analyzed the four strains separately. In these analyses, only B6-bacEMS4A showed a significant effect of genotype ($F(1,8) = 66501$, $P < 0.005$). These results collectively suggest that only B6-bacEMS4A transgenic mice show an effect of over-transcription of *Nr2e1* on brain morphology.

Table 4.3 Gross brain measurements in the four transgenic strains

	bacEMS4A			bacEMS4B		
	Wt (n = 6)	Tg (n = 6)	*Post-hoc P*	Wt (n = 6)	Tg (n = 7)	*Post-hoc P*
Olfactory bulb area (dorsal) (mm^2)	9.53 ± 0.40	10.1 ± 0.36	0.952	10.2 ± 0.32	10.8 ± 0.18	0.893
Olfactory bulb area (ventral) (mm^2)	13.4 ± 0.35	13.1 ± 0.50	1.00	13.2 ± 0.26	13.4 ± 0.53	0.977
Cerebrum area (dorsal) (mm^2)	73.2 ± 1.02	70.1 ± 1.91	0.479	74.6 ± 0.23	75.2 ± 0.91	1.00
Cerebrum area (ventral) (mm^2)	68.4 ± 0.70	68.8 ± 1.44	0.488	65.7 ± 0.64	66.6 ± 0.82	1.00
Cerebral cortex length (mm)	6.19 ± 0.13	5.95 ± 0.30	0.959	6.45 ± 0.11	6.46 ± 0.13	1.00
Cerebral cortex width (mm)	10.4 ± 0.06	10.2 ± 0.08	0.427	10.3 ± 0.04	10.5 ± 0.07	0.715
Colliculi exposure (mm)	1.90 ± 0.07	2.18 ± 0.05	0.175	2.05 ± 0.06	2.17 ± 0.07	0.951
Hypothalamus area (mm^2)	7.77 ± 0.42	7.03 ± 0.38	0.934	8.27 ± 0.33	8.71 ± 0.30	0.998
Hypothalamus length (mm)	3.00 ± 0.18	2.83 ± 0.14	0.982	3.22 ± 0.16	3.50 ± 0.10	0.911
Hypothalamus width (mm)	3.47 ± 0.06	3.31 ± 0.04	0.956	3.50 ± 0.06	3.52 ± 0.03	1.00
Cerebellum area (mm^2)	26.2 ± 1.10	26.2 ± 1.22	1.00	23.0 ± 0.34	23.8 ± 0.68	0.993
Cerebellum width (mm)	8.24 ± 0.04	8.19 ± 0.08	0.997	8.22 ± 0.05	8.32 ± 0.08	0.934
Brainstem width (mm)	5.49 ± 0.14	5.74 ± 0.28	0.887	5.52 ± 0.03	5.89 ± 0.21	0.241

	pacEMS1B			pacEMS1D		
	Wt (n = 6)	Tg (n = 6)	*Post-hoc P*	Wt (n = 6)	Tg (n = 7)	*Post-hoc P*
Olfactory bulb area (dorsal) (mm^2)	8.20 ± 0.24	8.17 ± 0.32	1.00	9.24 ± 0.40	9.41 ± 0.38	1.00
Olfactory bulb area (ventral) (mm^2)	10.1 ± 0.38	9.72 ± 0.37	0.999	10.1 ± 0.30	10.1 ± 0.39	1.00
Cerebrum area (dorsal) (mm^2)	64.4 ± 0.83	63.7 ± 1.15	1.00	70.7 ± 0.89	68.1 ± 0.80	0.725
Cerebrum area (ventral) (mm^2)	57.5 ± 1.01	57.3 ± 0.45	1.00	61.6 ± 0.86	60.3 ± 0.42	0.976
Cerebral cortex length (mm)	5.98 ± 0.09	5.80 ± 0.14	0.991	6.68 ± 0.04	6.50 ± 0.12	0.992
Cerebral cortex width (mm)	9.72 ± 0.05	9.73 ± 0.09	1.00	10.1 ± 0.04	9.84 ± 0.06	0.127
Colliculi exposure (mm)	2.08 ± 0.09	2.00 ± 0.09	0.991	1.76 ± 0.05	1.90 ± 0.10	0.885
Hypothalamus area (mm^2)	6.61 ± 0.27	6.98 ± 1.08	0.999	7.56 ± 0.16	7.00 ± 0.25	0.985
Hypothalamus length (mm)	3.10 ± 0.16	2.72 ± 0.16	0.468	3.02 ± 0.06	2.82 ± 0.09	0.962
Hypothalamus width (mm)	2.85 ± 0.05	3.14 ± 0.29	0.544	3.08 ± 0.06	3.01 ± 0.04	1.00
Cerebellum area (mm^2)	23.0 ± 0.85	22.4 ± 0.54	1.00	20.1 ± 0.32	19.9 ± 0.30	1.00
Cerebellum width (mm)	7.72 ± 0.04	7.74 ± 0.03	1.00	8.01 ± 0.04	7.76 ± 0.05	0.0809
Brainstem width (mm)	5.01 ± 0.03	5.08 ± 0.08	1.00	5.21 ± 0.07	5.23 ± 0.04	1.00

4.3.5 B6-bacEMS4A mice show altered transcription level of *Gfap* and *Gsk3β*

The transcription levels of *Aqp4*, *Ccnd1*, *Dcx*, *Gfap, Gsk3β*, *Nes*, *Nr4a2*, *Pten*,

and *S100β* were examined in the anterior portion of adult brains in all four transgenic

strains. With the exception of *Gfap* that is not transcribed at E12.5, the rest of the gene set

was examined in E12.5 whole heads. These genes were selected for analysis based on

literature showing an interaction with *Nr2e1* or their involvement in cell cycle regulation.

Since we had no *a priori* hypothesis that gene transcription had to be concordant

throughout time, we analyzed the two time points separately. A multifactorial ANOVA

was first performed on transcription data of all target genes from adult brains of the four

transgenic strains. From this analysis, significant effects of strain ($F(3,27) = 50.3$, $P <$

0.001) and genotype ($F(1,9) = 271.5$, $P < 0.001$), and a significant interaction between

strain and genotype ($F(3,27) = 51.8$, $P < 0.001$) were observed. *Post-hoc* analysis

revealed that genotype differences were only observed in the B6-bacEMS4A strains. B6-

bacEMS4A transgenic adult brain showed significantly increased *Gsk3β* and a trend for

reduced *Gfap* transcription compared to Wt brains (Table 4.4a). These results are

consistent with the brain morphological data indicating that the B6-bacEMS4A strain is

the only significantly affected transgenic strain.

Analysis of the transcription data from E12.5 whole brain were treated identically

to that of adult brain, except for *Gfap* that was removed from the gene set because it is

not transcribed in E12.5 whole head. The multifactorial ANOVA revealed significant

main effects of strain ($F(3,24) = 5.99$, $P < 0.001$) and genotype ($F(1,8) = 23.4$, $P <$

0.001), and a significant interaction between strain and genotype ($F(3,24) = 6.77$, $P <$

0.001). When we performed *post-hoc* analysis, we did not identify any significant

genotype effect in any particular gene in the four strains (Table 4.4b). Therefore, at E12.5

the presence of increased *Nr2e1* transcripts results in minor transcriptional differences

that only collectively contribute to the main effects detected.

Table 4.4 Fold change of target gene transcript in the four transgenic strains

a) Anterior portion of adult brain

Gene symbol	Age	bacEMS4A			Age	bacEMS4B		
		Wt (n = 5)	Tg (n = 5)	Post-hoc P		Wt (n = 5)	Tg (n = 5)	Post-hoc P
Aqp4	Adult	1.00 ± 0.14	1.12 ± 0.18	0.893	Adult	1.00 ± 0.09	1.01 ± 0.11	1.00
Ccnd1	Adult	1.00 ± 0.09	1.15 ± 0.08	0.923	Adult	1.00 ± 0.14	1.05 ± 0.15	1.00
Dcx	Adult	1.00 ± 0.43	1.44 ± 0.47	0.675	Adult	1.00 ± 0.20	1.31 ± 0.38	0.886
Gfap	Adult	1.00 ± 0.06	0.70 ± 0.10	0.0811^	Adult	1.00 ± 0.14	1.17 ± 0.16	0.556
Gsk3β	Adult	1.00 ± 0.18	1.51 ± 0.23	0.0152*	Adult	1.00 ± 0.11	0.93 ± 0.10	0.999
Nes	Adult	1.00 ± 0.59	1.72 ± 0.74	0.411	Adult	1.00 ± 0.25	0.73 ± 0.16	0.987
Nr4a2	Adult	1.00 ± 0.36	1.34 ± 0.37	0.763	Adult	1.00 ± 0.23	0.72 ± 0.16	0.863
Pten	Adult	1.00 ± 0.15	1.34 ± 0.18	0.230	Adult	1.00 ± 0.21	0.91 ± 0.18	0.996
S100b	Adult	1.00 ± 0.25	0.97 ± 0.18	1.00	Adult	1.00 ± 0.20	1.22 ± 0.21	0.891

Gene symbol	Age	pacEMS1B			Age	pacEMS1D		
		Wt (n = 5)	Tg (n = 5)	Post-hoc P		Wt (n = 5)	Tg (n = 5)	Post-hoc P
Aqp4	Adult	1.00 ± 0.06	0.82 ± 0.08	0.636	Adult	1.00 ± 0.13	0.98 ± 0.13	1.00
Ccnd1	Adult	1.00 ± 0.15	1.05 ± 0.17	1.00	Adult	1.00 ± 0.22	0.93 ± 0.20	0.999
Dcx	Adult	1.00 ± 0.20	0.82 ± 0.24	0.997	Adult	1.00 ± 0.19	1.13 ± 0.20	1.00
Gfap	Adult	1.00 ± 0.13	1.02 ± 0.11	1.00	Adult	1.00 ± 0.08	1.01 ± 0.09	1.00
Gsk3β	Adult	1.00 ± 0.18	0.62 ± 0.15	0.117	Adult	1.00 ± 0.10	0.97 ± 0.11	1.00
Nes	Adult	1.00 ± 0.18	0.69 ± 0.23	0.980	Adult	1.00 ± 0.33	1.09 ± 0.28	1.00
Nr4a2	Adult	1.00 ± 0.22	0.72 ± 0.13	0.851	Adult	1.00 ± 0.26	1.03 ± 0.20	1.00
Pten	Adult	1.00 ± 0.06	0.86 ± 0.10	0.964	Adult	1.00 ± 0.18	1.07 ± 0.17	0.999
S100b	Adult	1.00 ± 0.11	1.21 ± 0.30	0.855	Adult	1.00 ± 0.20	0.89 ± 0.14	0.997

b) E12.5 whole head

Gene symbol	Age	bacEMS4A			Age	bacEMS4B		
		Wt (n = 5)	Tg (n = 5)	Post-hoc P		Wt (n = 5)	Tg (n = 5)	Post-hoc P
Aqp4	E12.5	1.00 ± 0.30	0.94 ± 0.33	1.00	E12.5	1.00 ± 0.45	1.21 ± 0.53	0.999
Ccnd1	E12.5	1.00 ± 0.16	1.05 ± 0.13	1.00	E12.5	1.00 ± 0.16	1.06 ± 0.16	1.00
Dcx	E12.5	1.00 ± 0.11	1.02 ± 0.12	1.00	E12.5	1.00 ± 1.17	1.52 ± 1.18	0.989
Gsk3β	E12.5	1.00 ± 0.10	1.03 ± 0.11	1.00	E12.5	1.00 ± 0.13	0.95 ± 0.12	1.00
Nes	E12.5	1.00 ± 0.09	1.05 ± 0.11	1.00	E12.5	1.00 ± 0.20	1.01 ± 0.20	1.00
Nr4a2	E12.5	1.00 ± 0.16	1.20 ± 0.16	0.999	E12.5	1.00 ± 0.21	1.06 ± 0.19	1.00
Pten	E12.5	1.00 ± 0.10	1.06 ± 0.10	1.00	E12.5	1.00 ± 0.16	1.09 ± 0.16	0.999
S100b	E12.5	1.00 ± 0.18	0.91 ± 0.16	1.00	E12.5	1.00 ± 0.43	0.88 ± 0.41	1.00

Gene symbol	Age	pacEMS1B			Age	pacEMS1D		
		Wt (n = 5)	Tg (n = 5)	Post-hoc P		Wt (n = 5)	Tg (n = 5)	Post-hoc P
Aqp4	E12.5	1.00 ± 0.56	0.69 ± 0.35	0.976	E12.5	1.00 ± 0.51	1.08 ± 0.49	1.00
Ccnd1	E12.5	1.00 ± 0.25	1.21 ± 0.22	0.960	E12.5	1.00 ± 0.34	1.24 ± 0.40	0.909
Dcx	E12.5	1.00 ± 0.27	1.08 ± 0.23	1.00	E12.5	1.00 ± 0.30	1.16 ± 0.27	1.00
Gsk3β	E12.5	1.00 ± 0.38	1.31 ± 0.36	0.803	E12.5	1.00 ± 0.30	0.95 ± 0.25	1.00
Nes	E12.5	1.00 ± 0.18	1.41 ± 0.22	0.471	E12.5	1.00 ± 0.37	1.14 ± 0.39	0.996
Nr4a2	E12.5	1.00 ± 0.63	1.53 ± 0.69	0.832	E12.5	1.00 ± 0.44	1.53 ± 0.56	0.799
Pten	E12.5	1.00 ± 0.30	1.08 ± 0.23	1.00	E12.5	1.00 ± 0.21	1.22 ± 0.21	0.869
S100b	E12.5	1.00 ± 0.51	0.83 ± 0.31	0.997	E12.5	1.00 ± 0.50	0.91 ± 0.35	1.00

* statistical significance
^ statistical trend

4.3.6 Cell proliferation in the subventricular zone was altered in B6-bacEMS4A

Cell proliferation in neurogenic regions was quantified in the subventricular zone (SVZ) and dentate gyrus (DG) using Ki67 labeling. B6-bacEMS4A showed a significant increase in cell proliferation in the SVZ (Fig. 4.4a; Wt = 232.0 ± 31.7 Ki67+ cells/count area, Tg = 319.7 ± 46.6 Ki67+ cells/count area, $P = 0.05$), but not in the DG (Fig. 4.4b; Wt = 31.4 ± 3.1 Ki67+ cells/count area, Tg = 29.1 ± 4.3 Ki67+ cells/count area, $P > 0.1$) compared to Wt. However, B6-bacEMS4B showed no significant differences in cell proliferation in the SVZ (Fig. 4.4a; Wt = 117.1 ± 9.6 Ki67+ cells/count area, Tg = 122.5 ± 18.3 Ki67+ cells/count area, $P > 0.1$) or the DG (Fig. 4.4b; Wt = 17.3 ± 5.3 Ki67+ cells/count area, Tg = 19.1 ± 2.5 Ki67+ cells/count area, $P > 0.1$).
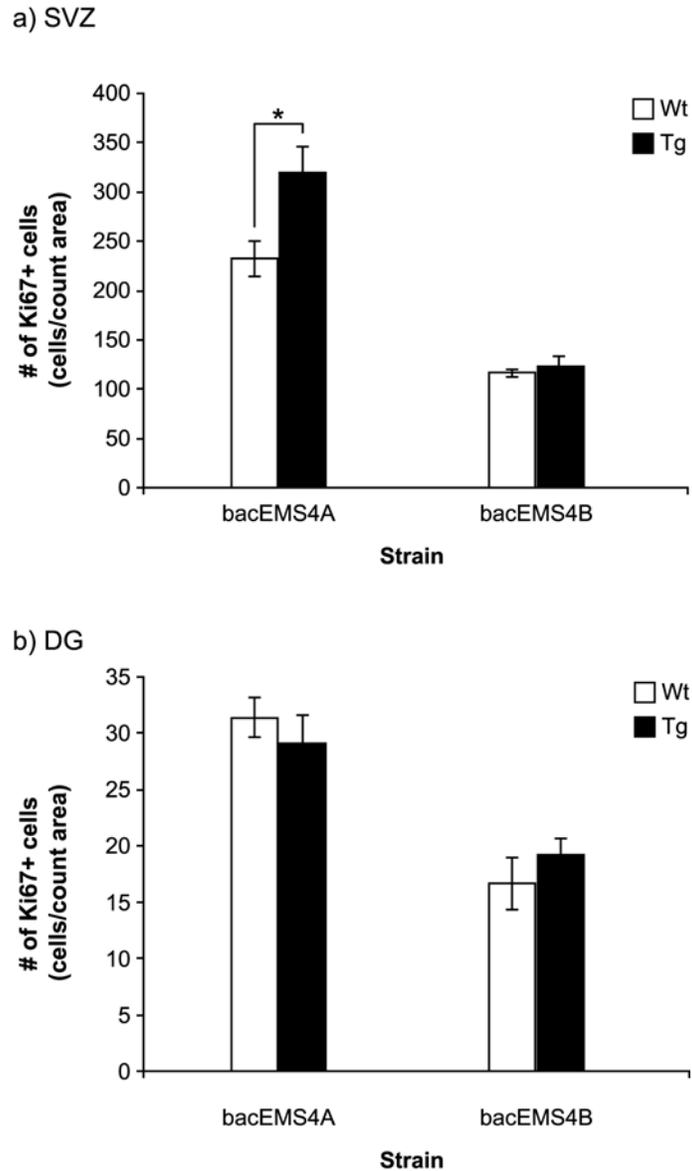
**Figure 4.4** B6-bacEMS4A showed significant increase in cell proliferation in the subventricular zone

(a) In the subventricular zone (SVZ), there were significantly more Ki67+ cells in B6-bacEMS4A, but not B6-bacEMS4B mice compared to Wt mice. * $P < 0.05$. (b) In the dentate gyrus (DG), there were no significant differences in Ki67+ cells in either B6-bacEMS4 strains compared to Wt. N = 3 per strain/genotype.

4.3.7 B6-bacEMS4A eyes showed thinning and disorganization of retinal cell layers

Since B6-bacEMS4A was the only strain to show overt eye phenotypes, further

effects of *Nr2e1* overexpression in the eye were examined only in B6-bacEMS4A. The

adult neural retina consists of 5 layers: the outer nuclear layer (ONL), the outer plexiform

layer (OPL), the inner nuclear layer (INL), the inner plexiform layer (IPL), and the

ganglion cell layer (GCL) (labeled in Fig. 4.6a and b). We performed

immunofluorescence with cell type specific markers and nuclear staining to compare

retinal organization of the B6-bacEMS4A transgenic and Wt mice. In Wt retina, Gfap

staining of Müller glia was observed in the GCL, however in B6-bacEMS4A transgenic

mice intraretinal Gfap staining indicated that there was gliosis, likely from Muller glia

(Fig. 4.5a and b). Rhodopsin staining of rods was reduced and sparse in B6-bacEMS4A

transgenic retina compared to Wt retina, consistent with thinning of the ONL indicative

of fewer photoreceptors (Fig. 4.5c and d). Syntaxin staining was observed in the IPL of

Wt and B6-bacEMS4A transgenic retina (Fig. 4.5e and f); however, Hoechst staining

showed cells protruding into the IPL from the normally tightly packed GCL indicating

disorganization of the GCL in the B6-bacEMS4A transgenic retina (Fig. 4.6b).

Staining for a nuclear marker showed that the ONL, INL, and IPL layers of the

B6-bacEMS4A retina were significantly thinner than Wt retina (Fig. 4.6). A

multifactorial ANOVA identified a significant main effect of genotype ($F(1,145) = 52.3$,

$P < 0.001$) and layers ($F(4,145) = 76.6$, $P < 0.001$), and a significant interaction between

genotype and layers ($F(4,145) = 13.1$, $P < 0.001$). *Post-hoc* analysis identified significant

genotype differences in the ONL, INL, and IPL (Fig. 4.6c-g; $P < 0.01$).
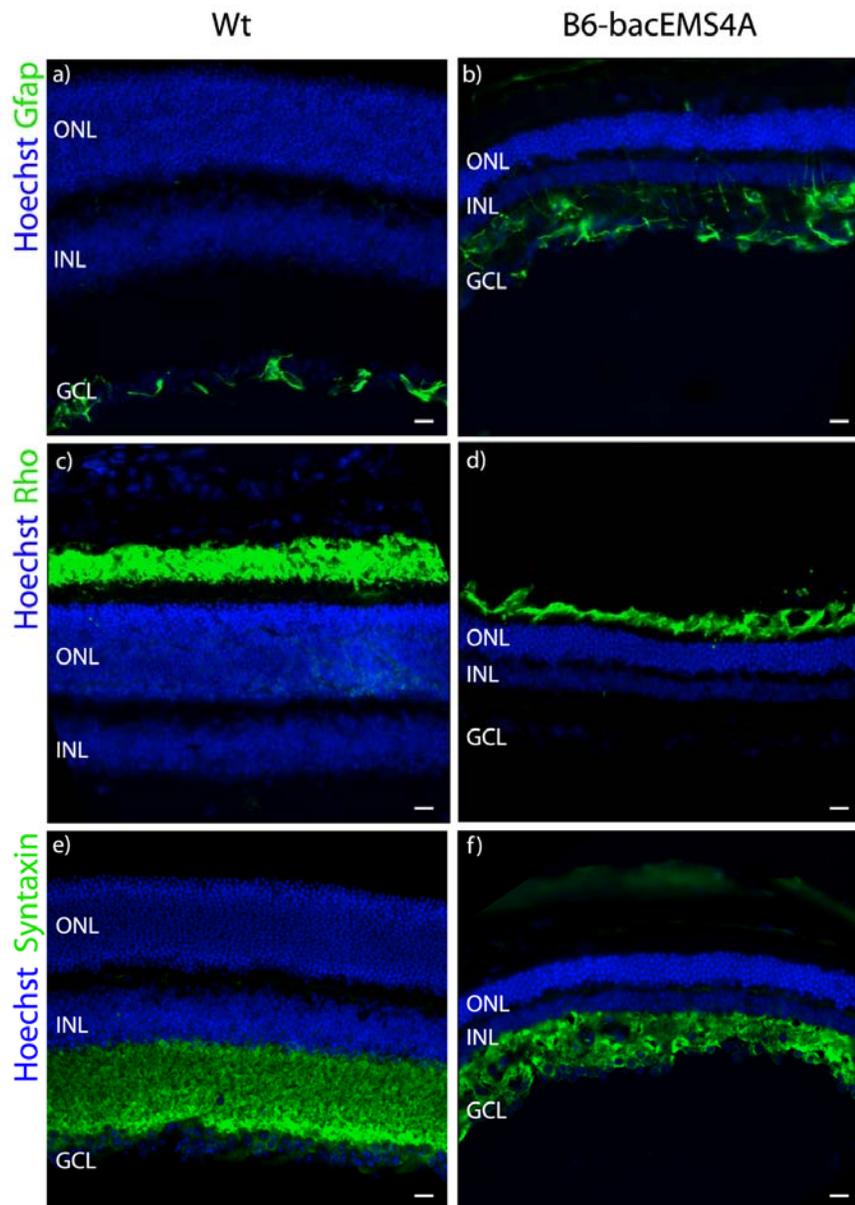
Figure 4.5 Adult B6-bacEMS4A eyes show abnormal cellular staining

(a & b) Gfap staining (green) of Müller glia in (a) Wt and (b) B6-bacEMS4A eyes, respectively, showed differences in staining between transgenic and Wt eyes. (c & d) Rhodopsin staining (green) of rod photoreceptors in (c) Wt and (d) B6-bacEMS4A eyes, respectively, showed reduced staining in transgenic eyes. (e & f) Syntaxin staining (green) of amacrine cells in (e) Wt and (f) B6-bacEMS4A eyes, respectively, showed abnormal staining in transgenic eyes. All nuclei were counterstained using Hoechst 33342 (blue). Outer nuclear layer (ONL); inner nuclear layer (INL); ganglion cell layer (GCL). White scale bar = 20 μm. N = 3 per genotype.
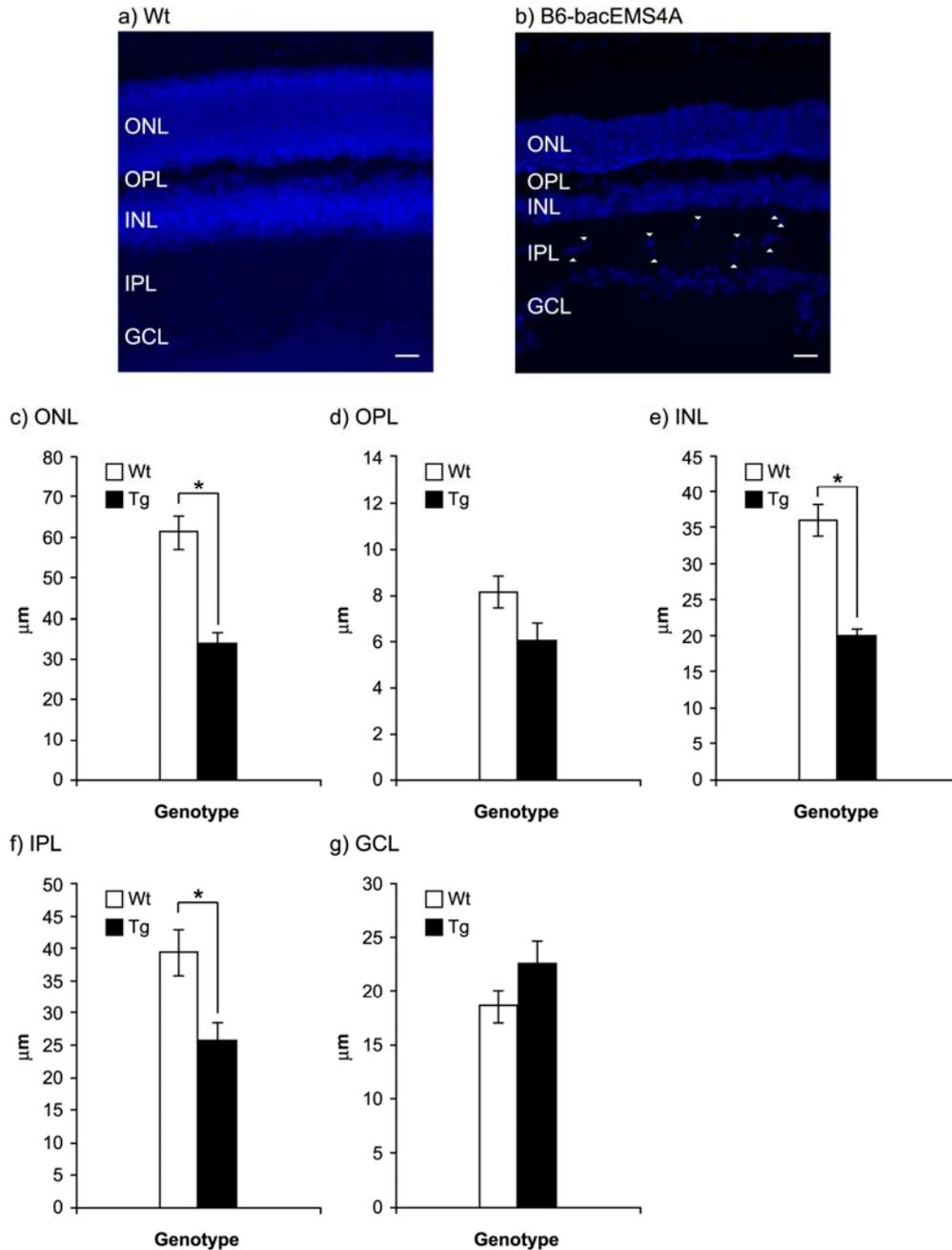
Figure 4.6 Adult B6-bacEMS4A eyes show thinning of retinal layers

Representative pictures of (a) Wt and (b) B6-bacEMS4A retina showed thinning of retinal layers. White arrowheads indicate cells seen in the IPL, which are not present in Wt retina. White scale bar = 20 μm. Five retinal layers: (c) outer nuclear layer (ONL); (d) outer plexiform layer (OPL); (e) inner nuclear layer (INL); (f) inner plexiform layer (IPL); and (g) ganglion cell layer (GCL), were measured for thickness in Wt and transgenic eyes. Significant thinning of the (c) ONL, (e) INL, and (f) IPL were observed in transgenic versus Wt retina. * $P < 0.001$. N = 3 per genotype.

4.3.8 Gene transcription is altered in B6-bacEMS4A eyes

Transcription of *Nr2e1* and other important developmental and retinal cell marker genes (*Gfap*, *Nr2e3*, *Opsin1sw*, and *Pax6*) were examined using quantitative reverse transcriptase PCR (qRT-PCR) in the B6-bacEMS4A adult eye. B6-bacEMS4A transgenic adult eye showed a significant increase in *Nr2e1* transcript level compared to Wt eyes (Fig. 4.7a; Wt = 1.00 ± 0.48-fold change, Tg = 3.34 ± 1.23-fold change, $P < 0.05$).

A significant effect of genotype ($F(1,4) = 23469$, $P < 0.005$) was observed for gene transcription of target genes in the adult eye. Similar to gene expression results from the brain, the level of *Gfap* transcript was also significantly decreased in B6-bacEMS4A transgenic adult eyes compared to Wt eyes (Fig. 4.7b; Wt = 1.00 ± 0.10-fold change, Tg = 0.67 ± 0.10-fold change, $P < 0.05$). Interestingly, transcript level of *Nr2e3*, a gene known to be involved in eye disease and the closest relative to *Nr2e1*, was significantly reduced in B6-bacEMS4A adult eyes (Fig. 4.7c; Wt = 1.00 ± 0.16-fold change, Tg = 0.28 ± 0.05-fold change, $P < 0.01$). *Opsin1sw*, expressed specifically in cones, was not significantly different in B6-bacEMS4A transgenic eyes (Fig. 4.7d; Wt = 1.00 ± 0.14-fold change, Tg = 0.74 ± 0.12-fold change, $P = 0.07$) compared to Wt eyes. And given the similarities observed between the B6-bacEMS4A transgenic and *Pax6*$^{+/Sey}$ adult eyes, we found, as expected, significant reduction of *Pax6* transcripts in B6-bacEMS4A transgenic eyes compared to Wt eyes (Fig. 4.7e; Wt = 1.00 ± 0.17-fold change, Tg = 0.56 ± 0.10-fold change, $P < 0.05$).
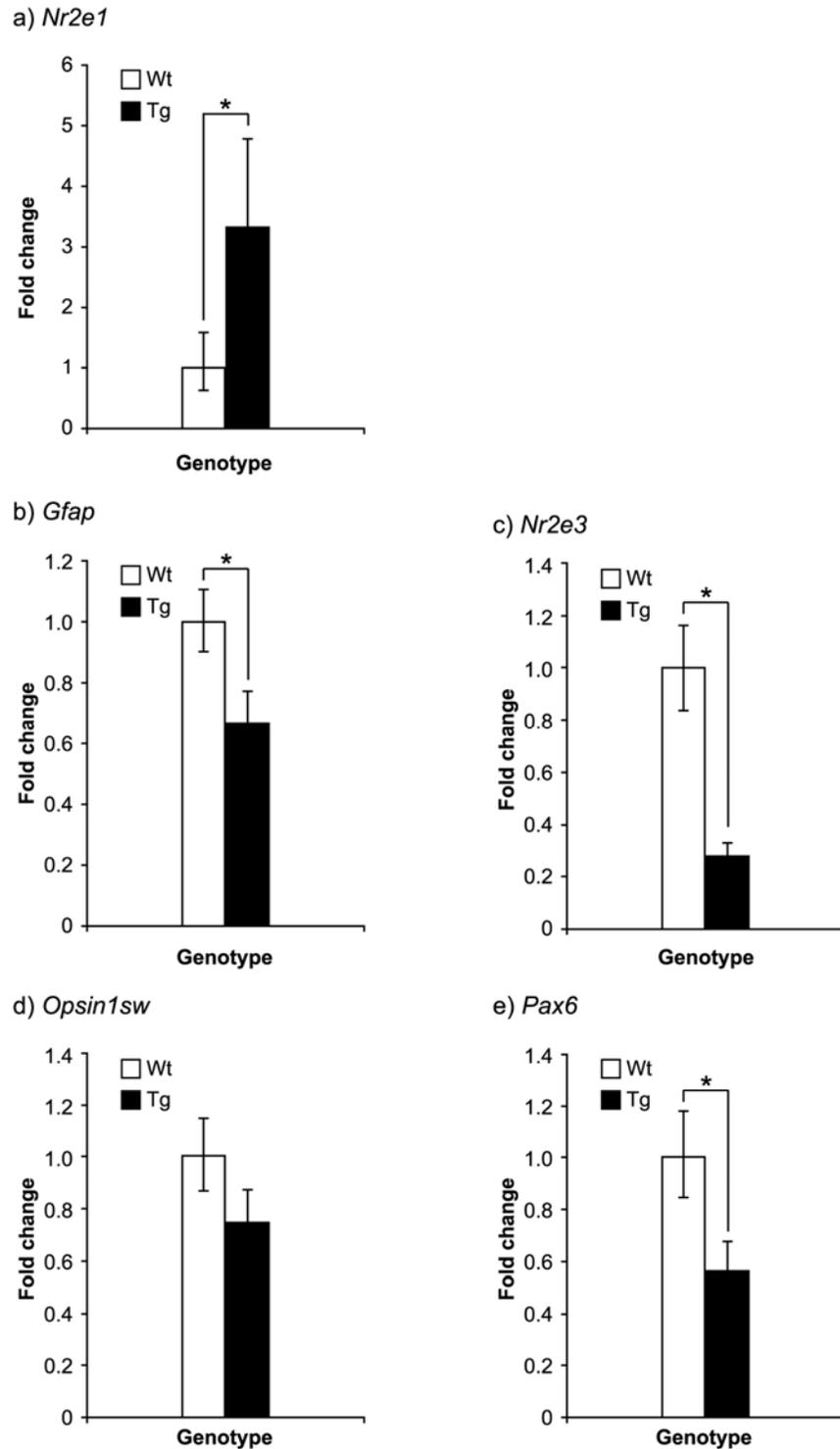
Figure 4.7 Adult B6-bacEMS4A eyes showed significant alteration in gene transcription
Adult B6-bacEMS4A eyes were examined for fold differences in (a) *Nr2e1*, (b) *Gfap*, (c) *Nr2e3*, (d) *Opsin1sw*, and (e) *Pax6* expression. * *P* < 0.05. N = 5 per genotype.

4.4 Discussion

This is the first study to characterize the neurological, proliferative, and ocular effects of increased *Nr2e1* transcription in mice. Although these mouse strains carry high copies of inserts, quantification of *Nr2e1* and *NR2E1* transcript levels was necessary to show that transgene transcription was indeed increased. Genes studied for transcriptional changes in these mice were chosen based on (1) previous literature demonstrating differences in Wt versus *Nr2e1*-null mice (Li *et al.*, 2008, Liu *et al.*, 2008, Miyawaki *et al.*, 2004, Shi *et al.*, 2004, Sun *et al.*, 2007) and (2) genes that are shown to be involved in cell cycle regulation (Eom & Jope, 2009, Ke *et al.*, 2004, Li *et al.*, 2006). The two bacEMS4 strains were analyzed for *Nr2e1* transcript levels, where B6-bacEMS4B showed no significant increase and B6-bacEMS4A showed a four-fold increase in the transcriptional level of *Nr2e1* in both the brain and eyes of adult mice. Consistent with the over transcription of *Nr2e1* in the bacEMS4 strains, only B6-bacEMS4A showed significant transcriptional changes of its target genes. In both pacEMS1 strains, although increased transcription of human *NR2E1* was observed, no significant difference in transcription of target genes were detected. Furthermore, increased *Nr2e1* transcription was observed in both embryonic and adult time points but significant target gene transcription differences were only observed in adults. These results all point towards a complex effect of *Nr2e1* level and its role in transcriptional regulation.

Since *Nr2e1* is generally known to act as a transcriptional repressor, we had anticipated that *Nr2e1* overexpression might result in increased repression of its direct genetic targets (i.e. *Aqp4*, *Gfap*, *Pten*, *S100β*). However, as evidenced by our qRT-PCR data, this is not necessarily the case. In fact, of the four direct target genes only *Gfap*

expression showed a statistical trend for reduction in B6-bacEMS4A transgenic mice, while others showed no significant differences. Several possibilities may explain these results. First, Nr2e1 is known to recruit histone demethylases (LSD1) and deacetaylases (HDAC3, 5, and 7) for transcription repression (Sun *et al.*, 2007, Yokoyama *et al.*, 2008). The lack of gene expression differences in the presence of *Nr2e1* overexpression may be due to the availability of these corepressor proteins. If these corepressors were not proportionally increased with Nr2e1, then transcriptional repression would reach a plateau. Secondly, although our null hypothesis was to predict a linear relationship between transcription level of target genes and *Nr2e1* transcript levels, this simplistic model was unlikely to hold up based on the dynamic expression pattern of *Nr2e1* (Land & Monaghan, 2003, Stenman *et al.*, 2003b), indicating that *Nr2e1* levels requires strict regulation for normal development. And finally, although we have shown increased transcription of mouse and human *NR2E1* in the transgenic strains, we have been unable to demonstrate that this transcriptional increase results in increased translation of Nr2e1 protein. Nr2e1 protein levels have to be quantified in these strains before we can accurately correlate the transcriptional data presented here with phenotypes observed. Our work has been impeded by the performance failure of the commercial antibodies for Nr2e1 currently available.

In B6-bacEMS4A transgenic brains, aside from the reduction in *Gfap* transcription, the other transcriptionally-affected gene was *Gsk3β*. This result strengthens the connection between *NR2E1* and bipolar I disorder (BPI). A relationship between *NR2E1* and BPI has now been demonstrated by different lines of evidence (Kumar *et al.*, 2008, Mcqueen *et al.*, 2005) and lithium is the standard treatment for mania in patients

with BPI (Shastry, 2005). Lithium has been shown to inhibit Gsk3β leading to an increase of CyclinD1 (Ccnd1) that initiates cell cycle re-entry (Chen *et al.*, 2005, Williams & Harwood, 2000), as well as reducing *Aqp4* transcription (Mcquillin *et al.*, 2007), all genes shown to be regulated by *Nr2e1* (Miyawaki *et al.*, 2004, Shi *et al.*, 2004). B6-bacEMS4A brains showed that increased levels of *Nr2e1* transcripts resulted in increased *Gsk3β* transcription, therefore implying a functional role of Nr2e1 in pathways mediated by drugs effective in treating BPI.

Since B6-bacEMS4A and the two B6-pacEMS1 strains showed an increase in mouse and human *NR2E1* levels, respectively, and assuming that the over transcription of the human transgene results in increased NR2E1 protein, then the lack of transcriptional changes in the pacEMS1 strains might be the result of subtle functional variation between human and mouse *NR2E1*. Previously, human *NR2E1* has successfully rescued the *Nr2e1*-null mouse brain and behavioural phenotypes, indicating a functional conservation between mouse and human NR2E1 (Abrahams *et al.*, 2005). Although brain morphology of PAC transgenic mice was deemed to be normal, detailed measurements of various brain regions were not performed. It was also noted that the presence of the human *NR2E1* was unable to entirely correct mutant eye phenotypes (Abrahams *et al.*, 2005), which was either the result of the eyes being sensitive to *Nr2e1* dose or slight differences in functional efficiency between mouse and human *NR2E1*. This study shows that there were no significant neuroanatomical differences in pacEMS1 transgenic strains when compared to Wt brains. B6-bacEMS4A was the only strain to show a significant genotype effect, when all brain measurements were analyzed together. The most noticeable difference in the B6-bacEMS4A brains was the significant reduction in brain

weight, which was not observed in any other transgenic strains studied here. However, this reduction in brain weight was not accompanied by any significant decrease in size of various brain regions.

The proliferative deficit of neural stem/progenitor cells in *Nr2e1*-null mice is characterized by a significant decrease in BrdU incorporation in the neurogenic areas of the adult brain: the subventricular zone (SVZ) and the dentate gyrus (DG) of the hippocampus (Shi *et al.*, 2004). We examined whether increased *Nr2e1* levels will alter neural stem/progenitor cell proliferation in these two areas. Based on the transcriptional and morphological data, we had a strong hypothesis that B6-bacEMS4A, our most affected strain, would show altered proliferation in the SVZ and DG. Although the pacEMS1 strains showed increased transcription of *NR2E1*, data from qRT-PCR of target genes and gross brain and eye morphology does not provide support for increased NR2E1 protein. Since B6-bacEMS4B mice showed no significant increase in *Nr2e1* transcript level, proliferating cells in the SVZ and DG of these brains were counted as a control experiment. Proliferation was not significantly different between B6-bacEMS4B transgenic brains and Wt brains in either the SVZ or DG, as expected. Cell proliferation in B6-bacEMS4A was significantly increased only in the SVZ but not in the DG. Neural stem/progenitor cells found throughout the brain have been demonstrated to be characteristically different (Lagace *et al.*, 2007, Merkle *et al.*, 2007) and can respond differently to regional regulatory signals (Palmer *et al.*, 1995). Therefore, the disparity in the proliferative effect of *Nr2e1* overexpression in the two areas might reflect varying roles of *Nr2e1* that are region- and cell type-specific. This ability of *Nr2e1* overexpression to increase cell proliferation and reduce *Gfap* expression is of great

144

interest for understanding and potential treatment of numerous neurological disorders, including Alzheimer's disease that shows increased Gfap expression (Jesse *et al.*, 2009) and treatments for depression and mania that attenuate symptoms by increasing proliferation in the brain (David *et al.*, 2009).

The eye phenotypes observed in B6-bacEMS4A, and not in other strains, were reminiscent of those seen in *Pax6* mutants (Hill *et al.*, 1991, Ramaesh *et al.*, 2003). *Pax6$^{+/Sey}$* mice show reduced *Pax6* expression resulting in decreased retinal ganglion cell genesis and enhanced cone photoreceptor and amacrine interneuron production (Hsieh & Yang, 2009). Interestingly, the closest relative of *Nr2e1*, *Nr2e3* controls photoreceptors fate by repressing cone-specific gene transcription and when mutated shows increased expression of cone-specific genes and enhanced cone generation (Webber *et al.*, 2008). A previous study in *Xenopus* showed that a fusion protein consisting of Nr2e1 DNA-binding domain (DBD) and the Engrailed repressor ligand-binding domain (LBD) that increases Nr2e1-specific gene repression resulted in a significant decrease in Pax6 expression (Hollemann *et al.*, 1998). This study is the first to demonstrate that overexpression of *Nr2e1* in mice results in significant reduction of both *Pax6* and *Nr2e3* expression. These results place *Nr2e1* in these important genetic pathways of eye development.

Given that *Nr2e1* and *Nr2e3* are expressed in different cell types (Müller glia and photoreceptor layer, respectively (Kobayashi *et al.*, 2008, Miyawaki *et al.*, 2004)), the reduction of *Nr2e3* is likely the result of a decrease in cone photoreceptors in these transgenic eyes, as supported by the trend for reduced expression of *Opsin1sw*, a cone-specific gene. Similarly, rod photoreceptors appear to be reduced in B6-bacEMS4A

retina. The significant thinning of the ONL provides further support for the reduction of photoreceptors. Müller cells, the astrocytic cells of the retina, are shown to be reduced and have defective ultrastructure in *Nr2e1*-null mice (Miyawaki *et al.*, 2004). Gfap immunofluorescent analysis of Müller cells in B6-bacEMS4A retina showed increased and dispersed GFAP staining. In addition to the staining abnormalities seen in the B6-bacEMS4A adult retina, there was significant thinning of the different retinal layers, especially the ONL, INL, and IPL. Similarly, thinning of retinal layers had also been previously reported for mice lacking *Nr2e1* (Young *et al.*, 2002). Therefore, proper development and/or maintenance of the retinal layers are not only regulated by presence and absence of Nr2e1, but also by its levels. Since gross eye abnormalities are observed in neonatal B6-bacEMS4A mice, ocular phenotypes are likely developmental instead of degenerative. However, since B6-bacEMS4A mice showed increased cell proliferation in the SVZ, cell proliferation in the retina will also need to be analyzed. If increased cell proliferation was also observed in the retina, then the thinning of the layers may be a result of increased apoptosis. Interestingly, mice with variable levels of *Pax6*, ranging from underexpressors to overexpressors, also exhibit thinning of the retinal and cortical layers (Sansom *et al.*, 2009, Schedl *et al.*, 1996). The levels of Pax6 have been shown to regulate the balance between self-renewal and differentiation. In the developing cortex, the loss of Pax6 leads to a failure to self-renew resulting in increased early differentiation, where increase in Pax6 enhances division of stem cells and promotes basal progenitor fate that leads to overproduction of early-born cortical neurons; in both cases there is a depletion of cortical stem cell pool (Sansom *et al.*, 2009). Therefore, future experiments are necessary for examining the effect of *Nr2e1* overexpression on

cell cycle and cell fate determination that underlie the cortical and retinal abnormalities in the B6-bacEMS4A transgenic mice.

Collectively, these results suggest that overexpression of *Nr2e1* may have a detrimental effect on the development of the mouse retina by significantly reducing *Pax6* and *Nr2e3* transcript levels, while generally sparing brain development. This study has identified a potential of overexpressing *Nr2e1* to increase neural stem/progenitor cell proliferation, as well as several target genes affected by *Nr2e1* overexpression that proposes molecular pathways on which varying dosage of *Nr2e1* may affect in human disorders.

4.5 References

Abrahams, B.S., Chong, A.C., Nisha, M., Milette, D., Brewster, D.A., Berry, M.L., Muratkhodjaev, F., Mai, S., Rajcan-Separovic, E. & Simpson, E.M. (2003) Metaphase FISHing of transgenic mice recommended: FISH and SKY define BAC-mediated balanced translocation. *Genesis,* **36,** 134-141.

Abrahams, B.S., Kwok, M.C., Trinh, E., Budaghzadeh, S., Hossain, S.M. & Simpson, E.M. (2005) Pathological aggression in "fierce" mice corrected by human nuclear receptor 2E1. *J Neurosci,* **25,** 6263-6270.

Bandah, D., Merin, S., Ashhab, M., Banin, E. & Sharon, D. (2009) The spectrum of retinal diseases caused by NR2E3 mutations in Israeli and Palestinian patients. *Arch Ophthalmol,* **127,** 297-302.

Chen, B., Pan, H., Zhu, L., Deng, Y. & Pollard, J.W. (2005) Progesterone inhibits the estrogen-induced phosphoinositide 3-kinase-->AKT-->GSK-3beta-->cyclin D1-->pRB pathway to block uterine epithelial cell proliferation. *Mol Endocrinol,* **19,** 1978-1990.

Christie, B.R., Li, A.M., Redila, V.A., Booth, H., Wong, B.K., Eadie, B.D., Ernst, C. & Simpson, E.M. (2006) Deletion of the nuclear receptor Nr2e1 impairs synaptic plasticity and dendritic structure in the mouse dentate gyrus. *Neuroscience,* **137,** 1031-1037.

David, D.J., Samuels, B.A., Rainer, Q., Wang, J.W., Marsteller, D., Mendez, I., Drew, M., Craig, D.A., Guiard, B.P., Guilloux, J.P., Artymyshyn, R.P., Gardier, A.M., Gerald, C., Antonijevic, I.A., Leonardo, E.D. & Hen, R. (2009) Neurogenesis-dependent and -independent effects of fluoxetine in an animal model of anxiety/depression. *Neuron,* **62,** 479-493.

Eom, T.Y. & Jope, R.S. (2009) Blocked inhibitory serine-phosphorylation of glycogen synthase kinase-3alpha/beta impairs in vivo neural precursor cell proliferation. *Biol Psychiatry,* **66,** 494-502.

Fradot, M., Lorentz, O., Wurtz, J.M., Sahel, J.A. & Leveillard, T. (2007) The loss of transcriptional inhibition by the photoreceptor-cell specific nuclear receptor (NR2E3) is not a necessary cause of enhanced S-cone syndrome. *Mol Vis,* **13,** 594-601.

Haider, N.B., Demarco, P., Nystuen, A.M., Huang, X., Smith, R.S., McCall, M.A., Naggert, J.K. & Nishina, P.M. (2006) The transcription factor Nr2e3 functions in retinal progenitors to suppress cone cell generation. *Vis Neurosci,* **23,** 917-929.

Hill, R.E., Favor, J., Hogan, B.L., Ton, C.C., Saunders, G.F., Hanson, I.M., Prosser, J., Jordan, T., Hastie, N.D. & van Heyningen, V. (1991) Mouse small eye results from mutations in a paired-like homeobox-containing gene. *Nature,* **354,** 522-525.

Hollemann, T., Bellefroid, E. & Pieler, T. (1998) The Xenopus homologue of the Drosophila gene tailless has a function in early eye development. *Development,* **125,** 2425-2432.

Hsieh, Y.W. & Yang, X.J. (2009) Dynamic Pax6 expression during the neurogenic cell cycle influences proliferation and cell fate choices of retinal progenitors. *Neural Dev,* **4,** 32.

Jesse, S., Steinacker, P., Cepek, L., Arnim, C.V., Tumani, H., Lehnert, S., Kretzschmar, H.A., Baier, M. & Otto, M. (2009) Glial Fibrillary Acidic Protein and Protein S-100B: Different Concentration Pattern of Glial Proteins in Cerebrospinal Fluid of Patients with Alzheimer's Disease and Creutzfeldt-Jakob Disease. *J Alzheimers Dis*.

Ke, N., Claassen, G., Yu, D.H., Albers, A., Fan, W., Tan, P., Grifman, M., Hu, X., Defife, K., Nguy, V., Meyhack, B., Brachat, A., Wong-Staal, F. & Li, Q.X. (2004) Nuclear hormone

receptor NR4A2 is involved in cell transformation and apoptosis. *Cancer Res,* **64,** 8208-8212.

Kobayashi, M., Hara, K., Yu, R.T. & Yasuda, K. (2008) Expression and functional analysis of Nr2e3, a photoreceptor-specific nuclear receptor, suggest common mechanisms in retinal development between avians and mammals. *Dev Genes Evol,* **218,** 439-444.

Kobayashi, M., Yu, R.T., Yasuda, K. & Umesono, K. (2000) Cell-type-specific regulation of the retinoic acid receptor mediated by the orphan nuclear receptor TLX. *Mol Cell Biol,* **20,** 8731-8739.

Kumar, R.A., Leach, S., Bonaguro, R., Chen, J., Yokom, D.W., Abrahams, B.S., Seaver, L., Schwartz, C.E., Dobyns, W., Brooks-Wilson, A. & Simpson, E.M. (2007) Mutation and evolutionary analyses identify NR2E1-candidate-regulatory mutations in humans with severe cortical malformations. *Genes Brain Behav,* **6,** 503-516.

Kumar, R.A., McGhee, K.A., Leach, S., Bonaguro, R., Maclean, A., Aguirre-Hernandez, R., Abrahams, B.S., Coccaro, E.F., Hodgins, S., Turecki, G., Condon, A., Muir, W.J., Brooks-Wilson, A.R., Blackwood, D.H. & Simpson, E.M. (2008) Initial association of NR2E1 with bipolar disorder and identification of candidate mutations in bipolar disorder, schizophrenia, and aggression through resequencing. *Am J Med Genet B Neuropsychiatr Genet,* **147B,** 880-889.

Lagace, D.C., Whitman, M.C., Noonan, M.A., Ables, J.L., DeCarolis, N.A., Arguello, A.A., Donovan, M.H., Fischer, S.J., Farnbauch, L.A., Beech, R.D., DiLeone, R.J., Greer, C.A., Mandyam, C.D. & Eisch, A.J. (2007) Dynamic contribution of nestin-expressing stem cells to adult neurogenesis. *J Neurosci,* **27,** 12623-12629.

Land, P.W. & Monaghan, A.P. (2003) Expression of the transcription factor, tailless, is required for formation of superficial cortical layers. *Cereb Cortex,* **13,** 921-931.

Li, Q.X., Ke, N., Sundaram, R. & Wong-Staal, F. (2006) NR4A1, 2, 3--an orphan nuclear hormone receptor family involved in cell apoptosis and carcinogenesis. *Histol Histopathol,* **21,** 533-540.

Li, W., Sun, G., Yang, S., Qu, Q., Nakashima, K. & Shi, Y. (2008) Nuclear receptor TLX regulates cell cycle progression in neural stem cells of the developing brain. *Mol Endocrinol,* **22,** 56-64.

Liu, H.K., Belz, T., Bock, D., Takacs, A., Wu, H., Lichter, P., Chai, M. & Schutz, G. (2008) The nuclear receptor tailless is required for neurogenesis in the adult subventricular zone. *Genes Dev,* **22,** 2473-2478.

McQueen, M.B., Devlin, B., Faraone, S.V., Nimgaonkar, V.L., Sklar, P., Smoller, J.W., Abou Jamra, R., Albus, M., Bacanu, S.A., Baron, M., Barrett, T.B., Berrettini, W., Blacker, D., Byerley, W., Cichon, S., Coryell, W., Craddock, N., Daly, M.J., Depaulo, J.R., Edenberg, H.J., Foroud, T., Gill, M., Gilliam, T.C., Hamshere, M., Jones, I., Jones, L., Juo, S.H., Kelsoe, J.R., Lambert, D., Lange, C., Lerer, B., Liu, J., Maier, W., Mackinnon, J.D., McInnis, M.G., McMahon, F.J., Murphy, D.L., Nothen, M.M., Nurnberger, J.I., Pato, C.N., Pato, M.T., Potash, J.B., Propping, P., Pulver, A.E., Rice, J.P., Rietschel, M., Scheftner, W., Schumacher, J., Segurado, R., Van Steen, K., Xie, W., Zandi, P.P. & Laird, N.M. (2005) Combined analysis from eleven linkage studies of bipolar disorder provides strong evidence of susceptibility loci on chromosomes 6q and 8q. *Am J Hum Genet,* **77,** 582-595.

McQuillin, A., Rizig, M. & Gurling, H.M. (2007) A microarray gene expression study of the molecular pharmacology of lithium carbonate on mouse brain mRNA to understand the neurobiology of mood stabilization and treatment of bipolar affective disorder. *Pharmacogenet Genomics,* **17,** 605-617.

Merkle, F.T., Mirzadeh, Z. & Alvarez-Buylla, A. (2007) Mosaic organization of neural stem cells in the adult brain. *Science,* **317,** 381-384.

Miyawaki, T., Uemura, A., Dezawa, M., Yu, R.T., Ide, C., Nishikawa, S., Honda, Y., Tanabe, Y. & Tanabe, T. (2004) Tlx, an orphan nuclear receptor, regulates cell numbers and astrocyte development in the developing retina. *J Neurosci,* **24,** 8124-8134.

Monaghan, A.P., Bock, D., Gass, P., Schwager, A., Wolfer, D.P., Lipp, H.P. & Schutz, G. (1997) Defective limbic system in mice lacking the tailless gene. *Nature,* **390,** 515-517.

Monaghan, A.P., Grau, E., Bock, D. & Schutz, G. (1995) The mouse homolog of the orphan nuclear receptor tailless is expressed in the developing forebrain. *Development,* **121,** 839-853.

Pachydaki, S.I., Klaver, C.C., Barbazetto, I.A., Roy, M.S., Gouras, P., Allikmets, R. & Yannuzzi, L.A. (2009) Phenotypic features of patients with NR2E3 mutations. *Arch Ophthalmol,* **127,** 71-75.

Palmer, T.D., Ray, J. & Gage, F.H. (1995) FGF-2-responsive neuronal progenitors reside in proliferative and quiescent regions of the adult rodent brain. *Mol Cell Neurosci,* **6,** 474-486.

Ramaesh, T., Collinson, J.M., Ramaesh, K., Kaufman, M.H., West, J.D. & Dhillon, B. (2003) Corneal abnormalities in Pax6+/- small eye mice mimic human aniridia-related keratopathy. *Invest Ophthalmol Vis Sci,* **44,** 1871-1878.

Rasband, W.S., ImageJ, U. S. National Institutes of Health, Bethesda, Maryland, USA, http://rsb.info.nih.gov/ij/, 1997-2009.

Roy, K., Kuznicki, K., Wu, Q., Sun, Z., Bock, D., Schutz, G., Vranich, N. & Monaghan, A.P. (2004) The Tlx gene regulates the timing of neurogenesis in the cortex. *J Neurosci,* **24,** 8333-8345.

Roy, K., Thiels, E. & Monaghan, A.P. (2002) Loss of the tailless gene affects forebrain development and emotional behavior. *Physiol Behav,* **77,** 595-600.

Rudolph, K.M., Liaw, G.J., Daniel, A., Green, P., Courey, A.J., Hartenstein, V. & Lengyel, J.A. (1997) Complex regulatory region mediating tailless expression in early embryonic patterning and brain development. *Development,* **124,** 4297-4308.

Sansom, S.N., Griffiths, D.S., Faedo, A., Kleinjan, D.J., Ruan, Y., Smith, J., van Heyningen, V., Rubenstein, J.L. & Livesey, F.J. (2009) The level of the transcription factor Pax6 is essential for controlling the balance between neural stem cell self-renewal and neurogenesis. *PLoS Genet,* **5,** e1000511.

Schedl, A., Ross, A., Lee, M., Engelkamp, D., Rashbass, P., van Heyningen, V. & Hastie, N.D. (1996) Influence of PAX6 gene dosage on development: overexpression causes severe eye abnormalities. *Cell,* **86,** 71-82.

Schorderet, D.F. & Escher, P. (2009) NR2E3 mutations in enhanced S-cone sensitivity syndrome (ESCS), Goldmann-Favre syndrome (GFS), clumped pigmentary retinal degeneration (CPRD), and retinitis pigmentosa (RP). *Hum Mutat*.

Shastry, B.S. (2005) Bipolar disorder: an update. *Neurochem Int,* **46,** 273-279.

Shi, Y., Chichung Lie, D., Taupin, P., Nakashima, K., Ray, J., Yu, R.T., Gage, F.H. & Evans, R.M. (2004) Expression and function of orphan nuclear receptor TLX in adult neural stem cells. *Nature,* **427,** 78-83.

Stenman, J., Yu, R.T., Evans, R.M. & Campbell, K. (2003a) Tlx and Pax6 co-operate genetically to establish the pallio-subpallial boundary in the embryonic mouse telencephalon. *Development,* **130,** 1113-1122.

Stenman, J.M., Wang, B. & Campbell, K. (2003b) Tlx controls proliferation and patterning of lateral telencephalic progenitor domains. *J Neurosci,* **23,** 10568-10576.

Sun, G., Yu, R.T., Evans, R.M. & Shi, Y. (2007) Orphan nuclear receptor TLX recruits histone deacetylases to repress transcription and regulate neural stem cell proliferation. *Proc Natl Acad Sci U S A,* **104,** 15282-15287.

Wang, N.K., Fine, H.F., Chang, S., Chou, C.L., Cella, W., Tosi, J., Lin, C.S., Nagasaki, T. & Tsang, S.H. (2009) Cellular origin of fundus autofluorescence in patients and mice with a defective NR2E3 gene. *Br J Ophthalmol,* **93,** 1234-1240.

Webber, A.L., Hodor, P., Thut, C.J., Vogt, T.F., Zhang, T., Holder, D.J. & Petrukhin, K. (2008) Dual role of Nr2e3 in photoreceptor development and maintenance. *Exp Eye Res,* **87,** 35-48.

Williams, R.S. & Harwood, A.J. (2000) Lithium therapy and signal transduction. *Trends Pharmacol Sci,* **21,** 61-64.

Yokoyama, A., Takezawa, S., Schule, R., Kitagawa, H. & Kato, S. (2008) Transrepressive function of TLX requires the histone demethylase, LSD1. *Mol Cell Biol*.

Young, K.A., Berry, M.L., Mahaffey, C.L., Saionz, J.R., Hawes, N.L., Chang, B., Zheng, Q.Y., Smith, R.S., Bronson, R.T., Nelson, R.J. & Simpson, E.M. (2002) Fierce: a new mouse

deletion of Nr2e1; violent behaviour and ocular abnormalities are background-dependent. *Behav Brain Res,* **132,** 145-158.

Yu, R.T., Chiang, M.Y., Tanabe, T., Kobayashi, M., Yasuda, K., Evans, R.M. & Umesono, K. (2000) The orphan nuclear receptor Tlx regulates Pax2 and is essential for vision. *Proceedings of the National Academy of Sciences USA,* **97,** 2621-2625.

Zhang, C.L., Zou, Y., Yu, R.T., Gage, F.H. & Evans, R.M. (2006) Nuclear receptor TLX prevents retinal dystrophy and recruits the corepressor atrophin1. *Genes Dev,* **20,** 1308-1320.

Chapter 5: General discussion

The work presented in this thesis examined the effects of varying *Nr2e1* levels on brain and eye phenotypes, with particular focus on (1) the validity of using *Nr2e1$^{frc/frc}$* mice as a model of bipolar I disorder (BPI) and (2) to identify novel target genes to place *Nr2e1* in genetic pathways important in human disease. In my discussion, I will comment on the findings of the three manuscript chapters as a whole, make suggestions on behavioural modeling of human psychiatric disorders, and propose future experiments, in both *in vivo* (mouse and human) and *in vitro* systems that will further identify roles of *NR2E1* in disease and as a potential therapeutic molecule.

5.1 Overview of major findings

Prior to evaluating the validity of *Nr2e1$^{frc/frc}$* mice as a model of BPI, the discriminatory power of dark- versus light-phase testing was examined. Results presented in Chapter 2 supported our hypothesis that dark-phase testing will affect and improve discrimination between genetically distinct mouse strains using high-throughput behavioural tests. The increased ability of dark-phase testing to distinguish behavioural difference in genetically distinct mouse strains influenced the experimental design of Chapter 3 which assessed *Nr2e1$^{frc/frc}$* mice for behavioural anomalies similar to those seen in some patients with BPI. *Nr2e1$^{frc/frc}$* mice showed several behavioural characteristics that are also observed in other rodent models of mania, including hyperactivity and learning deficits. We also showed reduced cell proliferation in the subventricular zone (SVZ) and dentate gyrus (DG) of *Nr2e1$^{frc/frc}$* mice, a trait that is seen in some patients with BPI. To further evaluate the pharmacological validity of *Nr2e1$^{frc/frc}$* mice as a model

for BPI, the effect of adult lithium administration on behavioural phenotypes and cell proliferation was examined. Chapter 3 represents the first report of drug assessment on mice lacking *Nr2e1*. Our results indicated that adult administration of lithium was unable to ameliorate behavioural and proliferation deficits in *Nr2e1^{frc/frc}* mice. Future work employing various drugs with different treatment regimes will be required to fully test the efficacy of drug treatments in *Nr2e1^{frc/frc}* mice. We began by examining *Nr2e1^{frc/frc}* mice as a model for BPI because (1) the heterozygous *Nr2e1* mice show no observable behavioural phenotypes and only mild cellular and transcriptional alterations (Liu *et al.*, 2008, Roy *et al.*, 2004) and (2) a null mutation would increase our ability to observe potentially subtle behavioural abnormalities; however, the role of *NR2E1* in human diseases is unlikely to be a result of null mutations in this highly conserved and functionally important gene. Variants in *NR2E1* identified in patients have been located in conserved regions that are thought to be important in transcriptional regulation (Kumar *et al.*, 2007, Kumar *et al.*, 2008), and therefore it was necessary to examine the effects of variable *Nr2e1* levels. In Chapter 4, we examined four transgenic mouse strains carrying exogenous copies of either human or mouse *Nr2e1* to test the hypothesis that *Nr2e1* overexpression will result in dysmorphia of neuroanatomical and ocular development, and that target gene transcription levels will inversely correlate with *Nr2e1* levels. We identified significant neuroanatomical, ocular, and gene expression differences in one of the four transgenic strains, B6-bacEMS4A, when compared to Wt mice. The significance and future directions stemming from these findings are discussed in greater detail below.

5.2 Considerations for modeling behavioural traits of human disease in mice

5.2.1 Dark-phase behavioural testing can improve detection of behavioural differences in genetically distinct mice

Despite the wide use of mouse models to study behavioural phenotypes, there has been a lack of continuity in the testing protocol throughout the field resulting in inter-laboratory variability (Crabbe *et al.*, 1999, Wahlsten, 2001, Wahlsten *et al.*, 2003). The sensitivity of behaviour to changes in environment and testing conditions has been well documented and differences in testing conditions can result in unnecessary complications when deciphering genetic effects of behavioural outcomes. With the explosion of genome-wide association studies of human psychiatric disorders throughout the last decade, more and more candidate genes will arise and require examination in a model system. Therefore, the evaluation and optimization of current high-throughput behavioural testing conditions was essential.

In Chapter 2, we examined the effects of light- and dark-phase testing on the ability to discriminate behavioural phenotypes in three genetically distinct strains (C57BL/6J, 129S1/SvImJ, and B6129F1). We acknowledged the inconvenience of dark-phase testing for the experimenters if lights were on between 0600-1800 h; therefore, we raised our mice on a reversed light cycle (lights on 23:00-11:00 h), thereby allowing researchers to test mice in their dark-phase during normal work hours. We demonstrated that dark-phase testing was not only more ethologically correct, but also improved discriminatory power of high throughput tests, including SHIRPA primary screen, open-field test, and motor learning on the rotarod. From these results we would recommend that behavioural examination of mouse mutants carrying candidate mutations of human psychiatric disorders be performed in the dark phase. By using a reversed light cycle,

researchers could easily benefit from the increased discriminatory power of dark-phase high-throughput behavioural testing, and thus allow for the detection of potentially subtle behavioural phenotypes.

5.2.2 The power of dissecting complex disorders into endophenotypes

Human psychiatric disorders are essentially impossible to accurately model in rodents (Einat, 2006). Although genetic and drug models of BP (presented in Chapter 1.6.4) demonstrate a subset of behavioural and/or neuropathological traits, the variability of symptoms in patients given the same diagnosis indicates the underlying genetic heterogeneity of the group. By evaluating aspects of these disorders separately, instead of the disorder as a whole, we can improve our ability to identify genetic influences of specific traits. This concept of "endophenotypes" stems from dissecting a complex disease into more basic phenotypes that have a clear genetic connection (Gottesman & Gould, 2003, Gottesman & Shields, 1973). Endophenotypes of BP may include behavioural symptoms (e.g. cognitive deficits, olfactory deficits, hyperactivity, sleep disturbances) (Goldberg & Chengappa, 2009, Kruger *et al.*, 2006, Mccurdy *et al.*, 2006) and neuroanatomical differences (e.g. increased ventricular volume, reduced hippocampal and cerebral cortical volume, reduced neurogenesis) (Swayze *et al.*, 1990). By studying these endophenotypes, we can better detect genetic defects that ultimately contribute to the disease.

5.3 Nr2e1$^{frc/frc}$ mice – an appropriate model for bipolar disorder?

Linkage analysis and significant association have suggested a relationship between *NR2E1* and bipolar disorder (BP), especially bipolar I disorder (BPI) (Kumar *et*

al., 2008, Mcqueen *et al.*, 2005) (as outlined in Chapter 1.6.2). These findings laid the groundwork for experiments described in Chapter 3. Furthermore, the considerations discussed above (Chapter 5.1) were implemented in the experimental design of Chapter 3.

5.3.1 *Nr2e1$^{frc/frc}$* mice show phenotypes observed in bipolar disorder

The neurological abnormalities are well characterized in *Nr2e1*-null mice and similarities can be drawn between patients with BPI (outlined in Chapter 3.1). This is the first study to evaluate the validity of *Nr2e1$^{frc/frc}$* mice as a model for BPI. Behaviourally, *Nr2e1$^{frc/frc}$* mice showed extreme hyperactivity and deficits in learning tasks, behavioural traits that are seen in patients with BPI and rodent models of mania. The neurological abnormalities in *Nr2e1$^{frc/frc}$* mice, such as hypoplasia of the hippocampus and olfactory bulbs, could underlie both hyperactivity and learning deficit, as lesion models show similar behavioural outcomes (Chaillan *et al.*, 2005, Deacon *et al.*, 2002, Pullela *et al.*, 2006). Developmental abnormalities in *Nr2e1$^{frc/frc}$* mice have also resulted in impairment of the GABAergic interneurons and changes to this neurotransmitter system have been shown to be important in the regulation of activity level (Viggiano, 2008). Given that the structural and behavioural phenotypes observed in *Nr2e1$^{frc/frc}$* are consistent with the current understanding of brain regions and behavioural control, our findings suggest a neurodevelopmental role of *NR2E1* in BPI.

Deficits in neural stem/progenitor cell proliferation are also observed in some patients with BPI, and since *Nr2e1* has a role in adult neurogenesis, where the lack of *Nr2e1* reduces neural stem/progenitor cell proliferation, *NR2E1* variants may also alter the ability of neural stem/progenitor cells to proliferate. Furthermore, a potential

mechanism by which lithium acts to attenuate symptoms in patients with BPI is to promote proliferation of neural stem/progenitor cell. Although we show in Chapter 3 that adult lithium treatment was unable to correct for the proliferative deficit, we hypothesize that adult $Nr2e1^{frc/frc}$ cells may be too severely altered to respond to lithium treatment, and therefore for future pharmacological analysis of $Nr2e1^{frc/frc}$ mice, we suggest testing at prenatal time points. To fully characterize the molecular changes occurring in cells lacking $Nr2e1$, drug effects should be examined at early (E8-12), mid (E14-15), and late (E16-18) embryoic time points, when we know there are dynamic changes in cell cycle rates (Roy *et al.*, 2004).

The *in vivo* approach is invaluable in studying the genetic and neurological consequences of behavioural phenotypes of psychiatric diseases. However, because the brain is so severely affected by the loss of $Nr2e1$, it is conceivable that other pathways and/or mechanisms have taken on a compensatory role, a phenomenon shown in mouse models of stroke and mania (Liu *et al.*, 2007, Prickaerts *et al.*, 2006). Therefore, in an *in vivo* system these compensatory mechanisms might mask drug responses to more basic phenotypes, such as cell proliferation. From our Chapter 3 results, we would also recommend future *in vitro* studies of adult- and embryo-derived $Nr2e1^{frc/frc}$ neural stem/progenitor cells (e.g. neurosphere assays, neural differentiation assays), that will allow cell cycle regulation to be evaluated in a controlled environment resulting in improved detection of drug effects.

The high degree of sequence conservation at the genomic and amino acid level (Abrahams *et al.*, 2002, Yu *et al.*, 1994), as well as the ability of human *NR2E1* to rescue the mouse phenotype (Abrahams *et al.*, 2005) demonstrates the functional importance of

this gene. Taking into consideration the severity of the *Nr2e1*-null brain abnormalities

and the location of the *NR2E1* variants found in patients with BPI (i.e. conserved

regulatory regions) (Kumar *et al.*, 2004), it is highly unlikely that these variants result in

the complete loss of function or transcription of the *NR2E1* gene. Therefore, *NR2E1*

variants are likely to result in altered *NR2E1* function (i.e. hypomorph or hypermorph)

leading to abnormal development of forebrain regions and systems resulting in

behavioural traits seen in BPI. This hypothesis drove the work presented in Chapter 4 of

this thesis that examined the effects of *Nr2e1* overexpression.

5.3.2 New direction stemming from inconsistencies in *Nr2e1*-null behavioural abnormalities

For the most part, the behavioural phenotypes observed in $Nr2e1^{frc/frc}$ mice were

consistent with those seen in other *Nr2e1*-null strains (Monaghan *et al.*, 1997, Roy *et al.*,

2002) and models of mania (Prickaerts *et al.*, 2006). In our findings (Chapter 3), the lack

of startle reactivity and the lack of increased pain sensitivity in the tail flick test were

surprising and unexpected, as these behaviours were inconsistent with what was

previously known about behaviour of *Nr2e1*-null mice. Since these two unexpected

results were observed from tests requiring physical constraint, we hypothesized that

$Nr2e1^{frc/frc}$ mice demonstrated abnormal stress response when subjected to a stressor.

Although $Nr2e1^{frc/frc}$ mice have been previously tested for corticosterone levels, which

were statistically similar to levels seen in Wt controls, the levels observed in $Nr2e1^{frc/frc}$

mice were consistently higher in both sexes on the C57BL/6J and B6129F1 background

(Young *et al.*, 2002). It is conceivable that the statistically insignificant increase in

corticosterone level in $Nr2e1^{frc/frc}$ mice can easily become significant when these mice are

under restraint. The key structures controlling stress response is the hypothalamic-pituitary-adrenal axis (HPA axis) with connections from regions such as the amygdala and hippocampus that facilitates activation of the HPA axis (Herman *et al.*, 1996). Since several of these regions are affected in *Nr2e1^{frc/frc}* mice, the role of *Nr2e1* in altering stress response is an interesting new direction that warrants examination.

5.4 Overexpression of Nr2e1 illuminates important genetic pathways

The pathways in which *Nr2e1* exerts its function are beginning to be elucidated. Transcriptional changes resulting from the lack of *Nr2e1* has placed *Nr2e1* into genetic pathways involving *Pten*, *Gfap*, and *S100β*, just to name a few (Shi *et al.*, 2004). Analysis of *Nr2e1*-null developing brains had shown an interaction between *Nr2e1* and *Pax6* in boundary establishment (Stenman *et al.*, 2003). Our data further supports this interaction, by demonstrating that *Nr2e1* overexpression decreases *Pax6* expression in the mammalian eye. Based on our transcript data of brain and eye from *Nr2e1* overexpressing mice (presented in Chapter 4), we can now add *Gsk3β* and *Nr2e3* to this growing gene list.

The expression change in *Gsk3β* in *Nr2e1* overexpressing brains is of particular interest to the field of psychiatric and cancer genetics. Gsk3β plays a major role in regulating cell cycle progression by acting through the Wnt/β-catenin signaling pathway that controls expression of numerous cell cycle regulatory genes, in particular cyclinD1, which is also phosphorylated by Gsk3β, (Ryves & Harwood, 2003, Takahashi-Yanaga & Sasaguri, 2009). Undoubtedly, cell cycle dysregulation is one of the underlying mechanisms in cancer biology, and the interaction between *Nr2e1* and *Gsk3β* not only

supports the role of *Nr2e1* in cancer, but also places it in the Wnt/β-catenin signaling pathway. In respect to psychiatric genetics, alteration in Gsk3β levels had been observed in BP, schizophrenia, and Alzheimer's disease, and the regulation of *Gsk3β* may also be involved in the therapeutic effects of drugs used in psychiatry (Jope & Roh, 2006), as demonstrated with lithium, a standard treatment for BP and a known Gsk3β inhibitor. Given the support for the role of Gsk3β in BP and our new evidence of an interaction between *Nr2e1* and *Gsk3β*, these findings collectively imply a functional role of *NR2E1* in the pathology of BP.

The overt eye phenotypes and their similarities to *Pax6$^{+/Sey}$* eyes suggested that *Nr2e1*-overexpressing eyes would likely show reduction in *Pax6* expression, which is supported by our transcript data. Until now, *Nr2e3* expression had not been examined in its relationship to *Pax6* and *Nr2e1*. Since both *NR2E3* and *PAX6* mutations result in eye disorders, enhanced S-cone syndrome (ESCS) and Aniridia, respectively, *NR2E1* would be a good candidate gene for human eye disorders (future direction discussed below).

The quantitative reverse transcriptase PCR examination of known interactors and genes of interest in the *Nr2e1*-overexpressors was a good starting point to evaluate what effects *Nr2e1* overexpression would have on gene regulation on a smaller scale. I would recommend that high-throughput analysis be performed using serial analysis of gene expression (SAGE) or cDNA microarray for expression differences on *Nr2e1*-null, *Nr2e1*-overexpressing, and wild-type brains and eyes to identify new interactors that are affected by varying levels of *Nr2e1*.

5.5 Future directions: NR2E1, bipolar disorder, and eye disorders

5.5.1 Testing bipolar disorder variants in mice

Variants found in *NR2E1* are located in evolutionarily conserved non-coding sequences that reside in the proximal promoter and untranslated regions, suggesting functional importance for transcriptional regulation of *NR2E1* (Abrahams *et al.*, 2002, Kumar *et al.*, 2007, Kumar *et al.*, 2008). Sixty-three percent of the novel NR2E1 variants were also predicted to alter transcription factor binding site (Kumar *et al.*, 2007, Kumar *et al.*, 2008), and therefore, each variant should be examined for *NR2E1* expression level as well as difference in binding using *in vitro* techniques such as electrophoretic mobility shift assay. As demonstrated in Chapter 4, variations in *Nr2e1* expression results in transcriptional differences of target genes; expression analysis of these genes would identify the functional changes resulting from these *NR2E1* variants. The absence of behavioural phenotypes in *Nr2e1* heterozygous mice warrants the study of these variants on a genetic background that does not contain endogenous *Nr2e1*. This strategy is termed the "rescue paradigm" utilized by Abrahams *et al.* (2005), where human *NR2E1* successfully rescued the *Nr2e1$^{frc/frc}$* behavioural and neuroanatomical phenotypes. Therefore, even though results originating from Chapter 3 of this thesis do not provide support for *Nr2e1$^{frc/frc}$* mice to be an adequate model for BPI, as it fails to show behavioural improvement with adult lithium treatment, it did characterize the baseline for behavioural phenotypes relevant for modeling BPI on which the suspect disease *NR2E1* variants will be studied. Drug studies using this *in vivo* rescue system, as well as *in vitro* assays (discussed above in 5.2.1) can provide significant insight into the role of each variant in disease susceptibility.

5.5.2 Identifying *NR2E1* variants in human eye disorders

The role of *NR2E1* in human eye disorders has been significantly strengthened by the transcriptional changes observed in *Pax6* and *Nr2e3* in *Nr2e1*-overexpressing eyes (Chapter 4). Mouse mutants carrying mutations in both *Pax6* and *Nr2e3* have been used in modeling human Aniridia and enhanced S-cone syndrome (ESCS), respectively. Given the resemblance between *Nr2e1*-overexpressing and *Pax6*$^{+/Sey}$ eyes in mice, patients who have Aniridia not caused by mutations in *PAX6* would be suitable for genetic analysis for *NR2E1* mutations. Similarly, patients with ESCS, but no known mutation in *NR2E3* would also be an appropriate sample population. Based on the transcriptional data from Chapter 4 of this thesis, we would anticipate that at least a subset of patient-specific variants in *NR2E1* identified from human sequencing studies might result in increased expression of *NR2E1*, leading to reduced *PAX6* and *NR2E3* expression. Similar to patient variants found in psychiatric disorders, variants found in eye disorders could be tested in mouse models to determine the molecular pathways in which they disrupt.

5.5.3 The use of genetic crosses to identify novel pathways

By crossing *Nr2e1*-null mice with *Pax6*$^{+/Sey}$ mutants, the genetic interaction between these two genes was discovered to be important for setting boundaries during brain development (Stenman *et al.*, 2003). This technique allows for two distinct genotypes to interact and either enhance or ameliorate specific phenotypes, thereby illuminating the nature of the genetic interaction. For example, if crossing the *Nr2e1* overexpressors with *Pax6*$^{+/Sey}$ mice results in an eye phenotype more severe than the two single mutants, then the two genes are working in additive genetic pathways. However, if *Nr2e1* acts upstream to *Pax6,* then the phenotype might be unchanged because the *Nr2e1*

overexpression phenotype hides the phenotypic effects of *Pax6*$^{+/Sey}$. A combination of genetic crosses can be performed, using *Nr2e1*$^{frc/frc}$, B6-bacEMS4A, *Pax6*$^{+/Sey}$, and *Nr2e3*$^{-/-}$ mice, to reveal genetic interactions important in brain and eye development.

The reduction of *Gfap* expression in brains of *Nr2e1* overexpressors is an exciting first step towards the long-term goal of using *Nr2e1* in therapy. Of particular interest is *NR2E1* in the treatment of Alzheimer's disease (AD), the most common cause of dementia, which shows severe neuropathology in the hippocampus consisting of β-amyloid plaques and neurofibrillary tangles (Gotz & Ittner, 2008). Current stem cell therapies in Alzheimer models have shown improved cognitive functions in transgenic mice; however, increased amyloid precursor protein (APP) in these animals reduces neurogenesis and increases glial differentiation of the implanted neural stem cells (Sugaya *et al.*, 2007), and therefore hinders the effectiveness of the therapeutic potential of these stem cells. We hypothesize that *Nr2e1*-overexpressing neural stem cells would be less susceptible to the anti-neurogenic and pro-gliosis effects of increased APP because of their increased proliferative potential and their reduced levels of endogenous *Gfap*. This reduced sensitivity to high APP levels could allow for later onset of symptoms resulting from inflammation and subsequent neuronal loss. Although we only showed a significant increase in neural stem/progenitor cell proliferation in the subventricular zone and not the dentate gyrus of the hippocampus, we predict that a diseased hippocampus would provide an environment in which *Nr2e1*-overexpressing neural stem/progenitor cells would be challenged and so demonstrate their increased potential to proliferate. *Nr2e1* overexpressing mice can be subjected to exercise or intracranial lipopolysaccharide (LPS) injections to test the effect of *Nr2e1* overexpression in a

sensitized system. Similarly, *Nr2e1* overexpressing mice can be crossed to mouse models of AD and examined for amelioration of disease phenotypes, such as neuropathological hallmarks (e.g. increased GFAP staining, neuronal loss in dentate gyrus) and cognitive deficits (e.g. impairment in Morris water maze).

5.6 Conclusion

The work presented in this thesis was the first to evaluate the validity of *Nr2e1$^{frc/frc}$* mice as a model for BP by behavioural measures and drug treatment, as well as the first to examine the transcriptional and morphological effects of *Nr2e1* overexpression in the mouse brain and eye. Our results have set the foundation on which patient variants of *NR2E1* from brain-behavioural abnormalities can be studied and have identified novel target genes that place *Nr2e1* into important genetic pathways involved in psychiatric and eye disorders, warranting further investigation of *NR2E1* in these human disorders.

5.6 References

Abrahams, B.S., Kwok, M.C., Trinh, E., Budaghzadeh, S., Hossain, S.M. & Simpson, E.M. (2005) Pathological aggression in "fierce" mice corrected by human nuclear receptor 2E1. *J Neurosci,* **25,** 6263-6270.

Abrahams, B.S., Mak, G.M., Berry, M.L., Palmquist, D.L., Saionz, J.R., Tay, A., Tan, Y.H., Brenner, S., Simpson, E.M. & Venkatesh, B. (2002) Novel vertebrate genes and putative regulatory elements identified at kidney disease and NR2E1/fierce loci. *Genomics,* **80,** 45-53.

Chaillan, F.A., Marchetti, E., Soumireu-Mourat, B. & Roman, F.S. (2005) Selective impairment of subcategories of long-term memory in mice with hippocampal lesions accessed by the olfactory tubing maze. *Behav Brain Res,* **158,** 285-292.

Crabbe, J.C., Wahlsten, D. & Dudek, B.C. (1999) Genetics of mouse behavior: interactions with laboratory environment. *Science,* **284,** 1670-1672.

Deacon, R.M., Bannerman, D.M., Kirby, B.P., Croucher, A. & Rawlins, J.N. (2002) Effects of cytotoxic hippocampal lesions in mice on a cognitive test battery. *Behav Brain Res,* **133,** 57-68.

Einat, H. (2006) Modelling facets of mania - new directions related to the notion of endophenotypes. *J Psychopharmacol.*

Goldberg, J.F. & Chengappa, K.N. (2009) Identifying and treating cognitive impairment in bipolar disorder. *Bipolar Disord,* **11 Suppl 2,** 123-137.

Gottesman, II & Gould, T.D. (2003) The endophenotype concept in psychiatry: etymology and strategic intentions. *Am J Psychiatry,* **160,** 636-645.

Gottesman, II & Shields, J. (1973) Genetic theorizing and schizophrenia. *Br J Psychiatry,* **122,** 15-30.

Gotz, J. & Ittner, L.M. (2008) Animal models of Alzheimer's disease and frontotemporal dementia. *Nat Rev Neurosci,* **9,** 532-544.

Herman, J.P., Prewitt, C.M. & Cullinan, W.E. (1996) Neuronal circuit regulation of the hypothalamo-pituitary-adrenocortical stress axis. *Crit Rev Neurobiol,* **10,** 371-394.

Jope, R.S. & Roh, M.S. (2006) Glycogen synthase kinase-3 (GSK3) in psychiatric diseases and therapeutic interventions. *Curr Drug Targets,* **7,** 1421-1434.

Kruger, S., Frasnelli, J., Braunig, P. & Hummel, T. (2006) Increased olfactory sensitivity in euthymic patients with bipolar disorder with event-related episodes compared with patients with bipolar disorder without such episodes. *J Psychiatry Neurosci,* **31,** 263-270.

Kumar, R.A., Chan, K.L., Wong, A.H., Little, K.Q., Rajcan-Separovic, E., Abrahams, B.S. & Simpson, E.M. (2004) Unexpected embryonic stem (ES) cell mutations represent a concern in gene targeting: lessons from "fierce" mice. *Genesis,* **38,** 51-57.

Kumar, R.A., Leach, S., Bonaguro, R., Chen, J., Yokom, D.W., Abrahams, B.S., Seaver, L., Schwartz, C.E., Dobyns, W., Brooks-Wilson, A. & Simpson, E.M. (2007) Mutation and evolutionary analyses identify NR2E1-candidate-regulatory mutations in humans with severe cortical malformations. *Genes Brain Behav,* **6,** 503-516.

Kumar, R.A., McGhee, K.A., Leach, S., Bonaguro, R., Maclean, A., Aguirre-Hernandez, R., Abrahams, B.S., Coccaro, E.F., Hodgins, S., Turecki, G., Condon, A., Muir, W.J., Brooks-Wilson, A.R., Blackwood, D.H. & Simpson, E.M. (2008) Initial association of NR2E1 with bipolar disorder and identification of candidate mutations in bipolar disorder, schizophrenia, and aggression through resequencing. *Am J Med Genet B Neuropsychiatr Genet,* **147B,** 880-889.

Liu, H.K., Belz, T., Bock, D., Takacs, A., Wu, H., Lichter, P., Chai, M. & Schutz, G. (2008) The nuclear receptor tailless is required for neurogenesis in the adult subventricular zone. *Genes Dev,* **22,** 2473-2478.

Liu, S., Tang, J., Ostrowski, R.P., Titova, E., Monroe, C., Chen, W., Lo, W., Martin, R. & Zhang, J.H. (2007) Oxidative stress after subarachnoid hemorrhage in gp91phox knockout mice. *Can J Neurol Sci,* **34,** 356-361.

McCurdy, R.D., Feron, F., Perry, C., Chant, D.C., McLean, D., Matigian, N., Hayward, N.K., McGrath, J.J. & Mackay-Sim, A. (2006) Cell cycle alterations in biopsied olfactory neuroepithelium in schizophrenia and bipolar I disorder using cell culture and gene expression analyses. *Schizophr Res,* **82,** 163-173.

McQueen, M.B., Devlin, B., Faraone, S.V., Nimgaonkar, V.L., Sklar, P., Smoller, J.W., Abou Jamra, R., Albus, M., Bacanu, S.A., Baron, M., Barrett, T.B., Berrettini, W., Blacker, D., Byerley, W., Cichon, S., Coryell, W., Craddock, N., Daly, M.J., Depaulo, J.R., Edenberg, H.J., Foroud, T., Gill, M., Gilliam, T.C., Hamshere, M., Jones, I., Jones, L., Juo, S.H., Kelsoe, J.R., Lambert, D., Lange, C., Lerer, B., Liu, J., Maier, W., Mackinnon, J.D., McInnis, M.G., McMahon, F.J., Murphy, D.L., Nothen, M.M., Nurnberger, J.I., Pato, C.N., Pato, M.T., Potash, J.B., Propping, P.,

Pulver, A.E., Rice, J.P., Rietschel, M., Scheftner, W., Schumacher, J., Segurado, R., Van Steen, K., Xie, W., Zandi, P.P. & Laird, N.M. (2005) Combined analysis from eleven linkage studies of bipolar disorder provides strong evidence of susceptibility loci on chromosomes 6q and 8q. *Am J Hum Genet,* **77,** 582-595.

Monaghan, A.P., Bock, D., Gass, P., Schwager, A., Wolfer, D.P., Lipp, H.P. & Schutz, G. (1997) Defective limbic system in mice lacking the tailless gene. *Nature,* **390,** 515-517.

Prickaerts, J., Moechars, D., Cryns, K., Lenaerts, I., van Craenendonck, H., Goris, I., Daneels, G., Bouwknecht, J.A. & Steckler, T. (2006) Transgenic mice overexpressing glycogen synthase kinase 3beta: a putative model of hyperactivity and mania. *J Neurosci,* **26,** 9022-9029.

Pullela, R., Raber, J., Pfankuch, T., Ferriero, D.M., Claus, C.P., Koh, S.E., Yamauchi, T., Rola, R., Fike, J.R. & Noble-Haeusslein, L.J. (2006) Traumatic injury to the immature brain results in progressive neuronal loss, hyperactivity and delayed cognitive impairments. *Dev Neurosci,* **28,** 396-409.

Roy, K., Kuznicki, K., Wu, Q., Sun, Z., Bock, D., Schutz, G., Vranich, N. & Monaghan, A.P. (2004) The Tlx gene regulates the timing of neurogenesis in the cortex. *J Neurosci,* **24,** 8333-8345.

Roy, K., Thiels, E. & Monaghan, A.P. (2002) Loss of the tailless gene affects forebrain development and emotional behavior. *Physiol Behav,* **77,** 595-600.

Ryves, W.J. & Harwood, A.J. (2003) The interaction of glycogen synthase kinase-3 (GSK-3) with the cell cycle. *Prog Cell Cycle Res,* **5,** 489-495.

Shi, Y., Chichung Lie, D., Taupin, P., Nakashima, K., Ray, J., Yu, R.T., Gage, F.H. & Evans, R.M. (2004) Expression and function of orphan nuclear receptor TLX in adult neural stem cells. *Nature,* **427,** 78-83.

Stenman, J., Yu, R.T., Evans, R.M. & Campbell, K. (2003) Tlx and Pax6 co-operate genetically to establish the pallio-subpallial boundary in the embryonic mouse telencephalon. *Development,* **130,** 1113-1122.

Sugaya, K., Kwak, Y.D., Ohmitsu, O., Marutle, A., Greig, N.H. & Choumrina, E. (2007) Practical issues in stem cell therapy for Alzheimer's disease. *Curr Alzheimer Res,* **4,** 370-377.

Swayze, V.W., 2nd, Andreasen, N.C., Alliger, R.J., Ehrhardt, J.C. & Yuh, W.T. (1990) Structural brain abnormalities in bipolar affective disorder. Ventricular enlargement and focal signal hyperintensities. *Arch Gen Psychiatry,* **47,** 1054-1059.

Takahashi-Yanaga, F. & Sasaguri, T. (2009) Drug development targeting the glycogen synthase kinase-3beta (GSK-3beta)-mediated signal transduction pathway: inhibitors of the Wnt/beta-catenin signaling pathway as novel anticancer drugs. *J Pharmacol Sci,* **109,** 179-183.

Viggiano, D. (2008) The hyperactive syndrome: metanalysis of genetic alterations, pharmacological treatments and brain lesions which increase locomotor activity. *Behav Brain Res,* **194,** 1-14.

Wahlsten, D. (2001) Standardizing tests of mouse behavior: reasons, recommendations, and reality. *Physiol Behav,* **73,** 695-704.

Wahlsten, D., Metten, P., Phillips, T.J., Boehm, S.L., 2nd, Burkhart-Kasch, S., Dorow, J., Doerksen, S., Downing, C., Fogarty, J., Rodd-Henricks, K., Hen, R., McKinnon, C.S., Merrill, C.M., Nolte, C., Schalomon, M., Schlumbohm, J.P., Sibert, J.R., Wenger, C.D., Dudek, B.C. & Crabbe, J.C. (2003) Different data from different labs: lessons from studies of gene-environment interaction. *J Neurobiol,* **54,** 283-311.

Young, K.A., Berry, M.L., Mahaffey, C.L., Saionz, J.R., Hawes, N.L., Chang, B., Zheng, Q.Y., Smith, R.S., Bronson, R.T., Nelson, R.J. & Simpson, E.M. (2002) Fierce: a new mouse deletion of Nr2e1; violent behaviour and ocular abnormalities are background-dependent. *Behav Brain Res,* **132,** 145-158.

Yu, R.T., McKeown, M., Evans, R.M. & Umesono, K. (1994) Relationship between Drosophila gap gene tailless and a vertebrate nuclear receptor Tlx. *Nature,* **370,** 375-379.

Appendix A: Deletion of the nuclear receptor *Nr2e1* impairs synaptic plasticity and dendritic structure in the mouse dentate gyrus

DELETION OF THE NUCLEAR RECEPTOR *Nr2e1* IMPAIRS SYNAPTIC PLASTICITY AND DENDRITIC STRUCTURE IN THE MOUSE DENTATE GYRUS

B. R. CHRISTIE,[a,b,c*] A. M. LI,[a] V. A. REDILA,[a] H. BOOTH,[a] B. K. Y. WONG,[d] B. D. EADIE,[b] C. ERNST[b] AND E. M. SIMPSON[b,c,d]

[a]*Department of Psychology, University of British Columbia, 2136 West Mall, Vancouver, British Columbia, Canada V6T 1Z4*

[b]*Graduate Program in Neuroscience, University of British Columbia, Vancouver, British Columbia, Canada V6T 1Z4*

[c]*The Brain Research Centre, University of British Columbia, Vancouver, British Columbia, Canada V6T 1Z4*

[d]*Centre for Molecular Medicine and Therapeutics, Child & Family Research Institute, and Department of Medical Genetics, University of British Columbia, Vancouver, British Columbia, Canada V5Z 4H4*

Abstract—The spontaneous or targeted deletion of the nuclear receptor transcription factor *Nr2e1* produces a mouse that shows hypoplasia of the hippocampal formation and reduced neurogenesis in adult mice. In these studies we show that hippocampal synaptic transmission appears normal in the dentate gyrus and cornu ammonis 1 subfields of adult mice that lack *Nr2e1* (*Nr2e1*$^{-/-}$), and that fEPSP shape, paired-pulse responses, and short-term plasticity are not substantially altered in either subfield. In contrast, the expression of long-term potentiation is selectively impaired in the dentate gyrus, and not in the cornu ammonis 1 subfield. Golgi analysis revealed that there was a significant reduction in both dendritic branching and dendritic length that was specific to dentate gyrus granule cells in the *Nr2e1*$^{-/-}$ mice. These results indicate that *Nr2e1* deletion can significantly alter both synaptic plasticity and dendritic structure in the dentate gyrus. © 2005 Published by Elsevier Ltd on behalf of IBRO.

Key words: long-term potentiation, synapse, hippocampus, dentate gyrus, Golgi.

The *Nr2e1* receptor (also known as *Mtll* or *Tlx*) is a member of the orphan nuclear receptor family, a subset of nuclear receptors that are highly conserved across a divergent range of species ranging from *Drosophila* to humans (Yu et al., 1994; Jackson et al., 1998; Abrahams et al., 2002, 2005). *Nr2e1* transcription initiates around embryonic day (E) 8, and quickly spreads to the presumptive diencephalons and the newly formed optic and olfactory evaginations by E8.5 (Monaghan et al., 1995). Transcription peaks at E13.5 in the ventricular and subventricular zone (SVZ), and then subsides to almost undetectable levels in the perinatal brain (Monaghan et al., 1995), before it is again expressed in the dentate gyrus (DG) and SVZ of the adult brain (Shi et al., 2004).

There are three different mouse strains that exhibit mutations of *Nr2e1*; two are targeted strains that lack two to three exons of the total DNA sequence for *Nr2e1*, while the third is a spontaneous mutation that lacks all nine exons (Monaghan et al., 1997; Yu et al., 2000; Young et al., 2002; Kumar et al., 2004). These mouse strains are phenotypically similar, showing cerebral, retinal, and olfactory bulb hypoplasia (Monaghan et al., 1997; Yu et al., 2000; Young et al., 2002). They are also similar in that these animals are characterized by extreme aggression in both sexes, with males often killing their intended mate (Monaghan et al., 1997; Young et al., 2002).

Several recent studies have proposed that *Nr2e1* has a regulative role in neurogenesis (Miyawaki et al., 2004; Roy et al., 2004; Shi et al., 2004). The evidence suggests that *Nr2e1* maintains adult neural stem cells in an undifferentiated, proliferative state *in vitro*, and its absence severely impairs cellular proliferation *in vivo* resulting in animals with smaller hippocampi (Miyawaki et al., 2004; Roy et al., 2004; Shi et al., 2004). It is not clear how these alterations affect synaptic plasticity in, or the basic dendritic structure of, DG granule cells. We have previously shown that voluntary exercise can enhance cellular proliferation in the DG, and this leads to increases in synaptic plasticity (van Praag et al., 1999; Farmer et al., 2004), dendritic length, and spine density (Eadie et al., 2005). Thus, the question naturally arises, are reductions in neurogenic activity in the DG, like those observed in animals that lack *Nr2e1*, also accompanied by reduced synaptic plasticity, decreased dendritic length, and fewer synapses.

EXPERIMENTAL PROCEDURES

Subjects

Both *Nr2e1*$^{-/-}$ and *Nr2e1*$^{+/+}$ littermates were used as subjects in these experiments. The mice were all first generation offspring resulting from the mating of C57BL/6J.129-*Nr2e1*$^{+/-}$ females (N10–12) to 129S1/SvlmJ.Cg-*Nr2e1*$^{+/-}$ males (N11–13). All mice were 2–4 months of age when tested. All of the procedures used in these experiments were in accordance with the Canada Council on Animal Care and approved by the University of British Columbia Animal Care Committee. All experiments were conducted in accordance with Canadian and International standards for animal

*Correspondence to: B. R. Christie, Department of Psychology, University of British Columbia, 2136 West Mall, Vancouver, British Columbia, Canada V6T 1Z4. Tel: +1-604-822-2296; fax: +1-604-822-6923.
E-mail address: bchristie@psych.ubc.ca (B. R. Christie).
Abbreviations: ACSF, artificial cerebrospinal fluid; CA1, cornu ammonis 1; DG, dentate gyrus; E, embryonic day; fEPSP, field excitatory postsynaptic potential; I/O, input–output; MPP, medial perforant path; PCR, polymerase chain reaction; STP, short-term potentiation; SVZ, subventricular zone; WT, wildtype.

care. All efforts were made to minimize the number and suffering of any animals used in these experiments.

Genotyping

Genotypes were determined using allele-specific polymerase chain reaction (PCR). All samples were tested for the presence of wildtype (WT) bands (365 bp) using the *Nr2e1* assay (30 cycles; 94 °C for 30 s, 58 °C for 30 s, and 72 °C for 55 s using primers oEMS296 (5′-CTCCCAGCAATCTAGTTTCCC-3′) and oEMS298 (5′-CTCTAGCAAAACTGCAGCTGC-3′) and mutant bands (438 bp) using the *Nr2e1*⁻/⁻ assay (30 cycles; 94 °C for 30 s, 58 °C for 30 s, and 72 °C for 55 s using primers oEMS643 (5′-CTGTGT-GTGCTGCTCTTGGT-3′) and oEMS652 (5′-CCCACATACA-CATATACATACCGA-3′). PCR products were subjected to electrophoresis in 2% agarose gel. Heterozygous mice will have positive bands for both assays, whereas WT and mutants will be positive for their respective bands only (data not shown). For this study, only WT and *Nr2e1*⁻/⁻ mice were examined.

Electrophysiology

Electrophysiological recordings were performed as we have described previously (Froc et al., 2003) on mice aged 2–4 months. Briefly, animals were decapitated and the brains were rapidly removed while submerged in chilled artificial cerebrospinal fluid (ACSF; pH 7.2) containing (in mM) 125.0 NaCl, 2.5 KCl, 1.25 NaH_2PO_4, 25.0 $NaHCO_3$, 2 $CaCl_2$, 1.3 $MgCl_2$ and 10.0 dextrose and continuously bubbled with 95% O_2/5% CO_2. While submerged in chilled ACSF, 200 μm transverse slices containing the hippocampal formation were sectioned using a vibratome. For recovery, slices were maintained in warm ACSF (30 °C) continuously bubbled with 95% O_2/5% CO_2 for at least 30 min. Individual slices were transferred to the recording chamber as required. fEPSPs (field excitatory postsynaptic potentials) were obtained using a 1–3 MΩ recording electrode, filled with ACSF, and a Dagan BVC-700 amplifier. Responses were evoked with a sharpened tungsten electrode (A-M Systems, WA, USA) using biphasic current pulses (120 μs, 10–400 μA) and a digital stimulus isolation unit (Getting Instruments, CA, USA). All data acquisition and analysis was performed using software provided by Getting Instruments (Lee Campbell, CA, USA).

All electrodes were initially positioned visually using a Olympus BX50wi microscope (10× objective). Stimulating electrodes were positioned in the middle third of the molecular layer to activate medial perforant path (MPP) fibers. All evoked responses were initially tested with paired-pulse stimuli (50 ms interpulse interval). During experiments, individual synaptic responses were continuously elicited at 15 s intervals. After a minimum of 15 min of stable baseline responses, LTP was induced by applying four bursts of 50 pulses at 100 Hz (30 s between bursts). Single pulse stimulation was again initiated immediately following the last tetanus, and was continued for a minimum of 30 min. All data were acquired at 5–10 kHz, and the initial slope of the negative going waveform was used to assess changes in synaptic efficacy (Froc et al., 2003). Paired-pulse (PP) responses are presented as the normalized difference between the slopes of the two responses and are presented as a percentage change. LTP is quantified as the percentage change in individual response slopes collected 30 min following the application of conditioning stimuli, as compared with the average slope of 60 responses acquired prior to tetanic stimulation.

In all figures, data are presented as the mean±standard error of the mean for that data set. Unpaired *t*-tests were used to assess statistical differences between groups (Statistica, Statsoft, Inc., Tulsa, OK, USA) with the exception of the phenotypic data.

Golgi–Cox analysis

Brains were removed and placed intact into vials containing 20 ml Golgi–Cox solution (Gibb and Kolb, 1998) and were stored in the dark for 14 days. Following this, the brains were switched to a 20% sucrose solution, and stored in the dark for a further 4 days, before being blocked and sectioned at 200 μm. Individual sections were then saved and placed on 2% gelatinized slides and examined under a microscope using Image-Pro Plus software (MediaCybernetics, CA, USA). Slices were coded prior to quantitative analysis, however differences in the gross morphology of the hippocampus in *Nr2e1*⁻/⁻ mice made it virtually impossible for this analysis to be conducted in a truly blind fashion. From each brain, five to 10 cells from both the DG and cornu ammonis 1 (CA1) subfields of the hippocampus were selected based upon (1) dark and consistent impregnation throughout the extent of the dendrites, (2) relative isolation from neighboring impregnated cells, and (3) cell bodies that were located toward the middle of the slice with dendrites lying in the same plane as the cell body. To quantify dendritic complexity, we performed a Sholl analysis (Sholl, 1956). For this analysis, each neuron was traced using an upright epifluorescence microscope at 40× magnification with an attached drawing tube set at 10× zoom (Nikon Y-IDT). A series of concentric rings, spaced 20 μm apart, was placed over the neuron, centered on the cell body, and the number of bifurcations as a function of distance was recorded. Separate two-way mixed ANOVAs were used to analyze the mean number of dendrite ring intersections for all cells. The total dendritic length of each granule cell was also measured using a digital imaging computer program (Image-Pro Plus; MediaCybernetics, MD, USA) and planned comparisons were used to compare differences in mean total dendritic length between the groups.

RESULTS

Synaptic transmission and presynaptic transmitter release are normal in the CA1 and DG subfields of the hippocampus in *Nr2e1*⁻/⁻ mice

To determine whether the *Nr2e1* deletion altered synaptic transmission in the hippocampus, we examined synaptic responses evoked in both the CA1 and the DG subfields of *Nr2e1*⁻/⁻ mice ($n=5$) and compared them against WT control animals ($n=5$). Because the hippocampus was noticeably smaller in the *Nr2e1*⁻/⁻ mice, we visually positioned the electrodes with the assistance of an upright microscope and a 10× water immersion objective to ensure that the electrodes were placed in equivalent positions in each experiment. For CA1 recordings, the electrodes were positioned in the middle of the stratum radiatum, equidistant between the pyramidal cell layer and the fissure, as shown in Fig. 1 (A and B). Electrical stimulation of the Schaffer collateral inputs to the CA1 subfield resulted in fEPSPs that had a characteristic negatively going waveform in both WT and *Nr2e1*⁻/⁻ mice (Fig. 1C).

To quantify any possible effects of the *Nr2e1* deletion on neurotransmission, input–output (I/O) curves were constructed by administering constant amplitude single pulses with one of seven different pulse widths (0.02–0.24 ms duration). Mice from both groups showed stereotypic nonlinear I/O curves (Fig. 1D) and no differences were apparent between genotypes for the I/O curves constructed for CA1 evoked responses. Although there were no obvious differences in the responses evoked in slices taken from WT and *Nr2e1*⁻/⁻ mice, it was possible that presynaptic transmitter release was altered in *Nr2e1*⁻/⁻ mice. To determine if this was the case, we carried out paired-pulse
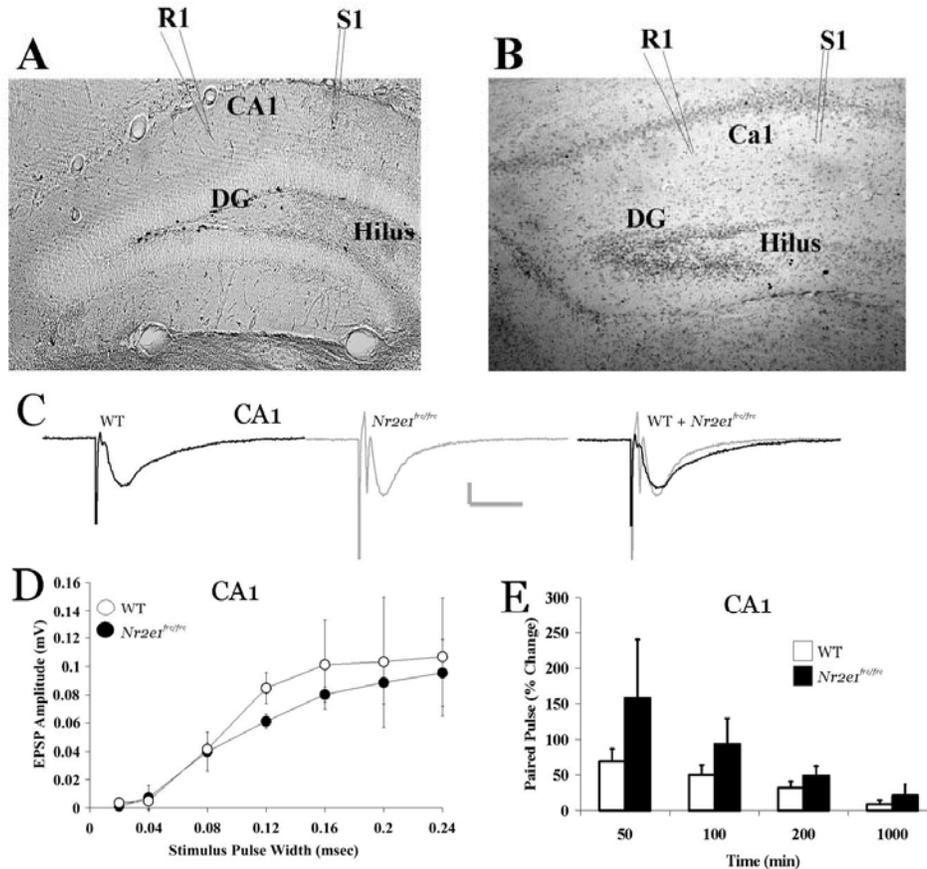
Fig. 1. Normal synaptic transmission in the CA1 subfield of $Nr2e1^{-/-}$ mice. (A, B) Photomicrographs depicting the position of stimulating (S1) and recording (R1) electrodes in the stratum radiatum layer of the CA1 subfield in WT (A) and $Nr2e1^{-/-}$ (B) mice. (C) No differences were found in evoked responses from WT and $Nr2e1^{-/-}$ mice. The fEPSP overlays illustrate that the responses are virtually identical in both strains of mice. (D) I/O curves were not significantly different for responses evoked in the CA1 subfield of WT and $Nr2e1^{-/-}$ mice. (E) Analysis of variance indicated that paired-pulse responses were not significantly different between the groups. Scale bar=0.25 mV; 20 ms.

analyses using four separate paired-pulse intervals (50, 100, 200, 1000 ms) (Fig. 1E). Analysis of variance across all of these intervals did not indicate that there was a significant difference between paired-pulse facilitation in the CA1 region of the WT and $Nr2e1^{-/-}$ mice ($P>0.05$).

To evoke fEPSPs in the DG, electrodes were also visually positioned equidistantly between the fissure and granule cell layer to stimulate the MPP inputs to the molecular layer of the DG (Fig. 2A, B). As shown in Fig. 2C, this also produced negative going fEPSPs in WT and $Nr2e1^{-/-}$ mice. IO curves were generated for the DG, as described above, and similar to the CA1 region,

no differences were observed between fEPSPs generated in WT and $Nr2e1^{-/-}$ mice (Fig. 2D). The application of paired-pulses to the MPP of the DG produces a characteristic paired-pulse depression (McNaughton and Barnes, 1977; Christie and Abraham, 1992a,b, 1994). Paired-pulse analyses of responses evoked in the DG of WT and $Nr2e1^{-/-}$ mice revealed there to be no significant difference between these two groups (Fig. 2E). These initial findings indicate that despite the gross morphological differences observed in the brains of WT and $Nr2e1^{-/-}$ mice, similar electrophysiological responses can still be elicited from both genotypes.
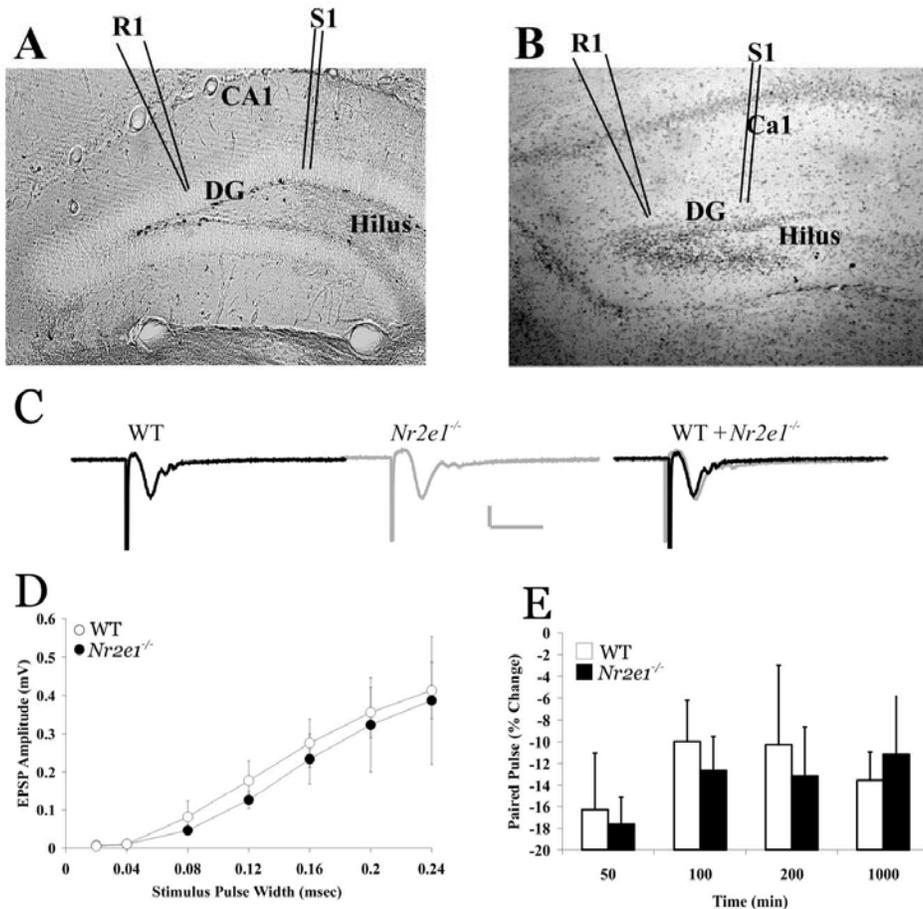
Fig. 2. Normal synaptic transmission in the DG subfield of $Nr2e1^{-/-}$ mice. (A, B) Photomicrographs depicting the position of stimulating (S1) and recording (R1) electrodes in the molecular layer of the DG subfield in WT (A) and $Nr2e1^{-/-}$ (B) mice. (C) No differences were found in evoked responses from WT and $Nr2e1^{-/-}$ mice. The fEPSP overlays illustrate that the responses are virtually identical in both strains of mice. (D) I/O curves were not significantly different for responses evoked in the DG subfield of WT and $Nr2e1^{-/-}$ mice. (E) Analysis of variance indicated that paired-pulse responses were not significantly different between the groups. Scale bar=0.25 mV; 20 ms.

LTP is impaired in the DG, but not the CA1 region, of $Nr2e1^{-/-}$ mice

To determine the capacity of WT and $Nr2e1^{-/-}$ mice to exhibit long-lasting changes in synaptic efficacy, high frequency stimuli (4×50 pulses at 100 Hz) were applied to electrodes situated in either the CA1 or DG subfields of the hippocampus. In the CA1 subfield, application of these conditioning stimuli produced a significant degree of short-term potentiation (STP) in WT ($348.6 \pm 85.5\%$) and $Nr2e1^{-/-}$ ($291.6 \pm 71.2\%$) mice. The amount of STP was not signifi-

cantly different between these two groups ($t_{(12)}=-0.5$; $P>0.05$). When we examined the capacity for Schaffer collateral inputs to the CA1 pyramidal neurons to express LTP lasting at least 30 min, we also found that there was not a significant difference ($t_{(12)}=-0.7$; $P>0.05$) between WT ($103.4 \pm 30.4\%$, $n=8$) and $Nr2e1^{-/-}$ ($78.2 \pm 18.2\%$, $n=6$) mice (Fig. 3A).

The application of these same stimuli to the MPP inputs to the DG had markedly different effects (Fig. 3B). WT and $Nr2e1^{-/-}$ mice showed normal and equivalent

178
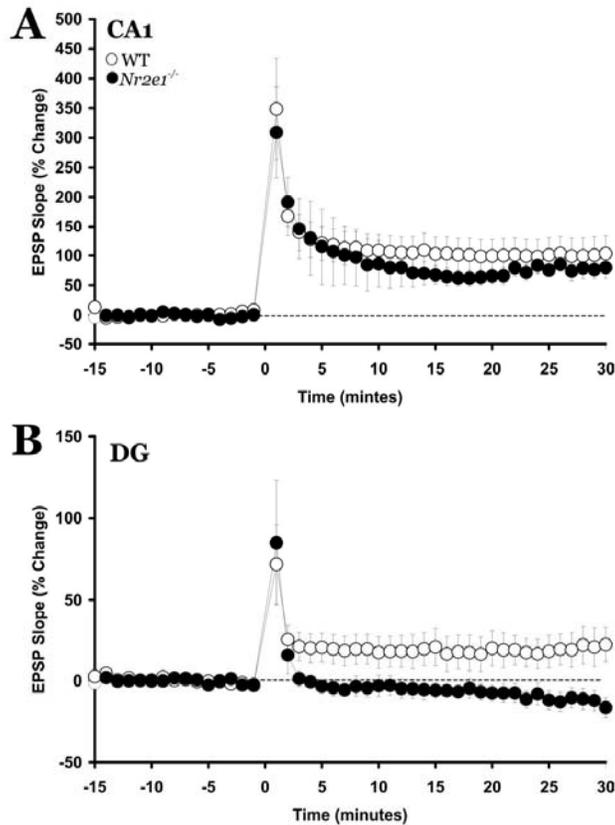
Fig. 3. Synaptic plasticity is severely impaired in the DG of $Nr2e1^{-/-}$ mice. (A) Graph depicts time course of experiment in WT and $Nr2e1^{-/-}$ mice that were administered 50 pulses of 100 Hz stimuli four times at time zero. (A) Note how robust STP and LTP is induced in WT and $Nr2e1^{-/-}$ mice in the CA1 subfield. (B) Although equivalent STP is observed in WT and $Nr2e1^{-/-}$ mice, LTP in the DG is significantly reduced in the $Nr2e1^{-/-}$ mice.

STP following the administration of the high-frequency stimuli (WT: 84.9±38.2%, $n=7$; $Nr2e1^{-/-}$: 71.8±24.2%, $n=6$). The STP translated into a modest but significant degree of LTP in WT mice (22.1%±10.6, $n=6$, $P<0.05$), while in contrast, a significant degree of LTP was not observed in $Nr2e1^{-/-}$ mice (−16.6±6.1%, $n=7$). The WT mice showed significantly more LTP than the $Nr2e1^{-/-}$ mice at 30 min post-conditioning ($t_{(11)}=−3.3$; $P<0.05$). It is noteworthy that the $Nr2e1^{-/-}$ mice did show STP, indicating that the lack of LTP was not due to the inability of DG cells in $Nr2e1^{-/-}$ mice to exhibit potentiation. Rather, in slices from $Nr2e1^{-/-}$ mice, the response was enhanced only briefly, and then rapidly attenuated towards baseline, indicating that the deficit involves some mechanism involved in the genesis of longer lasting forms of potentiation.

Mice lacking *Nr2e1* have abnormal dendritic structure in the DG

Previously Shi and colleagues (2004) have shown that neurogenesis is reduced in the DG of a targeted strain of $Nr2e1^{-/-}$ mice, but the reduced size of the hippocampus in these mice suggested that there might also be changes in the dendritic structure of hippocampal neurons. To examine this issue we used a modified Golgi–Cox procedure (Gibb and Kolb, 1998) to visualize individual hippocampal neurons.

Representative examples of DG granule cells and CA1 pyramidal cells in WT and Nr2e1$^{-/-}$ mice are shown in Fig. 4. Using a Sholl analysis, it was determined that granule cells in the $Nr2e1^{-/-}$ mice displayed significantly fewer branch points across the extent of the dentate mo-
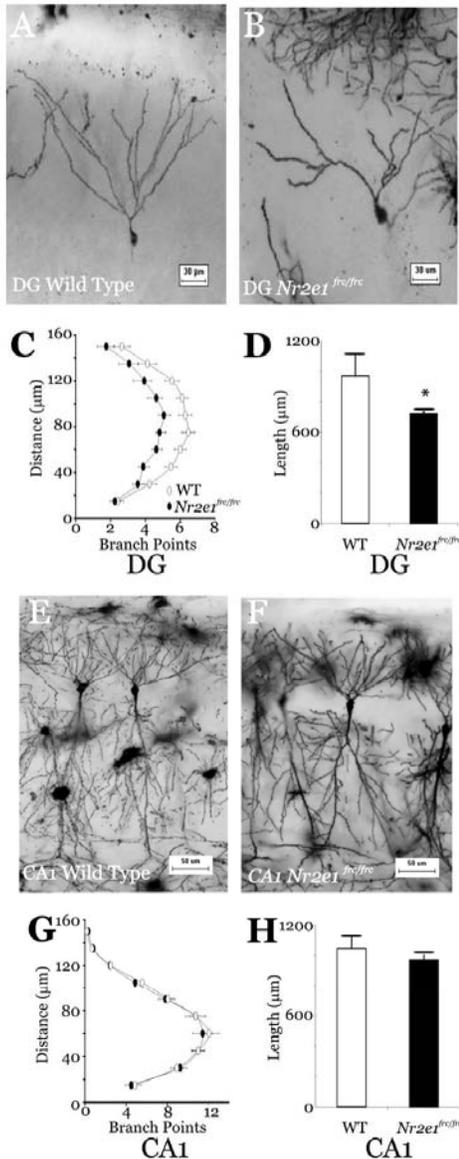
Fig. 4. DG granule neurons in $Nr2e1^{-/-}$ mice exhibit fewer branch points and reduced length. (A, B) Microphotographs of neurons labeled with Golgi–Cox impregnation in the DG of WT (A) and $Nr2e1^{-/-}$ mice (B). DG neurons in $Nr2e1^{-/-}$ mice typically displayed fewer branch points across the extent of the molecular layer (C) and overall were significantly shorter in length (D). Cells in the CA1 region of WT (E) and $Nr2e1^{-/-}$ (F) mice did not display any significant differences in dendritic complexity (G) or length (H). Scale bars=30 μm (A, B); 50 μm (C, D).

lecular layer than were seen in WT animals (Fig. 4C; $F_{(1,30)}$=11.5, P<0.05). In addition, these granule cells also exhibited a significant reduction in their total dendritic length when compared with WT animals ($F_{(1,30)}$=10.99, P<0.05). A similar Golgi analysis performed on pyramidal cells in the CA1 region did not reveal any significant differences between WT and $Nr2e1^{-/-}$ animals in either their apical or basal dendritic regions (P>0.05). Thus, marked alterations in dendritic structure appear to be restricted to DG granule cells in the $Nr2e1^{-/-}$ mice.

DISCUSSION

The initial results showed that $Nr2e1^{-/-}$ mice did not exhibit significantly altered field recordings in the DG and CA1 subfields, despite the reductions in hippocampal morphology and the changes in the granule cell dendrites we observed later in the Golgi analysis. WT and $Nr2e1^{-/-}$ mice had responses with similar amplitudes, latencies, and morphologies in both the DG and CA1 subfields of the hippocampus. In addition, paired-pulse analysis indicated that the loss of $Nr2e1$ did not significantly affect transmitter release in the DG and CA1 subfields. Despite the fact that there were no obvious electrophysiological deficits, when we administered high frequency stimuli, it was found that LTP was selectively impaired in the DG of $Nr2e1^{-/-}$ mice, even though normal STP was observed in all slices tested from both groups. The fact that STP was normal makes it unlikely that alterations in dendritic architecture alone resulted in decreased synaptic plasticity in $Nr2e1^{-/-}$ mice. It may be that some second messenger cascade, critical for the expression of LTP, is also impaired in the $Nr2e1^{-/-}$ mice. It is noteworthy that this selective reduction in DG LTP occurs in an adult animal that has also been reported to exhibit impaired neurogenesis. Conversely, we have shown previously that animals with increased neurogenesis can exhibit significantly increased LTP (van Praag et al., 1999; Farmer et al., 2004). Since these two processes are so tightly correlated, it may indicate that some mechanism involved in neurogenic activity plays a permissive role in establishing a 'plastic' environment for functional changes to occur. This would call into question the ubiquity of LTP in the different subregions, and suggest that the mechanisms for synaptic plasticity in the DG may differ substantially from those in the other hippocampal subfields.

Golgi impregnation did not differentiate between neurons in the CA1 region of WT and $Nr2e1^{-/-}$ mice, however there were substantial differences in the dendrites of DG granule cells. The sparse nature, and shorter overall length, of the dendrites of DG granule cells in $Nr2e1^{-/-}$ mice is reminiscent of early descriptions of immature neurons in the DG (Bayer, 1980). Functionally, dendrites have

been shown to be active contributors to a number of cellular processes, including LTP and LTD (Johnston et al., 2003). Furthermore, using compartmentalized models, it has been shown that a loss of dendritic area, similar to that shown here, severely impedes the ability of neurons to reliably transmit information (Mainen and Sejnowski, 1996). Thus, the inability of $Nr2e1^{-/-}$ mice to exhibit LTP in the DG may reflect that they lack sufficient dendritic processing area to sustain LTP, or that there is a loss of some underlying mechanism that is necessary for long-lasting changes in synaptic efficacy to be induced. This former position is strengthened by the fact that CA1 neurons in $Nr2e1^{-/-}$ mice, which did not exhibit changes in dendritic structure, also did not show impaired LTP.

In conclusion, we have shown that adult $Nr2e1^{-/-}$ mice exhibit marked deficits in synaptic plasticity and dendritic morphology in the DG that are not observed in the CA1 region of the hippocampus.

REFERENCES

Abrahams BS, Mak GM, Berry ML, Palmquist DL, Saionz JR, Tay A, Tan YH, Brenner S, Simpson EM, Venkatesh B (2002) Novel vertebrate genes and putative regulatory elements identified at kidney disease and NR2E1/fierce loci. Genomics 80:45–53.

Abrahams BS, Kwok MC, Trinh E, Budaghzadeh S, Hossain SM, Simpson EM (2005) Pathological aggression in "fierce" mice corrected by human nuclear receptor 2E1. J Neurosci 25:6263–6270.

Bayer SA (1980) Development of the hippocampal region in the rat. II. Morphogenesis during embryonic and early postnatal life. J Comp Neurol 190:115–134.

Christie BR, Abraham WC (1992a) Priming of associative long-term depression in the dentate gyrus by theta frequency synaptic activity. Neuron 9:79–84.

Christie BR, Abraham WC (1992b) NMDA-dependent heterosynaptic long-term depression in the dentate gyrus of anaesthetized rats. Synapse 10:1–6.

Christie BR, Abraham WC (1994) Differential regulation of paired-pulse plasticity following LTP in the dentate gyrus. Neuroreport 5:385–388.

Eadie BD, Redila VA, Christie BR (2005) Voluntary exercise alters the cytoarchitecture of the adult dentate gyrus by increasing cellular proliferation, dendritic complexity, and spine density. J Comp Neurol 486:39–47.

Farmer J, Zhao X, van Praag H, Wodtke K, Gage FH, Christie BR (2004) Effects of voluntary exercise on synaptic plasticity and gene expression in the dentate gyrus of adult male Sprague-Dawley rats in vivo. Neuroscience 124:71–79.

Froc DJ, Eadie B, Li AM, Wodtke K, Tse M, Christie BR (2003) Reduced synaptic plasticity in the lateral perforant path input to the dentate gyrus of aged C57BL/6 mice. J Neurophysiol 90:32–38.

Gibb R, Kolb B (1998) A method for vibratome sectioning of Golgi-Cox stained whole rat brain. J Neurosci Methods 79:1–4.

Jackson A, Panayiotidis P, Foroni L (1998) The human homologue of the Drosophila tailless gene (TLX): characterization and mapping to a region of common deletion in human lymphoid leukemia on chromosome 6q21. Genomics 50:34–43.

Johnston D, Christie BR, Frick A, Gray R, Hoffman DA, Schexnayder LK, Watanabe S, Yuan LL (2003) Active dendrites, potassium channels and synaptic plasticity. Philos Trans R Soc Lond B Biol Sci 358:667–674.

Kumar RA, Chan KL, Wong AH, Little KQ, Rajcan-Separovic E, Abrahams BS, Simpson EM (2004) Unexpected embryonic stem (ES) cell mutations represent a concern in gene targeting: lessons from "fierce" mice. Genesis 38:51–57.

Mainen ZF, Sejnowski TJ (1996) Influence of dendritic structure on firing pattern in model neocortical neurons. Nature 382:363–366.

McNaughton BL, Barnes CA (1977) Physiological identification and analysis of dentate granule cell responses to stimulation of the medial and lateral perforant pathways in the rat. J Comp Neurol 175:439–454.

Miyawaki T, Uemura A, Dezawa M, Yu RT, Ide C, Nishikawa S, Honda Y, Tanabe Y, Tanabe T (2004) Tlx, an orphan nuclear receptor, regulates cell numbers and astrocyte development in the developing retina. J Neurosci 24:8124–8134.

Monaghan AP, Grau E, Bock D, Schutz G (1995) The mouse homolog of the orphan nuclear receptor tailless is expressed in the developing forebrain. Development 121:839–853.

Monaghan AP, Bock D, Gass P, Schwager A, Wolfer DP, Lipp HP, Schutz G (1997) Defective limbic system in mice lacking the tailless gene. Nature 390:515–517.

Roy K, Kuznicki K, Wu Q, Sun Z, Bock D, Schutz G, Vranich N, Monaghan AP (2004) The Tlx gene regulates the timing of neurogenesis in the cortex. J Neurosci 24:8333–8345.

Shi Y, Chichung Lie D, Taupin P, Nakashima K, Ray J, Yu RT, Gage FH, Evans RM (2004) Expression and function of orphan nuclear receptor TLX in adult neural stem cells. Nature 427:78–83.

Sholl DA (1956) The measurable parameters of the cerebral cortex and their significance in its organization. Prog Neurobiol 2:324–333.

van Praag H, Christie BR, Sejnowski TJ, Gage FH (1999) Running enhances neurogenesis, learning, and long-term potentiation in mice. Proc Natl Acad Sci U S A 96:13427–13431.

Young KA, Berry ML, Mahaffey CL, Saionz JR, Hawes NL, Chang B, Zheng QY, Smith RS, Bronson RT, Nelson RJ, Simpson EM (2002) Fierce: a new mouse deletion of Nr2e1: violent behaviour and ocular abnormalities are background-dependent. Behav Brain Res 132:145–158.

Yu RT, McKeown M, Evans RM, Umesono K (1994) Relationship between Drosophila gap gene tailless and a vertebrate nuclear receptor Tlx. Nature 370:375–379.

Yu RT, Chiang MY, Tanabe T, Kobayashi M, Yasuda K, Evans RM, Umesono K (2000) The orphan nuclear receptor Tlx regulates Pax2 and is essential for vision. Proc Natl Acad Sci U S A 97:2621–2625.

Appendix B: Certificate of animal care

THE UNIVERSITY OF BRITISH COLUMBIA

ANIMAL CARE CERTIFICATE

Application Number: A07-0431

Investigator or Course Director: Elizabeth M. Simpson

Department: Medical Genetics

Animals:

Mice B6-bacEMS4A; nestinCFPnuc	12
Mice B6-pacEMS1D	52
Mice B6-pacEMS1D; nestinCFPnuc	12
Mice B6-pacEMS1B	52
Mice B6-bacEMS4B	52
Mice B6129-frc	40
Mice B6-pacEMS1D; nestinGFP	12
Mice B6-bacEMS4A	52
Mice B6-bacEMS4A; nestinGFP	12

Start Date:	September 4, 2007	**Approval Date:**	October 22, 2008

Funding Sources:

Funding Agency:	Canadian Institutes of Health Research (CIHR)
Funding Title:	The role of nuclear receptor 2E1 in Stem Cells, Neurogenesis, and Brain Development
Funding Agency:	British Columbia Research Institute for Children and Women's Health
Funding Title:	Modulation of neural stem cell pool by Nr2e1: Evaluation of over-expression as a therapeutic aid
Funding Agency:	Michael Smith Foundation for Health Research
Funding Title:	Role of Nr2e1 in Modulation of Neural Stem cell pool, neurogenesis, and behaviour

Unfunded title: N/A

The Animal Care Committee has examined and approved the use of animals for the above experimental project.

This certificate is valid for one year from the above start or approval date (whichever is later) provided there is no change in the experimental procedures. Annual review is required by the CCAC and some granting agencies.

A copy of this certificate must be displayed in your animal facility.

Office of Research Services and Administration
102, 6190 Agronomy Road, Vancouver, BC V6T 1Z3
Phone: 604-827-5111 Fax: 604-822-5093